UNIVERSITA' DEGLI STUDI DI MILANO-BICOCCA

Facoltà di Scienze Matematiche, Fisiche e Naturali

Scuola di Dottorato di Scienze

Dottorato di Ricerca in Biotecnologie Industriali

XXVII Ciclo

Exploitation of *Saccharomyces cerevisiae* for the challenging conversion of renewable substrates into biofuels and chemicals

Coordinatore: Prof. Marco Vanoni

Tutor: Prof.ssa Paola Branduardi

Dott.ssa: Nadia Maria Berterame

Matricola: 706115

Anno Accademico 2013-2014

Alla mia famiglia

INDEX

ABSTRACT

Fossil resources are the main source exploited by human society for the production of electricity and fuels, as well as raw materials for the production of fine and bulk chemicals. The gradual depletion of oil deposits, which in turn causes an increase in prices, along with the increasing demand and need for environmental sustainability have contributed to trigger the interest in alternative energy and chemical sources.

Within this context, the biorefinery concept arises. In this technological platform, microorganisms are used as (enzymatic) cell factories to transform organic material derived from biomass into biofuels, energy and chemicals.

The present work aimed at the production of one relevant chemical and two promising biofuels from different types of biomass feedstock, tailoring *Saccharomyces cerevisiae* as cell factory.

In particular, it is reported the use of glucose (representative of plant-derived sugars) and glycine (representative of aminoacids derived from industrial proteinaceous side stream) as renewable substrates for the respective production of lactic acid and butanol and isobutanol.

Lactic acid

Lactic acid is a monocarboxylic acid used in the food, cosmetic and pharmaceutical industries. Moreover, its polymer, polylactic acid (PLA), has attracted the attention of the market for the production of biodegradable plastics. It is nowadays produced mainly by lactic acid bacteria (LAB). *S. cerevisiae* is a promising alternative microorganism since it can grow at a lower pH than the LAB. This allows to partly avoid the use of bases and thus decreasing the costs associated with the recovery of the product, which must be in the acid form. Despite the high robustness of yeasts, the major

limitation for a viable production of organic acids is the toxic effect of the very high concentrations of product reached during the process; therefore, in this work the tolerance to lactic acid and its production in *S. cerevisiae* laboratory and industrial strains, respectively, have been evaluated.

In particular, the modulation of *SAM2* levels has been studied. This gene encodes for the enzyme S-adenosylmethionine synthetase, responsible for the synthesis of S-adenosylmethionine, a central cofactor of cellular metabolism. The deletion of *SAM2* resulted in an increased lactic acid tolerance in the BY4741 genetic background, and in an increased lactic acid production (~69 g/L, approximately 5% more than in the parental strain) in the industrial omolactic strain m850. Because of the results obtained with *SAM2* modulation and because we are highly interested in reprogramming cellular metabolism around the production of interest, the effects of lactic acid exposure on proteins and lipids of BY4741 and BY4741 *sam2Δ S. cerevisiae* strains were investigated. Remarkably, an effect on protein aggregation triggered by the stressful condition was observed in the parental strain. Moreover, an effect on the lipid composition, in particular a decrease in phosphatidylcholine level, was observed in both strains under investigation. Because of the central role of plasma membrane not only in physiological condition, but also and possibly even more during a process of production, the effect of the deletion of *OPI1* was examined. Its gene product is indeed involved in the biosynthetic pathway of phosphatidylcholine, the main membrane phospholipid. Remarkably, the deletion of *OPI1* resulted in an increased lactic acid tolerance in the laboratory strain BY4741.

Butanol and isobutanol

The current production of bio-fuels mainly refers to bioethanol and biodiesel. However, they are not ideal fuel substitutes in that they are not compatible

with the existing fuel infrastructures for distribution and storage. In particular, ethanol is very corrosive and hygroscopic and biodiesel has high viscosity and pour points. Moreover their energy content is lower if compered with gasoline and petrodiesel, respectively. As a consequence, interest in higher alcohols as gasoline substitutes has grown because of their higher energy density and lower vapor pressure compared to ethanol. In addition, they are less hygroscopic than ethanol, allowing their use in currently engine as well as storage and distribution using existing infrastructure.

The aim of this study was the production of two higher alcohols, butanol and isobutanol, in laboratory strains of *S. cerevisiae*. Although *Clostridia* are still the basis of the butanol production process, these microorganisms have strong limitations as a low tolerance to the product, the final cell differentiation in spores and the need to grow in total anaerobic conditions. In addition, the complex genetic manipulation makes the optimization process difficult. These limitations have led to focus the attention on alternative microorganisms, among which *S. cerevisiae*.

Specifically, our attention was focused on the pathway of keto-acids that branches from amino acid pathway. The keto-acid pathway appears to be promising since it might exploit as substrate the aminoacids released from proteins accumulated during industrial production processes starting from lignocellulosic biomass pre-treatment, rapresenting therefore a side byproduct now undervalued.

Villas-Boas (2005) proposed a metabolic model, supported by some wet data on metabolites, in which glycine, through glyoxylate, can be converted into α-ketovalerate, which in turn can be converted into α-isoketovalerate. It is known from literature that the conversion of α-ketovalerate can generate butanol as well as the conversion of α-isoketovalerate generates isobutanol.

Abstract

In the present work a novel pathway for the production of butanol and isobutanol from glycine was first hypothesized and then demonstrated in two different *S. cerevisiae* genetic background, CEN.PK and BY4741. In particular, starting from 15 g/L of glycine 92 mg/L of butanol and 58 mg/L of isobutanol have been obtained.

The versatility of the yeast *S. cerevisiae*, demonstrated both in terms of renewable substrates used and bio-products obtained, confirms this microorganism as a key cell factory that can be employed together with other bio-based processes in the view of a true bioeconomical development. Further efforts will therefore be focused to increase the robustness of this microorganism, in order to turn towards a biorefinery competitive with the processes currently available.

RIASSUNTO

Le risorse fossili sono attualmente la principale fonte sfruttata dall'uomo per la produzione di energia elettrica e combustibili, nonché come materia prima per l'industria, in particolare quella chimica. Il progressivo esaurimento dei giacimenti, che a sua volta determina un innalzamento dei prezzi, insieme alla crescente domanda e alla necessità di una maggior sostenibilità ambientale, hanno contribuito ad aumentare l'interesse verso fonti alternative.

All'interno di tale contesto sta emergendo il concetto di bioraffineria, in cui microrganismi, usati come *cell factories*, trasformano attraverso il loro metabolismo la materia organica derivante da biomasse in biocarburanti, energia e sostanze chimiche.

Il presente studio è finalizzato alla produzione di un composto chimico di notevole importanza e di due promettenti biocarburanti a partire da materie prime di diversa natura ottimizzando *Saccharomyces cerevisiae* come *cell factory*. In particolare, viene descritto l'utilizzo del glucosio (esempio di zucchero ottenuto da biomasse vegetali di scarto) e glicina (esempio di amminoacido derivante dalla frazione proteica di scarto degli attuali processi industriali) come substrati rinnovabili per la produzione rispettivamente di acido lattico e butanolo e isobutanolo.

Acido lattico

L'acido lattico è un acido monocarbossilico molto usato nell'industria alimentare, cosmetica e farmaceutica. Inoltre, il suo polimero, l'acido polilattico (PLA), si sta imponendo all'attenzione del mercato in quanto è utilizzabile per la produzione di plastiche biodegradabili, alcune delle quali

già in commercio. L'attuale bioprocesso si basa principalmente sull'attività di batteri lattici (LAB) omofermentanti, naturali produttori.

S. cerevisiae rappresenta una valida alternativa a tali microrganismi per la produzione industriale di acido lattico poiché è in grado di crescere a pH inferiori rispetto ai LAB. Ciò permette di evitare almeno in parte l'uso di basi e dunque di diminuire i costi associati al recupero del prodotto, che deve essere in forma acida. Nonostante l'elevata robustezza dei lieviti, il maggior limite per la produzione di acidi organici è rappresentato dall'effetto tossico delle alte concentrazioni di prodotto raggiunte durante il processo; per tali ragioni in questo lavoro è stata valutata sia la tolleranza che la produzione di acido lattico, rispettivamente, in ceppi di laboratorio e in un ceppo industriale di *S. cerevisiae*.

In particolare, è stata studiata la modulazione del livello genico di *SAM2*, codificante l'enzima S-adenosilmetionina sintetasi responsabile della sintesi dell'S-adenosilmetionina, cofattore centrale del metabolismo cellulare. La delezione di tale gene ha determinato sia un incremento della tolleranza all'acido, nel background genetico BY4741, che un incremento di circa il 5% della sua produzione (pari a circa 69 g/L) nel ceppo industriale omolattico-fermentante m850. Dati i risultati ottenuti dalla modulazione di *SAM2* e poiché siamo fortemente interessati nella riprogrammazione del metabolismo cellulare volta alla produzione d'interesse, l'esposizione all'acido lattico è stata indagata in termini di effetti sulle principali classi di biomolecole di *S. cerevisiae*, in particolare proteine e lipidi, nei ceppi BY4741 e BY4741 *sam2Δ*. I dati ottenuti tramite analisi spettroscopiche mostrano una transiente formazione di aggregati proteici intracellulari nel ceppo parentale e cambiamenti della composizione lipidica di membrana in entrambi i ceppi in analisi; in particolare sono stati osservati diminuiti livelli di fosfatidilcolina. Dato il ruolo centrale della membrana plasmatica non solo in

condizioni fisiologiche ma anche, e forse più, durante il processo di produzione, è stato valutato l'effetto della delezione del gene *OPI1*. Il suo prodotto genico è infatti un fattore di trascrizione in grado di reprimere i geni coinvolti nel *pathway* biosintetico della fosfatidilcolina, principale fosfolipide di membrana. La delezione di tale gene è risultata in una maggior tolleranza all'acido lattico nel ceppo di laboratorio BY4741.

Butanolo e isobutanolo

Le attuali produzioni di biocarburanti si riferiscono principalmente al bioetanolo e al biodiesel. Questi ultimi non sono però compatibili con le infrastrutture già esistenti. In particolare, l'etanolo ha un'elevata corrosività e igroscopicità mentre il biodiesel presenta una viscosità e un potere calorifico elevati. Inoltre possiedono un contenuto energetico più basso, se confrontati rispettivamente con la benzina e il petrodiesel. L'attenzione si sta quindi spostando verso possibili alternative. In particolare, gli alcoli superiori, data la loro maggiore densità energetica e la minore pressione di vapore, sono estremamente competitivi come sostituti della benzina rispetto all'etanolo. Inoltre possono essere utilizzati direttamente come biocarburanti nei motori e distribuiti attraverso le infrastrutture già esistenti grazie alla loro minore igroscopicità.

Nel presente lavoro ci si è focalizzati sulla produzione di butanolo e isobutanolo in ceppi di laboratorio di *S. cerevisiae*. Sebbene i *Clostridi*, produttori naturali di butanolo, siano alla base degli attuali processi di produzione, essi presentano forti limitazioni come la bassa tolleranza a elevate concentrazioni di prodotto, il differenziamento finale in spore e la necessità di crescere in totale anaerobiosi. Inoltre la difficile manipolazione genetica determina ridotti margini di miglioramento. Pertanto l'attenzione si sta spostando su microrganismi alternativi, tra cui *S. cerevisiae*. Nello

specifico il nostro interesse è stato volto al *pathway* dei chetoacidi che derivano dagli amminoacidi. Tale via metabolica, oltre ad essere promettente, permette di sfruttare le proteine che si accumulano nel corso degli attuali processi produttivi di biocarburanti e biomateriali, e che quindi costituiscono un sottoprodotto collaterale ora poco valorizzato.
Villas-Boas (2005) ha proposto un modello metabolico, supportato da dati sperimentali riguardanti i diversi metaboliti coinvolti, in cui a partire dall'amminoacido glicina, passando dal gliossilato, può generarsi il cheto-acido α-chetovalerato che a sua volta può essere convertito in α-isochetovalerato. Poiché in letteratura inoltre è riportata la conversione dell'α-chetovalerato in butanolo e dell'α-isochetovalerato in isobutanolo, nel presente lavoro è stato ipotizzato e dimostrato *step by step* un nuovo *pathway* per la produzione di tali alcoli a partire da glicina nei background genetici BY4741 e CEN.PK di *S. cerevisiae*. In particolare, a partire da 15 g/L di glicina sono stati ottenuti 92 mg/L di butanolo e 58 mg/L di isobutanolo.

La versatilità del lievito *S. cerevisiae* dimostrata sia in termini di substrati rinnovabili utilizzati che in termini di bioprodotti ottenuti, rende tale microrganismo una potente *cell factory* che può essere impiegata per far fronte alle problematiche economiche e ambientali, dovute allo sfruttamento di risorse fossili. Ulteriori sforzi saranno dunque mirati ad aumentare la robustezza del microrganismo in esame, al fine di volgere verso una bioraffineria realmente competitiva con i processi attualmente disponibili.

INTRODUCTION

Today, fossil resources are widely used to produce electricity, heat, and transportation fuels as well as the vast majority of the many chemicals that are required by contemporary society. In particular, about 85% and as much as 10% of all crude oil is used for the production of transportation fuels and industrial chemicals, respectively. During the 20th century, continuous scientific and technological developments led to ongoing refinements in these areas resulting in highly optimized and efficient technologies for utilizing fossil resources [1]. This increased use of fossil fuels has caused greenhouse gas emissions and created undesirable damage to the environment. Current instability of oil supplies and the continuous fluctuation of prices have further ignited widespread interest in alternative energy sources. These factors, which revolve around economical, environmental, and geopolitical issues, are central to current interest in renewable energy sources. An entire branch of biotechnology, referred to as “white biotechnology”, embraces the bioproduction of fuels and chemicals from renewable sources. These technologies use living cells and enzymes to synthesize products that require less energy and create less waste during their life cycle than those produced from fossil resources [2].

In fact, it is important to underline that with the development of genetic engineering in the 1970s, it became possible to transform microbes into ‘‘cell factories’’ for the recombinant production of chemicals through so-called metabolic engineering, a field dedicated to the design of microbial metabolism to efficiently convert a substrate (when possible, cheap) the desired product. With the further development of genomics and -omics analysis and advanced modeling tools in the field of systems biology, it has become possible to perform very detailed phenotypic characterization of

microorganisms that can serve as efficient cell factories for the production of fuels and chemicals [3].

In this context, the biorefinery concept arises and it is defined by the IEA Bioenergy Task 42 "Biorefineries" as "the sustainable processing of biomass into a spectrum of marketable products and energy" (http://www.biorefinery.nl/ieabioenergy-task42/) (Figure 1). In a biorefinery, plant based feedstock such as sugarcane, corn, starch and wood biomasses are converted into their building blocks (carbohydrates, proteins, triglycerides…) that are subsequently used by microorganisms to produce biofuels, power and chemicals through their fermentative metabolism. This concept is analogous to today's petroleum refinery, which produces multiple fuels and products from petroleum [4].

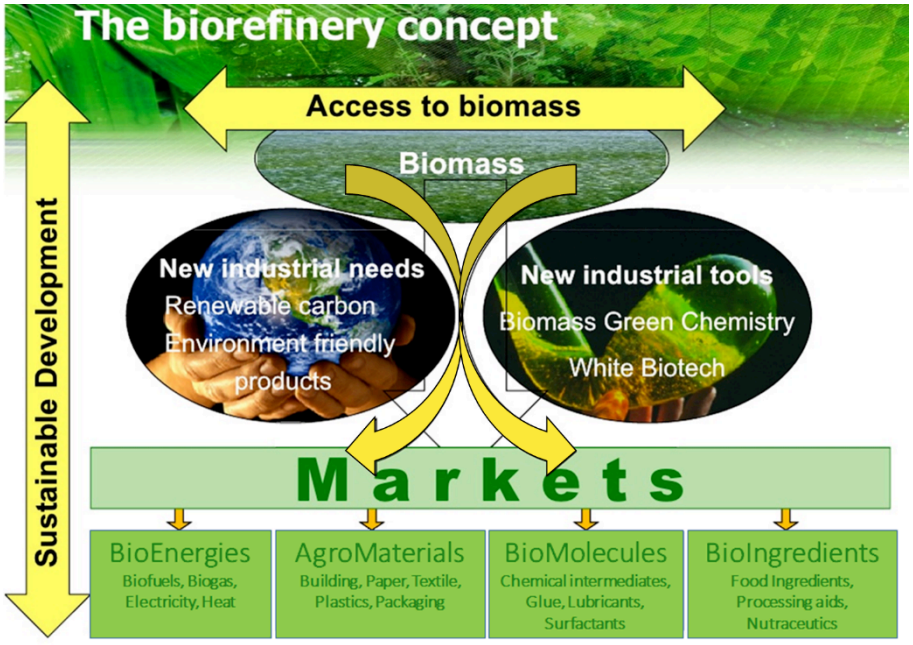

Figure 1: A schematic representation of the biorefinery concept. (BioMotion Congress Hannover 12 Nov. 2009 Biofuels in France from 1st to 2nd generation within a biorefinery strategy

Dr. Fabien DAURIAC Chambers of Agriculture of Picardy People, Plants, forever. France - Biomotion partner IAR - Competitiveness Cluster with a Worldwide Vocation).

This technological platform presents the inherent advantages of a clean process that can minimize wastes and CO_2 generation and can optimize the use of resources [5].

There are several examples of how the fuel and chemical industry is trying to develop novel bioprocesses that can change the primary feedstock from oil to agricultural-based products.

With regards to biofuels, they can be divided into primary and secondary biofuels. The latter can be categorized into three generations: first, second and third generation on the basis of different parameters, such as the type of processing technology, type of feedstock or their level of development (Figure 2) [6].

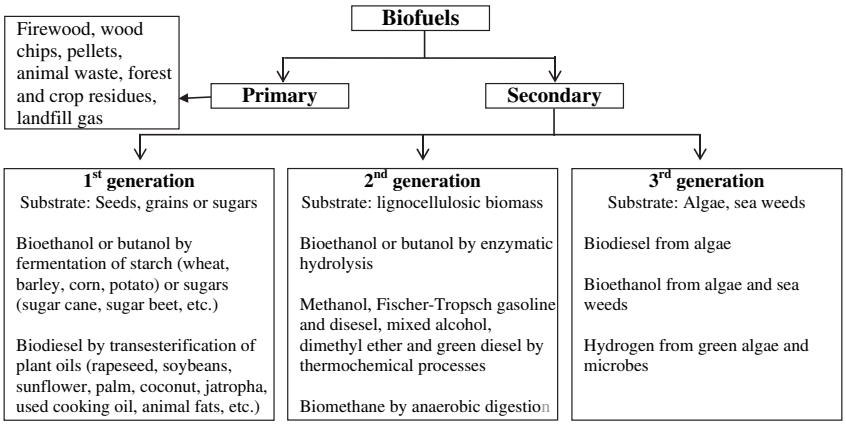

Figure 2: Classification of biofuels [6].

The first-generation liquid biofuels are the type of liquid fuels generally produced from sugars and grains or seeds and requires a relatively simple

process to produce the finished fuel product. The most well known first-generation biofuel is ethanol made by fermenting sugar extracted from crop plants and starch contained in maize kernels or other starchy crops. Biodiesel produced from straight vegetable oils of oleaginous plants by transesterification processes or cracking is another well known first-generation biofuels. First-generation fuels are being produced in significant commercial quantity in a number of countries. The viability of the first-generation biofuels production is, however, questionable because of the conflict with food supply. This limitation favours the search of non-edible biomass for the production of biofuels [6]. In addition, the intensive use of land with high fertilizer and pesticide applications and water use can cause significant environmental problems [7].

The advent of second generation biofuels is intended to produce fuels from lignocellulosic biomass, the woody part of plants that do not compete with food production. Sources include agricultural residues, forest harvesting residues or wood processing waste such as leaves, straw or wood chips as well as the non-edible components of corn or sugarcane. In particular, Dupont has entered into a joint venture with British Petroleum (BP), Butamax, on developing a bio-based production of butanol as a sustainable biofuel, and with Danisco for the development of a second-generation bioethanol production [3].

However, converting the woody biomass into fermentable sugars requires costly technologies involving pre-treatment with special enzymes, meaning that second generation biofuels cannot yet be produced economically on a large scale [7].

Therefore, third generation biofuels derived from microalgae are considered to be a viable alternative energy resource that is devoid of the major drawbacks associated with first and second generation biofuels. Microalgae

are able to produce 15–300 times more oil for biodiesel production than traditional crops on an area basis. In particular, ExxonMobil has entered into a joint venture with Synthetic Genomics to develop a novel microalgae-based process for the production of biodiesel [3]. Furthermore compared with conventional crop plants, which are usually harvested once or twice a year, microalgae have a very short harvesting cycle (≈1– 10 days depending on the process), allowing multiple or continuous harvests with significantly increased yields [7]. Moreover, the proteins, which are the major component of microalgae, could be converted into biofuels or biochemical products [8].

Regarding chemicals, table 1 lists a number of potential and current bulk chemicals that can be produced from biomass, together with some of the major players and alliances involved in the development and production from biomass resources. For each chemical, the market type is also indicated: either an existing or an emerging market [9].

Chemical	Market type	Market size ($Mt\,y^{-1}$)[a]	Major player(s)	Feedstock
acetic acid	existing	9.0	–	ethanol
acrylic acid	existing	4.2	Arkema, Cargill/Novozymes	glycerol or glucose
C_4 diacids	emerging	(0.1–0.5)	BASF/Purac/CSM, Myriant	glucose
epichlorohydrin	existing	1.0	Solvay, DOW	glycerol
ethanol	exisiting	60	Cosan, Abengoa Bioenergy, ADM	glucose
ethylene	existing	110	Braskem, DOW/Crystalsev, Borealis	ethanol
ethylene glycol	existing	20	India Glycols, Dacheng Industrial	glucose or xylitol
glycerol	existing	1.5	ADM, P&G, Cargill	vegetable oil
5-hydroxymethylfurfural	emerging	–	–	glucose/ fructose
3-hydroxypropionic acid	emerging	($\geq$0.5)	Novozymes/Cargill	glucose
isoprene	existing/ emerging	0.1 (0.1–0.5)	Danisco/Goodyear	glucose
lactic acid	existing/ emerging	0.3 (0.3–0.5)	Cargill, Purac/Arkema, ADM, Galactic	glucose
levulinic acid	emerging	($\geq$0.5)	Segetis, Maine Bioproducts, Le Calorie	glucose
oleochemicals	existing	10–15	Emery, Croda, BASF, Vantage Oleochemicals	vegetable oil/fat
1,3-propanediol	emerging	(0.1–0.5)	Dupont/Tate & Lyle	glucose
propylene	existing	80	Braskem/Novozymes	glucose
propylene glycol	existing/ emerging	1.4 ($\geq$2.0)	ADM, Cargill/Ashland, Senergy, Dacheng Industrial	glycerol or sorbitol
polyhydroxyalkanoate	emerging	(0.1–0.5)	Metabolix/ADM	glucose

Table 1: Overview of chemicals that are currently produced, or could be produced, from biomass together with their respective market type, size of the market, and potential biomass feedstock. Major players involved are also given [9].

[a] Market size of an existing market is given as its current size including production from fossil resources; for emerging markets the expected market size is reported in parenthesis.

The current research activities are focused on different relevant aspects for the implementation of biorefinery processes, such as optimization of the raw materials exploitation, valorisation of biomasses and the engineering of cell factories characterized by high rate of production, productivity and improved stress resistance. This in turn will allow to extend the array of products from biofuels to chemicals, possibly catching the final goal to substitute the oil

refinery with efficient and viable biorefineries. This is why increasing attention is given to the production of product other than biofuels from biomass and to the full utilization of said biomass, including side-stream wastes that still have high potential of bioconversion.

In this view, the present study has the aim to offer some examples about the utilization of different types of biomass feedstock and the optimization of a cell factory for the production of chemicals and biofuels. In particular, it is reported the use of glucose (representative of plant-derived sugars) and glycine (representative of aminoacids derived from industrial proteinaceous side stream) as renewable substrates for the respectively production of lactic acid and butanol and isobutanol, by the exploitation of *Saccharomyces cerevisiae* as cell factory.

1. Chemical: Lactic acid

Lactic acid (hydroxypropanoic acid) is a monocarboxylic acid discovered in 1780 by Carl Wilhelm Scheele, a Swedish chemist that isolated it in the form of dense brown liquid from milk. Lactic acid has a long history in the food industry for its application as an acidulant, flavoring agent, pH buffering or preservative [10]. It is also used as an additive in animal feed, in detergents and in pharmaceutical preparations. In the cosmetic field, the lactic acid can be used as a moisturizing agent, anti-acne, anti-tartar, and to brighten and rejuvenate the skin [10]. Furthermore, the presence of both carboxylic and hydroxyl groups in the lactic acid molecule enables its conversion into different technologically useful chemicals such as pyruvic acid, acrylic acid, 1,2-propanediol and lactate ester via chemical and biotechnological routes [11, 12, 13, 14], making it a primary chemical platform. However, the most interesting application from an environmental point of view, is the production

and the application of its derivative polylactic acid (PLA), since such biopolymer could replace traditional petrochemical-based plastic.

1.1 PolyLactic Acid (PLA)

Biopolymers are a wide and interesting class of materials that can replace in different applications the traditional plastics. Nowadays, the attention of both academic and industrial research is focused on their expanding market. Several restrictive measures concerning the use of conventional plastics have been issued by several states. One of the most important proposal comes from Japan, which promulgated the Biomass Nippon Strategy, a law that aims to replace by 2020, 20% of traditional plastics (about 2.5 / 3 million tons per year) with polymers derived from renewable resources (www.jbpaweb.net, Japan Bioplastic Association). At the European level in 2008, the European Commission Lead Market Initiative created the Ad-hoc Advisory Group for Bio-based products for the development of materials bio-based, including biopolymers, with the aim to suggest initiatives for promoting their introduction on the market. In addition, the US federal government has announced a directive important policy (the Federal Green Procurement), which designates products made from bio-based plastics as a preferred purchase. As shown by the data published recently in a joint study by the European Bioplastics and the Institute of Bioplastics and Biocomposites (Figure 2), the result of this combination of factors has led to a growing market of biopolymers.

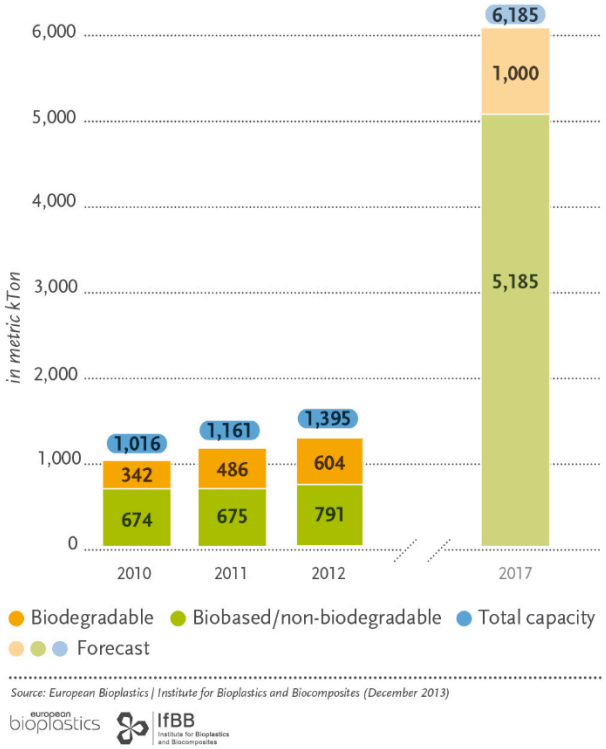

Figure 2: **Global production capacities of bioplastics** (http://en.european-bioplastics.org/).

Among the biopolymers, polyhydroxyalkanoates (PHA), a family of biopolyesters with different structures, are of considerable interest for their potential industrial applications and they are also the only bioplastics completely synthesized by microorganisms [15, 16]. However, as shown in Table 1 a market for this biopolymer does not yet exist. Conversely, polylactic acid (PLA) is now considered one of the most promising biopolymers thanks to its many industrial applications. In fact, it is used as a material for packaging, in the textile industry, and also in the biomedical field since it is biocompatible with living tissues (it is used in the production of suture threads and capsules for drugs) [17, 18]. The world leader in the production of PLA, marketed under the name of NatureWorks ©, is Cargill

USA, with a plant in Nebraska capable of producing 140,000 t/year (www.natureworksllc.com), but other production facilities are located, as well as in North America, in Europe and Asia.

The properties of PLA are closely linked to the presence of the D and L isomers of lactic acid. The polymer containing only the L-isomer is a semicrystalline material, rigid, with a high melting temperature (173-178 ° C), while the polymer containing both the L- and D-isomer presents an amorphous structure. Its properties can also be modified by the addition of plasticizers, fillers and other additives. The growing demand for this biopolymer has stimulated the development of industrial processes aimed at the production of lactic acid that is about 275,000 tons per year (www.essentialchemicalindustry.org). As previously mentioned, it is extremely important to obtain the acid in its enantiomerically pure forms; therefore, lactic acid is mainly produced by fermentation, where enzymes can ensure the sole production of the desired enantiomer. The chemical synthesis of lactic acid, based on the hydrolysis of acid lactonitrile, in fact leads to the obtaining of the racemic mixture. Currently, lactic acid bacteria (LAB), in particular *Lactobacillus* strains, are the microorganisms traditionally used for the lactic acid fermentation [10, 19]. Since they have several disadvantages (Chapter 1, Introduction), the attention is focusing on alternative microorganisms, among which *S. cerevisiae*.

Although the lactic acid required for the synthesis of PLA is mainly produced by fermentation, the current polymerization process occurs exclusively chemically. In particular, PLA has been principally produced by a multistep process including a production and an isolation of intermediate lactide, the cyclic dimer of lactic acid, followed by its ring-opening polymerization (ROP) catalyzed by organometal catalysts. The direct condensation process, instead, has been studied for many years by many scientists, but no one has

ever succeeded in obtaining a polylactic acid with a high enough molecular weight and useful properties [20]. The new challenge is therefore the production of PLA directly in microorganisms. Yang (2009) reported for the first time that PLA and its copolymers containing various lactate fractions can be produced in recombinant *E. coli* by establishing heterologous pathways employing evolved *Clostridium* propionicum propionate CoA transferase (Pct) and *Pseudomonas sp*. MBEL 6- 19 polyhydroxyalkanoate (PHA) synthase 1 [21].

2. Biofuels: Butanol and Isobutanol

The current gasoline-supplementing biofuel in use today is ethanol, of which the production in the world reached 23 billion gallons in 2013 (http://ethanolrfa.org/pages/World-Fuel-Ethanol-Production). Ethanol fermented from starch or sugar feedstocks is commonly added as a component to gasoline to control combustion and increase the octane rating of the fuel. High percentage blends of ethanol with gasoline such as E85 are also available, although slight modifications need to be made to conventional gasoline engines. Although ethanol provides the first model for biofuel commercialization, its reduced energy density (~70% of gasoline) and incompatibility with the current fuel infrastructure due to its high hygroscopicity and corrosiveness provide an opportunity for refinement. In addition to gasoline, renewable fuel replacements for diesel and jet fuel are also of great importance.

Petroleum-derived diesel is currently supplemented or replaced with biodiesel, which is typically made by the transesterification of waste oil and fat triglycerides with a short chain alcohol such as methanol to form fatty acid methyl esters (FAME). Although biodiesel shows promise in its ability to

power diesel engines, its portability and solvent properties remain to be improved [22].

To overcome those limitations, researchers are trying to turn biomass into more complex alcohols than ethanol, which can be either placed directly in the fuel tank or slotted into the processing chain in existing refineries. A said "higher alcohol", a molecule with more carbon and hydrogen atoms than ethanol such as butanol and isobutanol, seem to come closer to the ideal biofuel [23]. Butanol and isobutanol present several advantages compared to ethanol, reviewed in [22, 23, 24]:

- They have a higher energy content given by the higher number of carbons and hydrogens and consequently by the higher number of CH bonds, site where the useful energy is stored (Figure 3);
- They are compatible with the current infrastructure as they are less hygroscopic corrosive;
- They can be used not only as an additive to gasoline but also as a fuel by itself in conventional engines;
- Butanol (or isobutanol) might also be cheaper to make than ethanol. When a batch of yeast produces ethanol the alcohol comes out mixed with water. The water has to be boiled off, which means using more energy to produce the fuel. Butanol (or isobutanol) and water don't mix, so they can be separated by less energy-intensive processes.

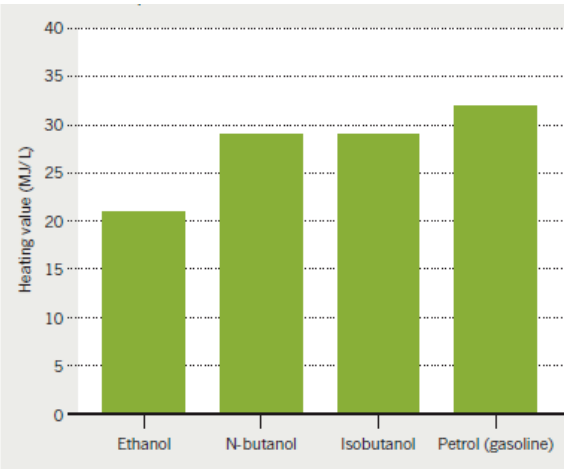

Figure 3: Biofuels energy density [23].

Several companies are trying to commercialize butanol or isobutanol production from biomass. In December 2010, the biotech company Green Biologics, of Abingdon, United Kingdom, announced a deal to provide its fermentation technology, based on a *Clostridium* strain, to two Chinese biochemical companies. Butamax Advanced Biofuels has opened a demonstration plant in Hull, United Kingdom. And Gevo, an advanced biofuels company in Englewood, Colorado, is converting an ethanol production facility in Minnesota to produce isobutanol [23].

Although *Clostridia* are still the basis of the butanol production process, these microorganisms have strong limitations as a low tolerance to the product, the final cell differentiation in spores and the need to grow in total anaerobic conditions. In addition, the complex genetic manipulation makes the optimization process difficult [22, 25, 26]. These limitations have led to focus the attention on alternative microorganisms, among which *S. cerevisiae* [27].

3. *Saccharomyces cerevisiae* as cell factory

With the further development of genomics and omics analyses and advanced modeling tools in the field of systems biology, it has become possible to perform very detailed phenotypic characterization of microorganisms that can serve as efficient cell factories for the production of fuels and chemicals. Yeasts, and in particular *Saccharomyces cerevisiae* is a very attractive cell factory. The vast knowledge on this organism (it was the first eukaryote to have its genome completely sequenced [28]) combined with the robustness of this organism to harsh industrial conditions makes it a preferred organism for production of many fermentation derived products. Compared to *E. coli*, which is widely used in academia and in industry as well, yeast cannot be contaminated by phages. It is very osmo-tolerant and can hence tolerate very high sugar concentrations, and it tolerates a lower pH than most bacteria [29]. *S. cerevisiae* is recognized by the American Food and Drug Administration as an organism generally regarded as safe (GRAS) (FDA, URL: www.fda.gov/default.html), it does not produce toxins harmful for humans and has been used safely for centuries in the brewing and baking industries. For these reasons it is one of the most widely used microorganisms for the production of many natural and recombinant compound of biotechnological interest [5,29] (Figure 4).

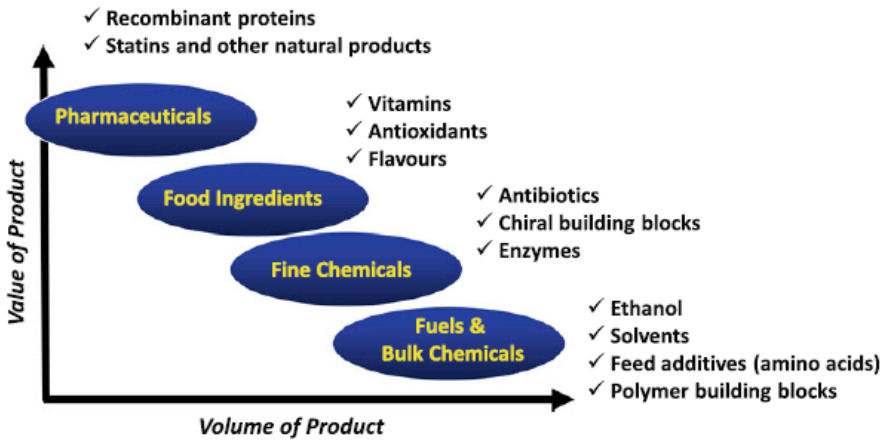

Figure 4: Biotech products range from high-value-added to low-value added products, with the latter being produced in large quantities and the former in small quantities. *S. cerevisiae* is used for the production of products in the whole spectrum [29].

Therefore, the yeast cells, and in particular *S. cerevisiae* is one of the best platforms to produce a number of different biochemicals and biofuels [3].

In particular, in the chapters 1 and 2 the tolerance to lactic acid and its production in *S. cerevisiae* laboratory and industrial strains, respectively, are discussed.

It is pointed out as the cofactor engineering is an additional tool to achieve desired metabolic engineering goals. In fact, the manipulation of SAM (S-adenosyl methionine, or AdoMet), a central cofactor of cell metabolism, has a strong impact on tolerance and lactic acid production. Moreover, lactic acid effects on the main classes of biomolecules are highlighted. The data obtained, never elucidated before, thus constitute a starting point for potential future metabolic engineering. Specifically, it is shown how changes in membrane lipid composition, by *OPI1* gene deletion, can increase tolerance to lactic acid.

Chapter 3 shows a possible valorization of the fraction of proteins that accumulates as a waste product in different microbial productions and currently is not totally absorbed by the market. The attention is indeed focused on the endogenous production of promising biofuel, butanol and isobutanol, starting from glycine in *S. cerevisiae*.

Chapters 1 and 3 are based on the published works (reported as such as appendix) but have been revised to include additional and novel experiments that do not appear in the papers, while chapter 2 is novel and currently under final preparation for submission.

REFERENCES

1. Christensen CH, Rass-Hansen J, Marsden CC, Taarning E, Egeblad K: **The renewable chemicals industry.** *ChemSusChem.* 2008, **1**(4):283-9.

2. Dellomonaco C, Fava F, Gonzalez R: **The path to next generation biofuels: successes and challenges in the era of synthetic biology.** *Microb Cell Fact*. 2010, **9**:3.

3. Hong KK, Nielsen J: **Metabolic engineering of *Saccharomyces cerevisiae*: a key cell factory platform for future biorefineries.** *Cell Mol Life Sci*. 2012, **69**(16):2671-90.

4. Cherubini F: **The biorefinery concept: Using biomass instead of oil for producing energy and chemicals.** *Energy Conversion and Management* 2010, **51**(7):1412–1421

5. Branduardi P, Smeraldi C, Porro D: **Metabolically engineered yeasts: 'potential' industrial applications.** *J Mol Microbiol Biotechnol.* 2008, **15**(1):31-40.

6. Nigam PS, Singh A: **Production of liquid biofuels from renewable resources**. *Prog. Energy Combust. Sci*. 2010, **37**(2011): 52-68.

7. Dragone G, Fernandes B, Vicente AA, Teixeira JA: **Third generation biofuels from microalgae** A Mendez-Vilas (Ed.), Current research, technology and education topics in applied microbiology and microbial biotechnology (Microbiology Book Series 2), Formatex, Badajoz 2010, 1355–1366.

8. Huo YX, Cho KM, Rivera JG, Monte E, Shen CR, Yan Y, Liao JC: **Conversion of proteins into biofuels by engineering nitrogen flux.** *Nat Biotechnol.* 2011, **29**(4):346-51.

9. Vennestrøm PN, Osmundsen CM, Christensen CH, Taarning E: **Beyond petrochemicals: the renewable chemicals industry.** *Angew Chem Int Ed Engl.* 2011, **50**(45):10502-9.

10. Wee YJ, Kim JN and Ryu HW: **Biotechnological Production of Lactic Acid and Its Recent Applications.** *Food Technol. Biotechnol.* 2006, **44**(2):163–172.

11. Sauer M, Porro D, Mattanovich D, Branduardi P: **Microbial production of organic acids: expanding the markets.** *Trends Biotechnol* 2008, **26**:100–108. 3.

12. Sauer M, Porro D, Mattanovich D, Branduardi P: **16 years research on lactic acid production with yeast - ready for the market?** *Biotechnol Genet Eng Rev* 2010, **27**:229–256.

13. Gao C, Ma C, Xu P: **Biotechnological routes based on lactic acid production from biomass.** *Biotechnol Adv* 2011, **29**:930–939.

14. Fan Y, Zhou C, Zhu X: **Selective catalysis of lactic acid to produce commodity chemicals.** *Catal Rev* 2009, **51**:293–324.

15. Chen GQ, Patel MK: **Plastics derived from biological sources: present and future: a technical and environmental review.** *Chem Rev.* 2012, **112**(4):2082-99.

16. Matsumoto K, Taguchi S: **Enzyme and metabolic engineering for**

the production of novel biopolymers: crossover of biological and chemical processes. *Curr Opin Biotechnol.* 2013, **24**(6):1054-60.

17. Albertsson AC, Varma IK: **Recent developments in ring opening polymerization of lactones for biomedical applications.** *Biomacromolecules* 2003, **4**(6):1466-862003.

18. Doi S, Clark JH, Macquarrie DJ, Milkowski K: **New materials based on renewable resources: chemically modified expanded corn starches as catalysts for liquid phase organic reactions.** *Chem Commun (Camb)* 2002, (**22**):2632-32002.

19. Datta R, Henry M: **Lactic acid: recent advances in products, processes and technologies — a review.** *J Chem Technol Biotechnol* 2006, **81**:1119–1129.

20. Rasal RM, Janorkar AV,Hirt DE: **Poly(lacticacid) modifications**. *Prog Polym Sci.* 2010, **35**:338–356.

21. Yang TH, Kim TW, Kang HO, Lee SH, Lee EJ, Lim SC, Oh SO, Song AJ, Park SJ, Lee SY: **Biosynthesis of polylactic acid and its copolymers using evolved propionate CoA transferase and PHA synthase.** *Biotechnol Bioeng.* 2010, **105**(1):150-60.

22. Connor MR, Liao JC: **Microbial production of advanced transportation fuels in non-natural hosts.** *Curr Opin Biotechnol.* 2009, **20**(3):307-15.

23. Savage N: **Fuel options: The ideal biofuel**. *Nature* 2011, **474**:S9–S11.

24. Lee SY, Park JH, Jang SH, Nielsen LK. Kim J, Jung KS: **Fermentative butanol production by Clostridia.** *Biotechnol. Bioeng.* 2008, **101**(2):209–228.

25. Zheng YN, Li LZ, Xian M, Ma YJ, Yang JM, Xu X, He DZ: **Problems with the microbial production of butanol.** *J Ind Microbiol Biotechnol.* 2009, **36**(9):1127-38.

26. Yan Y, Liao JC: **Engineering metabolic systems for production of advanced fuels.** *J Ind Microbiol Biotechnol*. 2009; **36**(4):471-9.

27. Branduardi P, de Ferra F, Longo V, Porro D: **Microbial *n*-butanol production from Clostridia to non-Clostridial hosts.** *Eng Life Sci* 2014, **14**:16–26.

28. Goffeau A, Barrell BG, Bussey H, Davis RW, Dujon B, Feldmann H, Galibert F, Hoheisel JD, Jacq C, Johnston M, Louis EJ, Mewes HW, Murakami Y, Philippsen P, Tettelin H, Oliver SG: **Life with 6000 genes.** *Science* 1996, **274**(5287):546, 563-7.

29. Hong KK and Nielsen J: **Recovery of phenotypes obtained by adaptive evolution through inverse metabolic engineering**. *Appl Environ Microbiol* 2012, **78**(21):7579-86.

CHAPTER 1

Changes in *SAM2* expression affect lactic acid tolerance and lactic acid production in *Saccharomyces cerevisiae*

INTRODUCTION

As discussed in the Introduction, lactic acid can be used for several industrial applications. Initially, the natural producers, lactic acid bacteria (LAB) were the "bio-catalysts" of choice for industrial lactic acid fermentations [1, 2]. However, LAB have complex nutrients requirements and are inhibited by the product, especially at low pH. Indeed, the most relevant bottleneck in lactic acid production by LAB is in all likelihood relates to the inhibitory effects of the low pH of the medium on cell growth, cell viability and in turn on lactic acid accumulation. Indeed, large amounts of $CaCO_3$ must be added during fermentation, to maintain a constant pH of the culture broth (at around 5) and sustain production. Under these conditions the final product is lactate, since the pKa of lactic acid is 3.86. This in turn increases the operation costs for separation and purification of the desired product, which is actually the free acidic form [3, 4, 5], therefore requiring the acidification of the spent medium at the end of the fermentation.

The use of naturally low-pH tolerant organisms, such as yeasts, represents an alternative production route. In 1994 Dequin and Barre [6] first described a metabolically engineered *Saccharomyces cerevisiae* strain expressing a heterologous L-lactate dehydrogenase, obtaining a hetero-fermentative strain producing both ethanol and lactic acid. Since then, many improvements have been obtained along the years. Among them, (*i*) the deletion of pyruvate decarboxylase gene(s) to avoid ethanol production and increase production, productivity and yield of lactic acid [7, 8, 9], (*ii*) the increased yields thanks to the effect of different *S. cerevisiae* backgrounds and heterologous L-lactate dehydrogenases [10], (*iii*) the development of high-producing strains following classical selection methods, by direct exposure of the cells to the stressor, and indirect screenings by sorting the

cells on the basis of tolerance-related traits like the capability to keep an higher intracellular pH [11, 12], and (*iv*) the effect of overexpression of the genes encoding for two hexose transporters (e.g. *HXT1* and *HXT7*) on glucose uptake and lactic acid productivity and production [13]. Metabolically engineered *S. cerevisiae* strains were also characterized for their energetic balance, showing that lactate production does not contribute to the net ATP production probably due to energy utilization for lactate export [14]. Recently, metabolically engineered yeast came on the market for lactic acid production (NatureWorks®) [15].

In spite of their ability to produce high levels of lactic acid at low pH, the presence of the undissociated weak acid in the growth medium imposes a high degree of stress also to the yeast cells [16, 17, 18, 19, 20]. The cell membrane is, in fact, selectively permeable to small polar and to hydrophobic molecules, like undissociated weak organic acids, which can cross it by passive diffusion following their gradient [21]. Because of the relatively high intracellular pH value, weak acids dissociate once into the cytoplasm, releasing H^+ and the corresponding anion. Accumulation of both species has detrimental effects on cells, ranging from lowering of intracellular pH and inhibition of metabolic activities, to interference with lipid organization and membrane permeability/functions and induction of oxidative stress and cell death (reviewed in [17, 18]), among others. Therefore, during detoxification, the protons are expelled via the H^+-ATPase pump and the anions via active export systems (or metabolized), consuming huge amounts of energy. There is no surprise then in finding that membrane lipids and proteins are among the first targets of modification induced by some specific stresses [22, 23, 24, 25, 26].

Stress responses induce a complex cellular reprogramming. Classically, most metabolic engineering studies have focused on enzyme levels and on

the effect of the amplification, addition, or deletion of a particular pathway directly linked with the product of interest. However, the current status of metabolic engineering is still hindered by the lack of our full understanding of cellular metabolism. Indeed, the complex aspects of integrated dynamics and overall control structure are the common obstacles for the optimal design of pathways to achieve a desired goal. Since cofactors are essential to a large number of biochemical reactions, their manipulation is expected to have large effects on metabolic networks. It is conceivable that cofactor availability and the proportion of cofactor in the active form may be critical in dictating the overall process yield. It has already been shown that cofactors play a major role in the production of different fermentation products (such as D-(-)-2,3-butanediol [27]). Furthermore, changes in cofactor pools induce changes at the transcriptional level as well as at the enzyme levels [28].

SAM (S-adenosyl methionine, or AdoMet) is a central coenzyme in the metabolism that participates to a very high number of reactions [29]. In particular it functions as a donor of methyl groups to proteins, lipids, nucleic acids, vitamin B12 and others by SAM-dependent methyltransferases; it is also a precursor molecule in the aminopropylation and transulfuration pathways [30] and it regulates the activities of various enzymes. SAM has a role in the modelling of the plasma membrane structure, since it donates three methyl groups during the synthesis of phosphatidylcholine (PC) from phosphatidyl-ethanolamine (PE). Malakar *et al*. [31] demonstrated a protective role of externally added SAM in *S. cerevisiae* cells growing under inorganic acid (HCl) stress, which they associated to the measured increase in PC:PE ratio and to the higher activity of the proton pump Pma1p. Moreover, SAM displays an anti-apoptotic role, acting as an indirect scavenger of reactive oxygen species (ROS) via enhancement of glutathione biosynthesis [32].

We therefore focused our attention on SAM-synthetase which catalyses the only known reaction that, starting from L-methionine (Met) and ATP, leads to the biosynthesis of SAM [33, 34, 35]. Notably, *S. cerevisiae* has two distinct SAM-synthetase genes, named *SAM1* and *SAM2*, which arose from gene duplication [36, 37] and share a high degree of similarity (83% identity in the ORF, 92% in the translated sequence) [37]. Although *SAM1* and *SAM2* have at least partially overlapping functions, their regulation is different. Both genes undergo feedback repression by SAM, like other genes of the sulfur aminoacids metabolism, but the expression of *SAM2* also increases during growth, in a Sam2p-dependent manner [38]. Remarkably, *SAM2* is repressed after the addition of myoinositol and choline, suggesting that Sam2p, but not Sam1p, is involved in phospholipid biosynthesis [39]. It can be therefore hypothesized that Sam2p is involved in this process also during lactic acid stress.

In this work, the expression and localization of Sam2p under lactic acid treatment were evaluated. To assess the role of this protein during lactic acid stress, *SAM2* was both overexpressed and deleted in *S. cerevisiae* laboratory strains. Moreover, when *SAM2* was deleted in the engineered and evolved homolactic acid producing strain CEN.PK m850 [12], higher lactic acid productivity and production were obtained.

Remarkably, this study also showed how *SAM2* localization can be affected by growing conditions. At the moment, we have not enough elements to draw functional hypothesis, but surely the data obtained opens novel doors for future investigations.

RESULTS

Sam2p as a putative responsive element to lactic acid stress

Based on the reported beneficial effects of SAM during inorganic acid (HCl) stress [31] and its involvement in membrane remodelling, the protein levels of Sam2p are evaluated by western blot analysis during lactic acid exposure. A chromosomal tagging approach by which the GFP coding sequence was fused in frame to the C-terminal coding region of the endogenous copy of the SAM2 gene has been applied (see Methods). The SAM2GFP strain was created in the CEN.PK 113-11C background, a robust *S. cerevisiae* reference strain, and also in the BY4741 background, commonly used for functional genetic studies (EUROSCARF collection http://web.uni-frankfurt.de/fb15/ mikro/euroscarf/). The BY4741 *SAM2*GFP and CEN.PK *SAM2*GFP strains were grown in minimal medium with 2% w/v glucose in the absence and in the presence of different concentrations of lactic acid (pH 5, pH 3, 12 g/L and 20 g/L lactic acid at pH 3) and Sam2p levels were estimated using an anti-GFP antibody at 16 and 40 hours after inoculation, respectively corresponding to the exponential and the early stationary phase of growth. The biomass accumulation and the growth phase among the different conditions within the same genetic background were similar, for each time point considered. As control, β-actin levels were also detected.

Two analyses were run in parallel: in the first, the total protein fraction was extracted with trichloroacetic acid (TCA); in the second, three sub-fractions resulting from sequential protein extraction were separated: the first containing only soluble proteins, the second containing insoluble proteins solubilized with urea, the third containing highly insoluble proteins excluded from the second fraction and solubilized with concentrated sodium dodecyl sulfate (SDS) (see Methods for details).

Figure 1 shows the western blots of the TCA extracts for CEN.PK (panel A) and BY (panel B) strains. Remarkably, in both strains the signal intensity of Sam2p-GFP increased in the presence of lactic acid, particularly in the BY strain (see panels B).

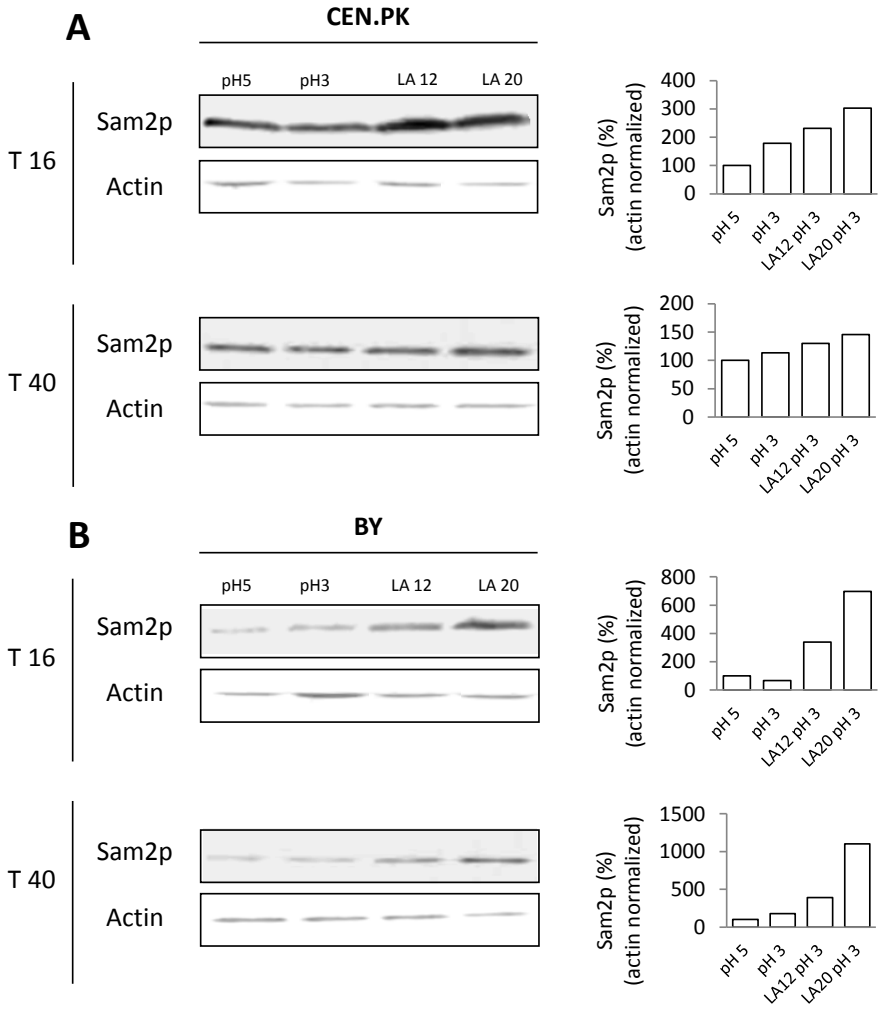

Figure 1: Western blot analysis of total Sam2p levels in cells grown in the absence and presence of lactic acid. CEN.PK 113-11C (**panel A**) and BY4741 SAM2GFP (**panel B**) cells were grown in shake flasks in minimal (YNB) medium with 2% w/v glucose without or with the addition of

different concentrations of lactic acid (pH 5, pH 3, 12 g/L and 20 g/L lactic acid at pH3) and the Sam2p-GFP levels were evaluated after 16 and 40 hours after inoculation in the total protein fraction, extracted with TCA, using an anti-GFP antibody. Samples were normalised according to cell number. β-actin levels have been detected as control. Bands have been quantified by ImageJ 1.48 software. Histograms refer to the ratio (%) of Sam2p/Actin normalized to the values at pH 5. LA: lactic acid.

Noteworthy, Sam2p was found in all the three protein sub-fractions after sequential extraction. Figure 2 shows the western blots obtained for CEN.PK. At 16 h, the signals detected in the soluble protein fractions were rather similar among the different conditions, thus the protein increase of the lactic acid samples was mainly ascribable to the highly insoluble protein fractions and to a lesser extent to the fractions solubilised with urea. This was also true for lactic acid samples collected at 40 h, when slight enrichments were also found in the native extracts (data not shown).

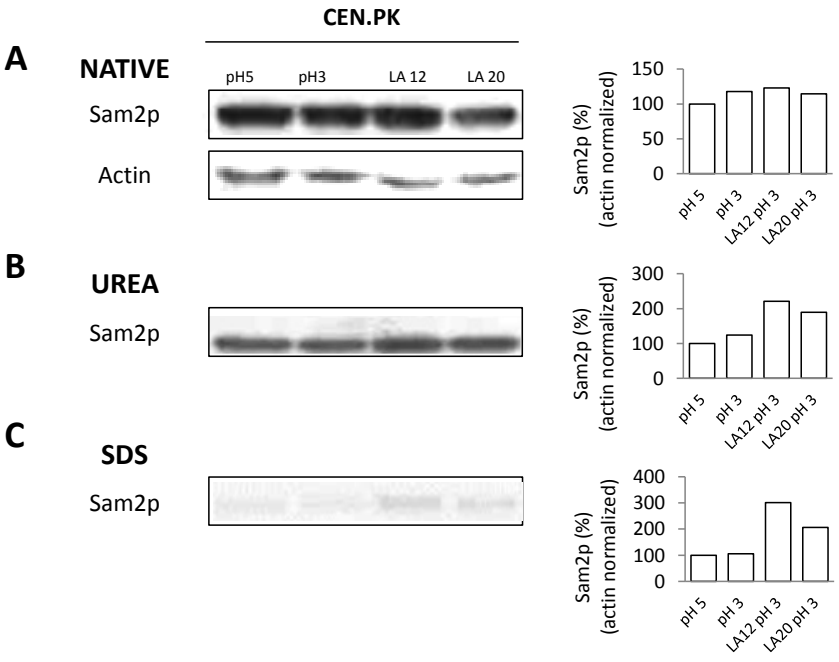

Figure 2: Western blot analysis of the fractions obtained from sequential protein extraction

for the strain CEN.PK 113-11C SAM2GFP. Cells were grown in shake flasks in minimal (YNB) medium with 2% w/v glucose without or with the addition of different concentrations of lactic acid (pH 5, pH 3, 12 g/L and 20 g/L lactic acid at pH3) and then three protein sub-fractions were obtained after sequential extraction in Tris buffer (Native, **A**), 8 M urea (**B**) and 10% SDS (**C**). The Sam2p-GFP levels were evaluated after 16 hours after inoculation using an anti-GFP antibody. Samples were normalised according to cell number. β-actin levels have been detected as control. Bands have been quantified by ImageJ 1.48 software. Histograms refer to the ratio (%) of Sam2p/Actin normalized to the values at pH5. LA: lactic acid.

Overall, lactic acid determined an increase in the total amount of the Sam2p in both yeast backgrounds.

Sam2p localization under stress conditions

The localization of Sam2p is still a matter of debate. In fact, while the LoQate database [40] and Tkach *et al.* [41] report a cytoplasmic localization, the Yeast GFP Fusion Database [42] reports it as ambiguous, the OrganelleDB (A. Kumar's Lab, Life Sciences Institute, University of Michigan; http:// organelledb.lsi.umich.edu/) reports it as unknown and finally the YPL+ Database (Oskolkova, Leitner and Kohlwein, personal communication) describes it as nuclear.

Based on our previous data, therefore, the possible effect of lactic acid exposure on Sam2p-GFP fusion protein localization in the BY4741 *SAM2*GFP and CEN.PK *SAM2*GFP was investigated by fluorescence microscopy. Moreover, the effect of ethanol and high temperature treatments, two other stresses of industrial interest, was also evaluated.

Lactic acid exposure

Yeast cells were grown in the same conditions described above and observed under epifocal microscope at 16 and 40 hours after inoculation. The images of Figure 3, depicting CEN.PK cells, show that the presence of

lactic acid had no significant effects on Sam2p-GFP distribution. At 16 h (upper panels) the signal was diffused into the whole cell, with the exclusion of extended dark areas representing the vacuoles and nuclei (based on DAPI staining, not shown). Therefore, the localization appeared to be mainly cytoplasmatic, although a contingent association with membranes cannot be excluded. At 40 h (bottom panels), instead, discrete spots emerging from the diffused fluorescence signal were visible. A similar situation was observed in BY4741 cells (data not shown). The number and dimensions of these foci were highly variable in all cells, irrespective of whether lactic acid was present or not. Therefore the data reported do not allow additional speculations on their relevance to stress tolerance. The nature of the observed Sam2p *foci*, never reported in literature before, is still unknown, and its biological significance needs to be further investigated.

In conclusion, Sam2p distribution within the cytosol in both yeast strains appeared to change in correlation with the growth phase.

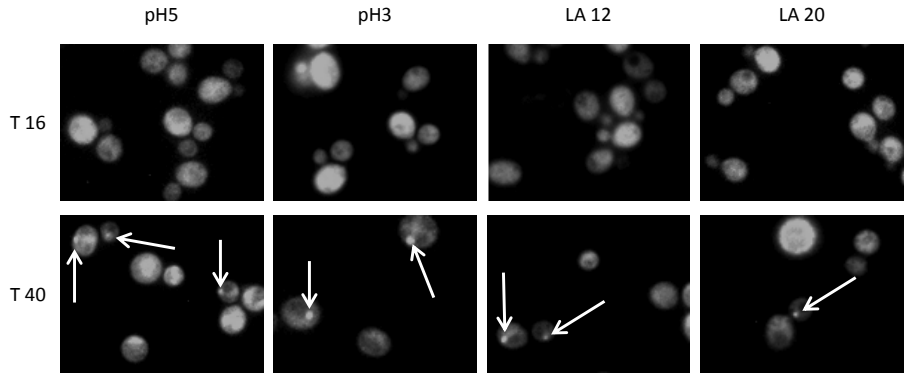

Figure 3: Sam2p-GFP fluorescence distribution during growth in the absence and presence of lactic acid. CEN.PK 113-11C *SAM2*GFP cells were grown in shake flasks in minimal (YNB) medium with 2% w/v glucose without or with the addition of different concentrations of lactic acid (pH 5, pH 3, 12 g/L and 20 g/L lactic acid at pH3). Epifocal microscope images were taken at 16 and 40 hours after inoculation, corresponding to exponential growth phase and early stationary phase,

respectively. Pictures show Sam2p-GFP fluorescence in the green field. White arrows indicate Sam2p-GFP *foci*. LA: lactic acid.

Ethanol stress

To evaluate the effect of ethanol exposure on Sam2p-GFP localization, the cells were grown in minimal medium, until the exponential phase was reached, and then collected and treated or not with 20% ethanol [43]. After 2 hours the cells were observed under epifocal microscope (Figure 4). Similarly to the previous experiment, the cells not exposed to the stressing agent showed fluorescence diffused mainly in the cytoplasm (left panel). On the contrary, the treatment with ethanol led to the formation of Sam2p aggregates (right panel). Furthermore, although also in this case the number of *foci* per cell was quite variable, it appeared to be on average higher than that observed during the stationary phase of growth (Figure 3, lower panel).

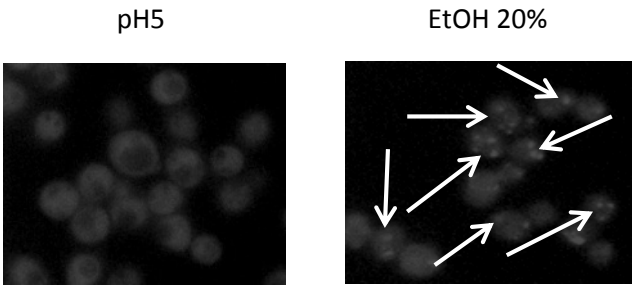

Figure 4: Sam2p-GFP fluorescence distribution in cells stressed or not with ethanol. CEN.PK 113-11C *SAM2*GFP cells were grown in minimal medium until the exponential phase and then collected and treated or not with 20% ethanol. Epifocal microscope images were taken after 2 hours of stressing agent incubation. Pictures show Sam2p-GFP fluorescence in the green field. White arrows indicate Sam2p-GFP *foci.* White arrows indicate Sam2p-GFP *foci.* EtOH: ethanol.

Heat shock

The cells were grown in minimal medium until the exponential phase and then shifted for 2 hours at 46 °C. Figure 5 shows how even heat shock was able to induce Sam2p aggregation (middle panel). The number of *foci* per

cell was variable but they seemed to be generally more numerous and smaller than those observed after ethanol stress. Subsequently, it was examined whether the protein aggregation was reversible. Therefore, the culture underwent shock was re-incubated at the yeast optimum temperature of growth (30 °C) and the cell fluorescence was monitored over time. As can be seen in the right panel, after 3 hours of incubation at 30 °C Sam2p-GFP fluorescence reverted to diffuse throughout the cell.

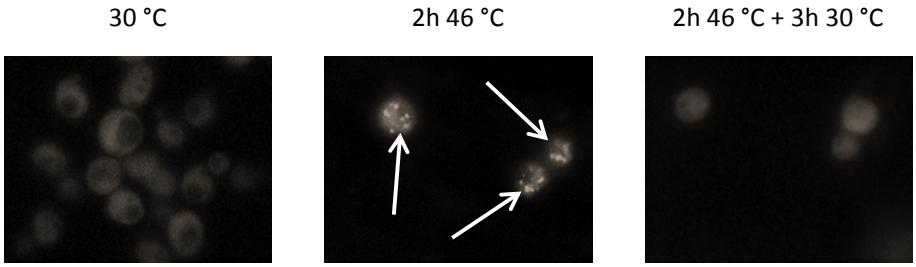

Figure 5: Sam2p-GFP fluorescence distribution in cells heat shocked. CEN.PK 113-11C *SAM2*GFP cells were grown in minimal medium until the exponential phase at 30 °C, control (**left panel**). The cells were then shifted to 42 °C and the epifocal microscope images were taken after 2 hours of incubation (**middle panel**). The cells underwent shock were re-incubated at 30 °C and the epifocal microscope images were taken after 3 hours of incubation (**right panel**). Pictures show Sam2p-GFP fluorescence in the green field. White arrows indicate Sam2p-GFP *foci*.

Overall, the data suggest that Sam2p is probably relocated in a different way in response to diverse stimuli, presumably requiring its function in different and specific pathways, which need to be further investigated. Because of our primary interest in this context to analyze lactic acid tolerance and production, this aspect was further investigated focussing on *SAM2* modulation.

Effect of *SAM2* overexpression and deletion on lactic acid tolerance

The differential accumulation of Sam2p observed by the western blot analysis opens the question about a possible role of this protein during the cellular response to lactic acid stress at low pH. Consequently, the effect of *SAM2* overexpression was examined for growing cells challenged with different concentrations of the stressing agent. The wild type CEN.PK 102-3A and BY4741 strains were transformed with the pTEF-L-SAM2 multicopy plasmid (see Methods), carrying *SAM2* under the control of the strong constitutive *S. cerevisiae* TEF1 promoter. CEN.PK 102-3A and BY4741 cells transformed with the respective empty plasmid were used as controls.

Figure 6 shows the results obtained by cultivation in minimal medium with 2% w/v glucose without or with lactic acid (40 g/L) at pH 3. No remarkable differences were observed between the control and the *SAM2* overexpressing strains during growth without lactic acid at low pH, in both yeast backgrounds (Figure 6A). Lactic acid had a clear negative effect on the growth of all strains, visible in terms of growth delay and lower biomass accumulation (Figure 6B). However, while wild type and *SAM2* overexpressing cells grew similarly in the stressed condition for the CEN.PK background, in the BY background a marked difference between the two strains was observed, where surprisingly the *SAM2* overexpressing strain was much more affected compared to the control.

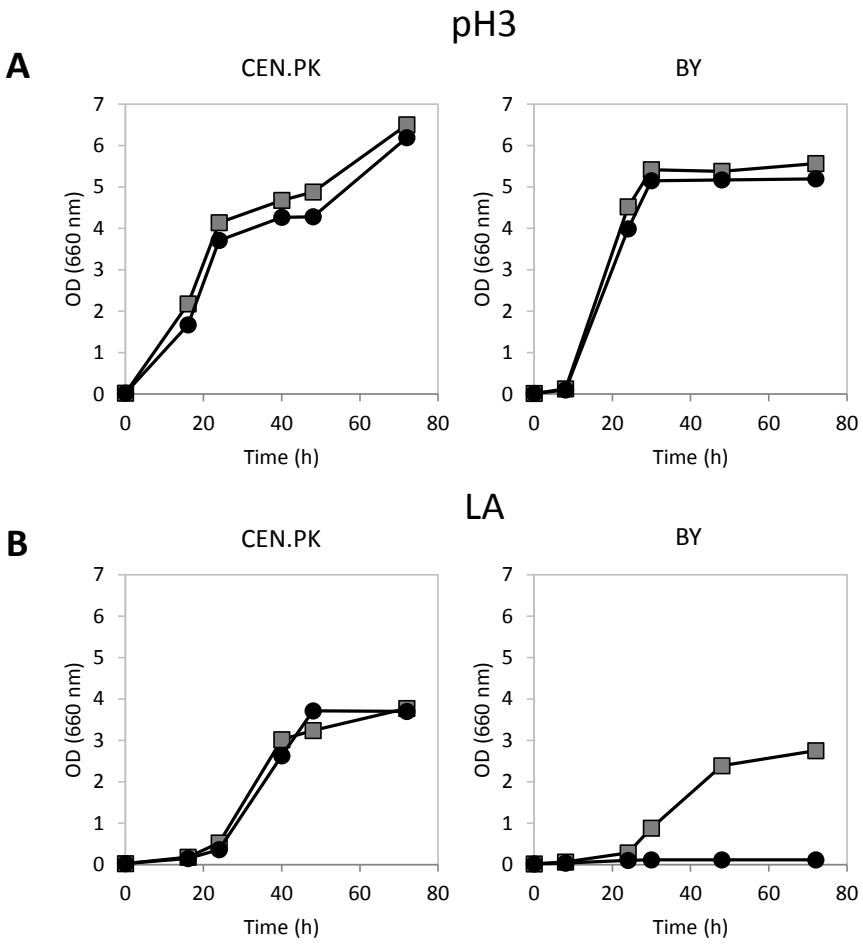

Figure 6: Growth of wild type and *SAM2* overexpressing cells in the absence and presence of lactic acid. Yeast cells were grown in shake flasks in minimal (YNB) medium with 2% w/v glucose at initial pH 3, without (**panel A**) or with (**panel B**) 40 g/l of lactic acid. Growth was determined as OD at 660 nm. Left panels: CEN.PK cells; right panels: BY cells. Dark grey squares: wild type control strains (CEN.PK 102-3A [pTEF-L], BY4741 [pTEF-L]). Black circles: cells overexpressing *SAM2* (CEN.PK 102-3A [pTEF-L-SAM2], BY4741 [pTEF-L-SAM2]).

Since unexpectedly *SAM2* gene overexpression did not help improving lactic acid tolerance in the CEN.PK background and caused severe growth

deficiencies in the BY4741 background, the effect of its deletion was also tested. *SAM2* was deleted in the CEN.PK 102-3A and BY4741 parental strains and in the same strains harbouring the pTEF-L plasmid (the backbone plasmid used for *SAM2* overexpression), complementing the leucine auxotrophy, to allow a direct comparison of all the data.

Figures 7 and 8 show the growth curves obtained, respectively for the parental strains and for the LEU^+ complemented strains. *SAM2* deletion had no effect, in all the tested strains, during growth in minimal medium at low pH (Figures 7A and 8A). When cells were stressed with lactic acid, once more no marked differences were observed in the CEN.PK background between the wild type and the deleted strain (Figures 7B and 8B). Interestingly, the BY4741 parental strain *sam2Δ* turned out to be less sensitive to the stressing agent than the wild type (Figure 7B): the specific growth rate in exponential phase was in fact 45% higher compared to control cells (0.11 ± 0.01 h^{-1} *vs* 0.16 ± 0.01 h^{-1}, mean and SD from three independent experiments).

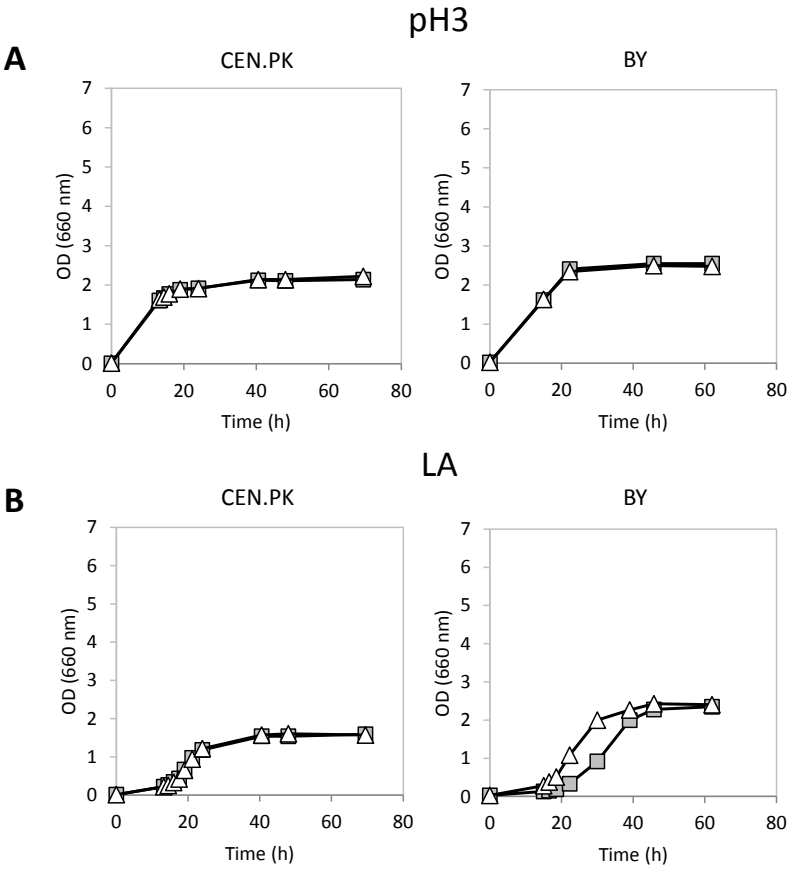

Figure 7: Growth of wild type and *sam2Δ* leucine nutritionally complemented strains in the absence and presence of lactic acid. Yeast cells were grown in shake flasks in minimal (YNB) medium with 2% w/v glucose and 50 mg/L of the necessary nutritional supplements at initial pH 3, without (**panel A**) or with (**panel B**) 34 and 38 g/l of lactic acid for CEN.PK (left panels) and BY (right panels), respectively. Growth was determined as OD at 660 nm. Light grey squares: parental wild type strains (CEN.PK 102-3A, BY4741). White triangles: *sam2Δ* cells (CEN.PK 102-3A *sam2Δ*, BY4741 *sam2Δ*).

However, the complementation of leucine auxotrophy made void the positive impact of *SAM2* deletion on cellular growth (Figure 8B).

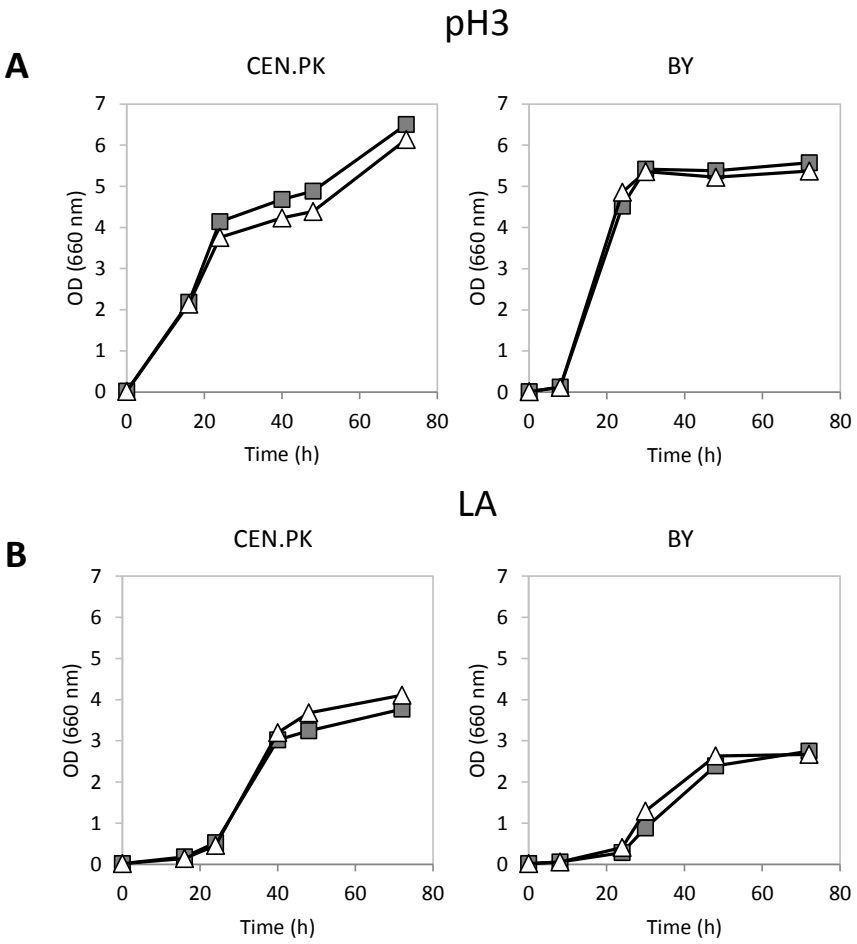

Figure 8: Growth of wild type and *sam2Δ LEU2* genetically complemented strains in the absence and presence of lactic acid. Yeast cells were grown in shake flasks in minimal (YNB) medium with 2% w/v glucose and 50 mg/L of the necessary nutritional supplements at initial pH 3, without (**panel A**) or with (**panel B**) 40 g/l of lactic acid. Growth was determined as OD at 660 nm. Left panels: CEN.PK cells; right panels: BY cells. Dark grey squares: wild type control strains (CEN.PK 102-3A [pTEF-L], BY4741 [pTEF-L]). White triangles: *sam2Δ* cells (CEN.PK 102-3A *sam2Δ* [pTEF-L], BY4741 *sam2Δ* [pTEF-L]).

It has to be noticed that the final OD reached by the *leu*$^-$ strains in the unstressed condition was lower compared to the values registered for LEU$^+$ complemented strains, possibly indicating that the standard amino acid supplementation (50 mg/L) was not sufficient in the case of leucine. This effect was stronger in the CEN.PK background (Figure 7A). Pronk [44] suggested complementation of the medium with 125 mg/L, 500 mg/L, 100 mg/L, 150 mg/L for histidine, leucine, methionine and uracil respectively. Accordingly, the growth experiments, in which the effect of *SAM2* modulation has been observed, were repeated in the presence of lactic acid at pH 3 with the supplemented relevant chemicals (Figure 9). While in this medium *SAM2* deletion did not affect the cellular growth in the presence of the stressing agent (panel A), *SAM2* overexpression was still detrimental to the cells (panel B). This confirms that Sam2p recombinant overproduction is not beneficial to improve the tolerance to this stress.

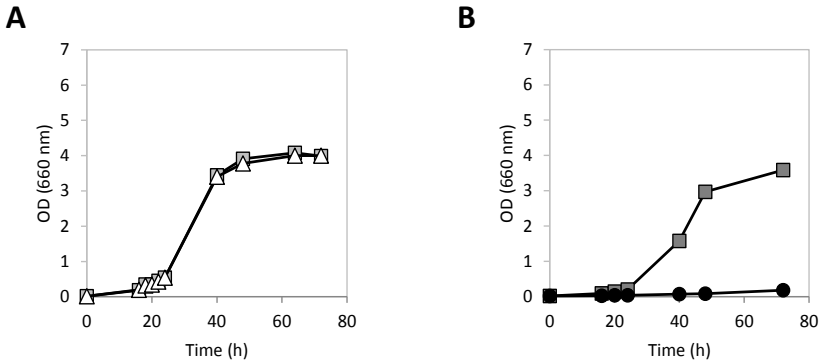

Figure 9: Growth of wild type, deleted or overexpressing *SAM2* BY strains in minimal supplemented medium with lactic acid. BY cells were grown in shake flasks in minimal (YNB) medium with 2% w/v glucose, 125 mg/L, 500 mg/L, 100 mg/L, 150 mg/L for histidine, leucine, methionine and uracil respectively, at initial pH 3, with 38 g/l of lactic acid. Growth was determined as OD at 660 nm. **Panel A**. Light grey squares: wild type control strain (BY4741) White triangles:

sam2Δ cells (BY4741 *sam2Δ*). **Panel B**. Dark grey squares: wild type control strain (BY4741 [pTEF-L]) Black circles: cells overespressing *SAM2* (BY4741 [pTEF-L-SAM2]).

Effect of lactic acid pulsed stress on cell viability

The effect of *SAM2* deletion and overexpression was also evaluated in terms of cellular viability in the aforementioned strains, i.e. CEN.PK 102-3A and BY4741 wild type, *SAM2* overexpressing and *sam2Δ* (complemented or not for leucine auxotrophy). Cells were grown in minimal medium, until the exponential phase was reached, and then treated with a pulse of lactic acid at different concentrations (0, 25, 30, 35, 40 and 45 g/L at pH 3). After 30 minutes the cells were collected, stained with propidium iodide (PI) and analyzed by flow cytometry to identify dead and/or severely compromised cells. Figure 10 shows the histograms obtained for the BY4741 strains, where the left peak corresponds to intact (PI-negative) cells, while the right peak corresponds to the dead/damaged (PI-positive) cells (we currently do not have an interpretation for the bimodal distribution visible in the plots).

As for the growth experiments, also in this case the effects of *SAM2* gene modulation were observed only in the BY background. In particular, the parental *leu*$^-$ strain *sam2Δ* showed a percentage of dead/damaged cells consistently lower than the control strain (Figure 10A). When the leucine auxotrophy was complemented, however, the differences between the two strains were not significant (Figure 10B). On the contrary, and in agreement with what already observed in the kinetics of growth, the *SAM2* overexpressing strain showed an increased sensitivity to lactic acid stress, with a higher percentage of dead/ damaged cells compared to the control (Figure 10B). It is worth to notice that for any tested lactic acid concentrations the BY *leu*$^-$ strains had a higher mortality compared to LEU$^+$ strains.

In the CEN.PK background, instead, the *SAM2* deletion and overexpression had no significant effect on cellular viability (data not shown).

A

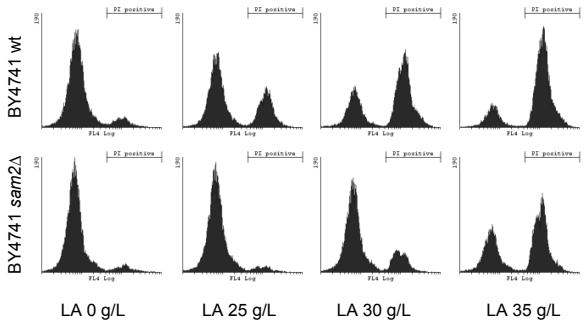

% Dead	LA 0 g/L	LA 25 g/L	LA 30 g/L	LA 35 g/L
wt	8.78	32.31	65.49	81.33
*sam2*Δ	6.33	5.05	19.92	59.84

B

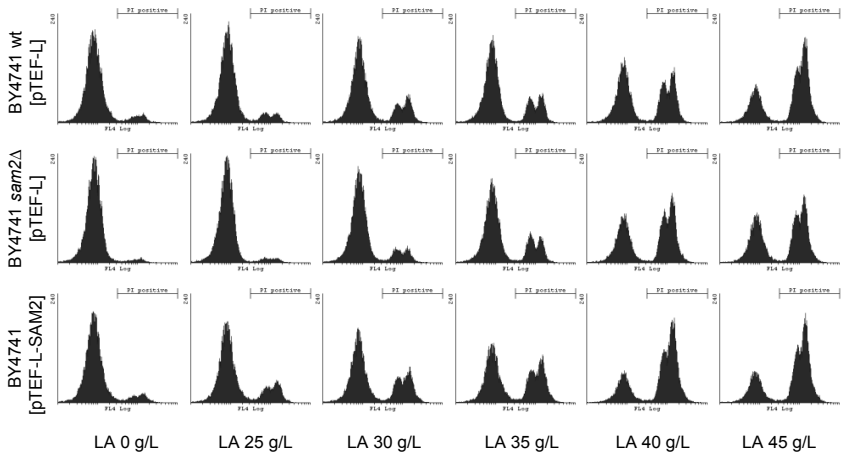

% Dead	LA 0 g/L	LA 25 g/L	LA 30 g/L	LA 35 g/L	LA 40 g/L	LA 45 g/L
wt pTEF-L	7.94	10.71	24.24	26.6	45.75	71.62
*sam2*Δ pTEF-L	3.42	4.93	14.97	26.67	56.62	55.94
pTEF-L-SAM2	9.36	22.33	33.97	44.59	73.19	71.62

Figure 10: Viability determination for cells stressed with lactic acid. Cells were grown in minimal medium until the exponential phase and then treated with a pulse of lactic acid. After 30 min

of incubation, cells were collected and stained with propidium iodide (PI) to detect dead and/or severely damaged cells by flow cytometry. The fluorescence emission was measured through a 670 nm long pass filter (FL3 parameter). For each sample, 25000 cells were analysed. The bar indicates the PI positive subpopulation. **Panel A**: BY4741 and BY4741 *sam2Δ*. **Panel B**: BY4741 [pTEF-L], BY4741 *sam2Δ* [pTEF-L] and BY4741 [pTEF-L-SAM2].

Analysis of intracellular AXP levels

Our data indicate that the Sam2 protein levels respond to lactic acid in both the CEN.PK and BY4741 yeast strains, but the effects of *SAM2* gene deletion and overexpression, at least in terms of growth and cell viability, are only detectable in the BY background. We considered the hypothesis that these differences might be correlated with different AXP pool composition. We therefore measured the adenine nucleotide content of CEN.PK 113-11C and BY4741 wt, *SAM2* overexpressing and *SAM2* deleted strains, complemented for leucine auxotrophy, during the exponential growth phase on minimal medium with 2% w/v glucose without or with lactic acid (samples were collected at OD ~1 if without and at OD ~0.3 if with lactic acid, respectively). The ATP, ADP and AMP (collectively referred as AXP) intracellular concentrations were determined by HPLC with the method from Ask *et al*. [45], as described in the Methods section. Data are reported in Figure 11, normalized for culture OD for consistency with the other data.

In the CEN.PK background (Figure 11A) similar levels of all the nucleotides were found in all the strains regardless the presence of lactic acid, and no differences were evident depending on *SAM2* expression levels. In the BY background, lower mean ATP levels were registered in the presence of lactic acid compared to control medium (Figure 11B), although again no specific differences were assessed in dependence on *SAM2* expression. Interestingly, a comparison of the data obtained for the two yeast backgrounds shows a lower mean ATP content in the BY strains compared

to CEN. PK. The differences are statistically significant, with a Student's *t*-test p-value of 0.012 for the comparison at pH 3 and of 0.004 for the comparison in lactic acid at pH 3. Also the ADP and AMP mean concentrations were lower in the BY strain, especially in the presence of lactic acid, so that the calculated energy charge resulted conserved in all the strains, at physiological levels higher than 0.8 (data not shown).

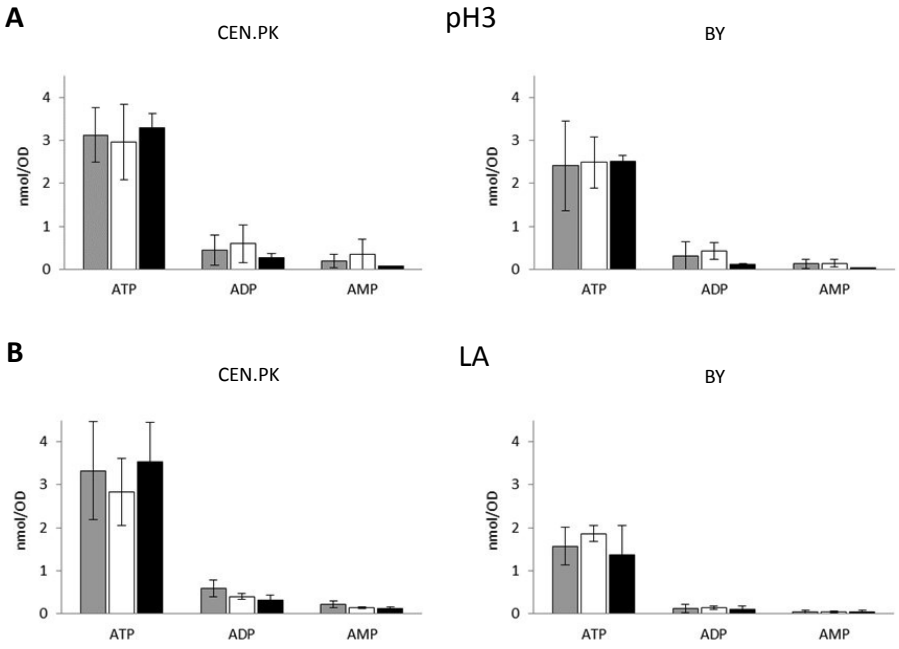

Figure 11: Intracellular adenine nucleotides concentrations in the absence and presence of lactic acid. Yeast cells were grown in shake flasks in minimal (YNB) medium with 2% w/v glucose at initial pH 3, without (**panel A**) or with (**panel B**) 40 g/l of lactic acid. ATP, ADP and AMP were extracted from samples collected during the exponential growth phase and determined by HPLC. Concentrations are expressed per OD of cell culture. The mean and SD for two independent experiments is reported. Left panels: CEN.PK cells; right panels: BY cells; Grey bars: CEN.PK 102-3A [pTEF-L], BY4741 [pTEF-L]; white bars: CEN.PK 102-3A *sam2Δ* [pTEF-L], BY4741 *sam2Δ* [pTEF-L]; black bars: CEN.PK [pTEF-L-SAM2], BY4741 [pTEF-L-SAM2].

Effect of *SAM2* deletion on lactic acid production by a *S. cerevisiae* strain engineered and evolved for the industrial process

Despite the fact that the mechanisms involved remain far from being elucidated, our data indicate that *SAM2* deletion might confer an advantage to cells exposed to lactic acid stress when the overall conditions are not optimal. Since the final goal of our studies is to find conditions that can bring advantages to lactic acid production, we tested the effects of *SAM2* deletion in the lactic acid producing strain during the production process. Indeed, even though the productive strain was originally derived from the robust CEN.PK background and does not bring any auxotrophies, still the production process puts it under extremely severe stress conditions.

The recombinant CEN.PK m850 strain is a homolactic fermenting cell factory able to produce up to 60 g/L in 60 h at pH values lower than 3. It was derived from the CEN.PK background via engineering steps that deleted all the pyruvate decarboxylase (PDC) genes and introduced the *L. plantarum* lactate dehydrogenase (LDH) activity, eliminating in this way all ethanol production in favour of lactic acid production from the free pyruvate. It furthermore underwent selection, following an adaptive laboratory evolution approach, for improved acid tolerance [12].

The *SAM2* gene was deleted in the CEN.PK m850 strain, and the performances of the parental and the *sam2Δ* strains were compared during the production of lactic acid in minimal medium in the presence of high amounts of initial glucose. Cells were first pre-cultivated for 24 hours in minimal medium with 10 g/L ethanol and 0.5 g/L glucose, to obtain the biomass, and then transferred to a fresh medium containing 5 g/L ethanol and 90 g/L glucose for the production phase (as previously described, [11]). Figure 12 reports the culture parameters monitored at time intervals throughout the production phase: cellular growth (panel A), residual glucose

and produced lactic acid in the medium, measured by HPLC (panel B), cell viability as determined by flow cytometry (panel C) and culture medium pH (panel D).

No differences ($p > 0.05$ Student's *t*-test) were observed between the two strains in terms of biomass accumulation (Figure 12A) and cell viability, the latter assessed after staining with either PI (Figure 12C) or fluorescein diacetate (whose signal is linked to metabolically active cells; data not shown), and extracellular pH values were almost identical (Figure 12D). Instead, differences were measured for the glucose and lactic acid concentrations (Figure 12B), indicating higher specific lactic acid production rates for the CEN.PK m850 *sam2Δ* strain compared to the control.

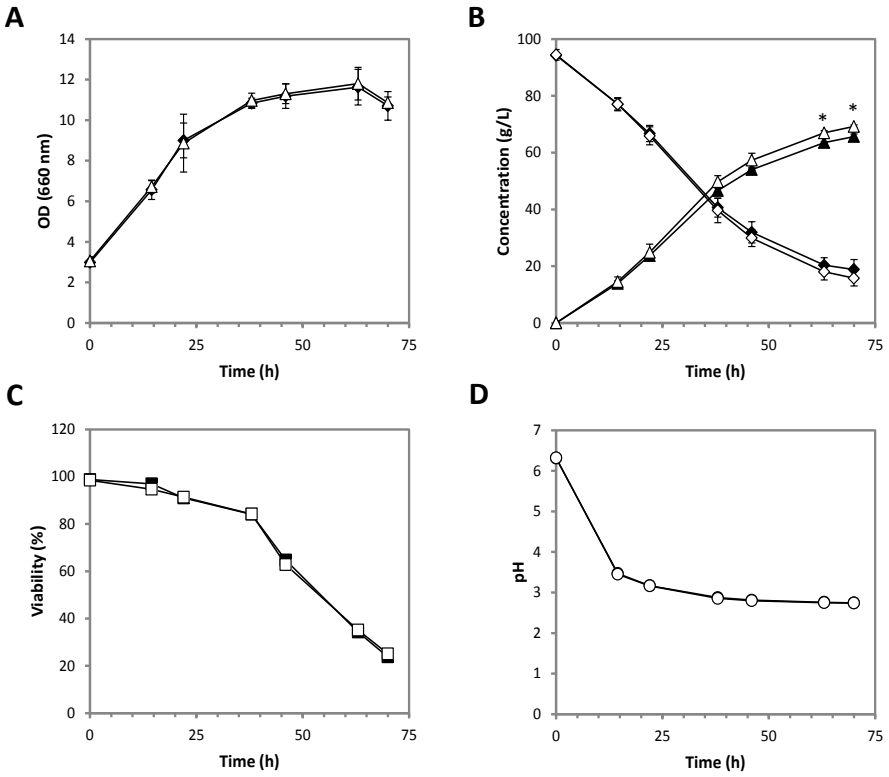

Figure 12: Batch lactic acid production in wt and *sam2Δ* strains. Fermentation profiles for CEN.PK m850 (filled symbols) and CEN.PK m850 *sam2Δ* (open symbols) pre-grown in shake flasks and then transferred in new flasks in minimal medium containing 90 g/L of glucose for the lactic acid production phase. (**A**) Biomass formation (OD at 660 nm). (**B**) Residual glucose (diamonds) and produced lactic acid (triangles). (**C**) Cellular viability was determined by PI staining followed by flow cytometry. (**D**) Culture medium pH. **Panel A** and **B** report the mean and SD for three independent experiments (*$p \leq 0.01$; Student's *t*-test); **Panel C** and **D** report data from a single representative experiment.

A mean 5.4% increase in lactic acid production was observed in the *sam2Δ* strain at the end of the process (69.2 ± 0.6 *vs* 65.6 ± 0.9 g/L, average and SD of three independent experiments). Based on a two-tails, unpaired, heteroscedastic Student's *t*-test, the differences in production at the last two

time points of the experiment are highly significant (*p*-values 0.0103 and 0.0087 respectively at 63 and 70 h). The 95% confidence intervals (CI) for lactic acid production throughout the process were also calculated (Table 1), indicating statistical significance for the differences found from the 46 h time point onward.

	95% CI[1] (*z* low and *z* up[2], g/L)				***t*-test *p*-values**
Time (h)	**m850**		**m850 *sam2Δ***		**m850 *vs* m850 *sam2Δ***
14,5	12.85	15	12.72	16.38	0.5997
22	22.41	25.06	21.56	28.18	0.5833
38	45.42	47.8	47.25	52.18	0.1167
46	53.71	54.29	54.55	60.11	0.1423
63	63.17	63.88	66.04	67.89	0.0103
70	64.58	66.7	68.57	69.82	0.0087

Table 1 – Statistical evaluation of differences in lactic acid production

Data for three independent experiments are reported.
[1] Confidence Interval
[2] Lower and upper endpoints of the CI

For both strains, the yields were similar (0.88 ± 0.01 and 0.87 ± 0.03 g of lactic acid per g of glucose consumed, respectively for the *sam2Δ* and the control strain). The differences observed between the two strains might be judged as small, but it must be considered that the cells were already pushed close to the theoretical limits (in terms of lactic acid yield) and in extreme conditions, therefore improvements of a high percentage cannot be expected.

To test if energetic balance might contribute to the observed differences, the intracellular AXP concentrations were determined in the control and *sam2Δ* strain during the process already described. Figure 13 shows the mean data and SD relative to cells analysed immediately before inoculation (indicated

as 0 h) and at 24 and 48 hours after the beginning of the production phase, respectively, in two independent experiments.

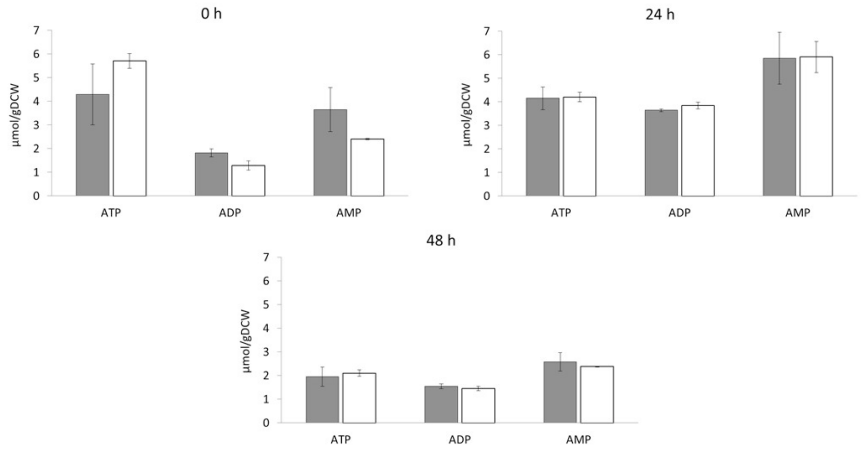

Figure 13: Intracellular adenine nucleotides concentrations in the lactic acid producing strains. CEN.PK m850 (grey bars) and CEN.PK m850 *sam2Δ* (white bars) were pre-grown in shake flasks and then transferred in new flasks in minimal medium containing 90 g/L of glucose for the lactic acid production phase. ATP, ADP and AMP were extracted and determined by HPLC, immediately before (0 h) or after the transfer in the production medium, at the indicated times (24 h and 48 h). Nucleotide concentrations are expressed per gram of dry cell weight (DCW). The mean and SD for two independent experiments is reported.

At time 0 h, the ADP and AMP contents were lower whereas the ATP content was higher in the *sam2Δ* strain compared to the control, despite a high variability in the case of ATP. After inoculation, no differences were found between the two strains. At 24 h, the ADP and AMP concentrations increased in both strains compared to 0 h, while at 48 h all the three species decreased.

Accordingly, the calculated energy charge (Table 2) was higher in the *sam2Δ* strain immediately before the production phase (0 h), while there was no difference between the two strains later during production. Note- worthy,

at all the time points and more pronouncedly during the production phase, the energy charge was below the physiological levels, differently from the laboratory strains, confirming the high stress experienced by the lactic acid producing strain.

Time (h)	m850		m850 *sam2Δ*	
0	0.53	±0.11	0.68	±0.01
24	0.44	±0.02	0.44	±0.03
48	0.45	±0.07	0.48	±0.01

Table 2: Energy charge values in the lactic acid producing strains

The mean and SD for two independent experiments are reported.

CONCLUSIONS

Cofactor engineering, *i.e.* the manipulation of cofactor levels, as exemplified by SAM in this work, in addition to providing means to study cellular metabolism has the potential to be used as an additional tool to achieve desired metabolic engineering goals and fits with current trends in systems biotechnology. Our findings confirm the potential of cofactor-engineering strategies for industrial application [46].

Western Blot analysis showed that lactic acid addition at low pH determines an increase of Sam2p in the cell. This increase was mainly associated to the insoluble protein fraction. To test a possible interaction with other proteins in complex(es) eventually associated to the membranes, the plasma membrane enriched fractions (PMEF) of the strain CEN.PK was analysed, finding a statistically non significant (*i.e.* present in two out of three replicates) enrichment of a spot corresponding to Sam2p (our unpublished results). This might reflect its association in (homo or hetero) protein complexes, and a co-sedimentation with plasma membrane proteins during the extraction protocols. The proneness of Sam2 to aggregate seems to find confirmation not only under lactic acid stress but also in other stressful conditions (see ethanol- and heat-shock data).

Nevertheless, the data obtained until now do not explain why the Sam2p levels increase when cells are exposed to lactic acid. It is however important to point out, as evidenced by FTIR analysis and widely discussed in Chapter 2, that the presence of Sam2p correlates in the BY4741 genetic background with the formation of protein aggregates under lactic acid stress. Therefore, it is possible to hypothesize that cells increase the levels of this protein to stimulate protein aggregation and thus slow down the cellular growth under the stressful condition. Consequently, the Sam2p recombinant

overproduction exacerbates this effect, determining a drastic fitness reduction on the laboratory strain BY4741 during lactic acid stress. Indeed, the *SAM2* deletion in the leucine auxotrophic BY4741 strain resulted in a higher (apparent) lactic acid tolerance, or to be more precise in a shorter lag phase during growth in media added with lactic acid at high concentration.
In respect to the increased lactic acid production observed in the CEN.PK m850 *sam2Δ,* our data on AXP concentrations suggest that the energetic balance might have a role. In fact, the higher ATP concentration found in the CEN.PK m850 *sam2Δ* strain before starting the lactic acid production phase, together with a higher energy charge value, might account for the superior performance of this strain compared to the CEN.PK m850 parental strain. Probably, a higher biosynthetic potential endows the cells with a larger pool of beneficial metabolites and/or better sustain the activity of energy-consuming detoxifying systems. As it was previously demonstrated that lactic acid production in engineered *S. cerevisiae* is limited by ATP availability [14], the fact that no ATP or energetic differences were detected later on during production is not surprising, since it is highly probable that in such a dynamic situation any ATP excess would be readily used by the cells.

All together, these data indicate Sam2p as a responsive element to lactic acid stress and suggest its modulation for lactic acid production improvement. Clarifying the nature of Sam2p interactions with other cellular components and their role in response to lactic acid stress might lead, in the future, to even higher resistance properties and productions via engineering of other interactors.

METHODS

Yeast strains, transformation, media and cultivation

The *S. cerevisiae* parental and derived strains used in this study are listed in Table 3.

Strain	Relevant genotype	Plasmid	Reference
CEN.PK 113-11C	*MATa, ura3-52, his3-Δ1*	-	P. Kotter[1]
CEN.PK 102-3A	*MATa, ura3-52, leu2-3,112*	-	P. Kotter[1]
CEN.PK [pTEF-L]	CEN.PK 102-3A	pTEF-L, multicopy (*Sc*TEF1, *LEU2*)	This work
CEN.PK [pTEF-L-SAM2]	CEN.PK 102-3A	pTEF-L-SAM2 (*Sc*TEF1, *ScSAM2*, *LEU2*)	This work
CEN.PK *sam2Δ*	CEN.PK 102-3A *sam2::KanMX4*	-	This work
CEN.PK *sam2Δ* [pTEF-L]	CEN.PK 102-3A *sam2Δ*	pTEF-L (*Sc*TEF1, *LEU2*)	This work
CEN.PK *SAM2*GFP	CEN.PK 113-11C *SAM2:: SAM2*GFP-*HIS3*	-	This work
CEN.PK m850	*MATa, pdc1(-6,-2)::loxP, pdc5(-6,-2)::loxP, pdc6 (-6,-2)::loxP, ura3-52, acid tolerant*	YEpLpLDH (*Sc*TPI, *Lp*LDH, *URA3*)	[18]
CEN.PK m850 *sam2Δ*	CEN.PKm850 *sam2::KanMX4*	YEpLpLDH (*Sc*TPI, *Lp*LDH, *URA3*)	This work
BY4741	*MATa, his3-Δ1, leu2-Δ0, met15-Δ0, ura3-Δ0*	-	EUROSCARF[2]
BY4741[pTEF-L]	BY4741	pTEF-L (*Sc*TEF1, *LEU2*)	This work
BY4741[pTEF-L-SAM2]	BY4741	pTEF-L-SAM2 (*Sc*TEF1, *ScSAM2*, *LEU2*)	This work
BY4741 *sam2Δ*	BY4741 *sam2::kanMX4*	-	This work
BY4741 *sam2Δ* [pTEF-L]	BY4741 *sam2Δ*	pTEF-L (*Sc*TEF1, *LEU2*)	This work
BY4741 *SAM2*GFP	BY4741 *SAM2:: SAM2*GFP-*HIS3*	-	This work

Table 3: Yeast strains used and created in this study

[1]Institut fur Mikrobiologie der Johann Wolfgang Goethe Universitat, Frankfurt, Germany.

[2]http://web.uni-frankfurt.de/fb15/mikro/euroscarf/.

Strain CEN.PK 102-3A was used for overexpression/deletion studies and CEN.PK 113-11C for GFP fusion. BY4741 (obtained from EUROSCARF) was used for overexpression/deletion studies and GFP fusion. The m850 lactic strain has been previously described [11, 12], obtained starting from a *PDC1*, *PDC5*, *PDC6* triple deleted CEN.PK strain [14], and was here deleted

in *SAM2*. Yeast transformations were performed according to the LiAc/PEG/ss-DNA protocol [47] and the strains were transformed with the constructs described below, in parallel with the corresponding empty plasmids. Integration of the constructs was confirmed by PCR analysis. For each set of transformation at least three independent transformants were initially tested, showing no significant differences among them.

Yeast cultures were performed in synthetic minimal medium (0.67% w/v YNB Biolife without amino acids) with 2% w/v D-glucose as carbon source. When required, supplements such as leucine, uracil, methionine and histidine were added to a final concentration of 50 mg/L, or to 125 mg/L, 500 mg/L, 100 mg/L, 150 mg/ L for histidine, leucine, methionine and uracil respectively for the experiment shown in Figure 6, while the antibiotic G418 (Roche Diagnostics) was added to a final concentration of 200 mg/L. Lactic acidic stress was imposed by adding the desired amount of L-lactic acid (Sigma-Aldrich) to the culture medium. The final media have been prepared starting from 2 different stock solutions, one of 100 g/L lactic acid and one of synthetic minimal medium 2X, in order to obtain the desired lac- tic acid concentration. The pH of the lactic acid and the culture media were adjusted to 3 with pellets of KOH and HCl 1 M, respectively. Cell growth was monitored by measuring the OD at 660 nm at regular time intervals and cells were inoculated at an initial OD of 0.02 for growth kinetics experiments and at an initial OD of 0.005 for western blot and fluorescence microscopy experiments in lactic acid.

For the ethanol shock treatment, exponentially growing cells were collected and observed after 2 hours of incubation with 20% ethanol at 30 °C. We choose this condition because, as reported by Hu [43], despite cells are subjected to a severe stress, the mortality is only of about 25%. The possible *foci* dissolution was not trivial to evaluate, in fact: the cells should have been

collected, washed and re-inoculated in minimal medium, therefore affecting the *foci* stability. For the heat shock treatment, exponentially growing cells were shifted to 42 °C for 2 hours and observed under epifocal microscope. Subsequently, the cells were re-incubated at 30 °C and the fluorescence was monitored over time.

All cultures were incubated in shake flasks at 30°C (expect for heat treatment) and 160 r.p.m. and the ratio of flask/ medium volume was 5/1.

For the lactic acid pulsed stress experiment, aliquots of exponentially growing cultures were transferred in tubes containing the desired amount of lactic acid, adjusted to pH 3, at a final OD of 0.1. The cells were incubated at 30°C and 160 r.p.m. for 30 min.

The producing strain CEN.PK m850 and the derived transformants were cultivated as previously described [11]. Briefly, after a first batch growth phase, cells were collected by centrifugation and resuspended in fresh medium at a final OD of 3; lactic acid production kinetics were then performed by incubating at 32°C and 185 r.p.m. in 250 mL quadruple baffled shake flasks in minimal medium containing 2.78 g/L CaCO3, 1.7 g/L YNB without amino acids and without (NH4)2SO4, 1 g/L urea, 5 ml/L ethanol, and with different glucose concentration (70, 80, 90 g/L) as carbon source. Each experiment was repeated at least three times.

Gene amplification and plasmids construction

The *S. cerevisiae SAM2* gene sequence was amplified by PCR using as a template the genomic DNA from CEN.PK strain, extracted by standard methods [48]. Pwo DNA polymerase (Roche catalogue no. 11 644 955 001) was used on a GeneAmp PCR System 9700 (PE Applied Biosystem, Inc.). Standard conditions used were 0.2 mM primers, 1.5 U of Pwo and 3 µL of genomic DNA. The program used for amplification of gene was as follows:

after 5 min at 94°C, 30 cycles (each cycle consisting of 45 sec at 94°C, 30 sec at 58°C and 1 min 30 sec at 72°C) were carried out, followed by 7 min at 72°C. Oligonucleotides pairs for SAM2 were as follows: SAM2_fw (5′-AATCATGTCCAAGAGCAAAACTTTCTTAT-3′) and SAM2_rev (5′-CATGGGAAAAACCAAAGAAATTGGAATTTTAA-3′). The amplified fragment was sub-cloned using the Perfectly Blunt Cloning kit (Novagen) into the Escherichia coli vector pSTBlue-1 obtaining the plasmid pSTBlue-SAM2. The insert was sequenced and it resulted identical to the deposited *S. cerevisiae* target sequence (*SAM2*, GeneID: 852113). This coding sequence was used for the construction of the multicopy expression plasmid pTEF-L-SAM2. This plasmid was derived from the commercial yeast multicopy expression plasmid p427-TEF (Dualsystems Biotechnology, CH), upon substitution of the selective marker Kan-MX with *LEU2* as follows: p427-TEF was NcoI digested, blunted and DraIII digested. The *LEU2* marker was excised from pYX042 (R & D Systems, Inc., Wiesbaden, D) by digestion with NotI, followed by blunting, and DraIII digestion, and then ligated to the recipient vector. The obtained vector pTEF-L was linearized with EcoRI and ligated to the *SAM2* ORF, excised with EcoRI from pSTBlue-SAM2.

The disruption of *SAM2* was performed using a standard recombination approach. pSTBlue-SAM2 was NcoI digested, blunted and EcoRV digested in the *SAM2* ORF. The excided fragment of about 200 nt was replaced with Kan-MX. The Kan marker was obtained from pFA6A- KanMX4 [49] digested with EcoRV and BamHI. The deletion cassette SAM2sx-KanMX-SAM2dx was excised from the resulting plasmid by cutting with NdeI and PvuII and used directly for yeast transformations. The obtained clones were screened by PCR using the following conditions: 5 min at 94°C, 30 cycles (45 sec at 94°C, 45 sec at 58°C and 2 min at 72°C) and 7 min at 72°C. The control primers, SAM2_fw_gen (5′-CGACGTCAAATCTTCATATGCAAGG-3′) and

Kan_fw (5′-AACGTGAGTCTTTTCCTTACCCAT-3′), were designed upstream of the ATG and in the KanMX marker cassette. The DyNAzymeTM II DNA Polymerase (Finnzymes Reagents) was utilized for those reactions. DNA manipulation, transformation and cultivation of *E. coli* (Novablue, Novagen) were performed following standard protocols [48]. All the restriction and modification enzymes utilised are from NEB (New England Bio- labs, UK) or from Roche Diagnostics.

The substitution of *SAM2* endogenous ORF with the construct *SAM2*GFP was performed using a standard recombination approach. The construct was obtained by PCR using as template the Longtine plasmid pFA6a-GFP (S65T)-His3MX6. Standard conditions used were 0.2 mM primers, 1.5 U of Pwo and 0.3 µL of plasmid DNA. The program used for amplification of construct was as fol- lows: 5 min at 94°C, 5 cycles (45 sec at 94°C, 30 sec at 50° C and 2 min at 72°C) and 7 min at 72°C, then 20 cycles (45 sec at 94°C, 30 sec at 65° C and 2 min at 72 °C) and 7 min at 72 ° C. Oligonucleotides pairs for *SAM2*GFP were as follows: SAM2_Fw_longtine (5'-TCAAGAGTACTCATGGGAAAAACCAAAGAAATTGGAATTTCGGATCCCC GGGTTAATTAA3') and SAM2_Rev_longtine (5'-TATAAAAATCAAAATAA AACATTTATTGTCTAAATGTTTAGAATTCGAGCTCGTTTAAAC-3'). The amplified fragment was used directly for yeast transformation.

The obtained clones were screened by PCR using the following conditions: 5 min at 94° C, 30 cycles (45 sec at 94° C, 45 sec at 57.5° C and 1 min 30 sec at 72 ° C) and 7 min. The control primers were as follows: SAM2_fw_gen (5'-CGAC GTCAAATCTTCATATGCAAGG-3') and Gfp_Rev (5'-AAGAATTGGGACAACTCCAGTGA-3'). The DyNAzymeTM II DNA Polymerase (Finnzymes Reagents) was utilized for those reactions.

Protein extractions for western blot analysis

Total protein extraction

10^8 cells were broken by glass beads in 20% TCA. After centrifugation, the pellet was resuspended in the Laemmli buffer system and in 1 M Tris, pH 7. The sample was boiled for 3 min and after centrifugation the supernatant was collected for the western blot analysis.

Tris-Urea-SDS sequential extraction

108 cells were resuspended in Tris buffer (50 mM Tris pH 8.7, 150 mM NaCl, 1 mM EDTA, 1 mM protease inhibitor cocktail, 1 mM PMSF) and broken by glass beads. After centrifugation the supernatant was collected (soluble fraction) and the pellet was resuspended in urea buffer (50 mM Tris pH 8.7, 150 mM NaCl, 1 mM EDTA, 1 mM protease inhibitor cocktail, 1 mM PMSF, 8 M urea). The sample was centrifuged and the supernatant was collected (urea fraction) while the pellet was resuspended in SDS buffer (SDS 10%, 1 mM protease inhibitor cocktail, 1 mM PMSF; SDS fraction).

SDS-PAGE and western blot analysis

The samples were boiled for 3 min in the Laemmli buffer system and then were loaded on a 12% poly-acrylamide analytical SDS gel. Electrophoresis in the separating gel was conducted at 30 mA for 5 hours. After the stacking gel was removed, transfer of proteins from SDS gels to 0.45 μM Protran Nitrocellulose Transfer Membrane was done for 1 hour at 250 mA.

Blocking and incubation with primary antibody to detect Sam2p-GFP

The nitrocellulose paper was then incubated in 5% milk made in TBS-Tween over night at 4°C with shaking. Monoclonal anti-GFP antibody (Living Colors A.v JL-8, Diatech Labline) was diluted 1:1000 in 5% milk/TBS- Tween and

applied to the nitrocellulose membrane. After incubation for 2 hours at room temperature with shaking, the membrane was washed in three changes of TBS-Tween over 25 min.

Blocking and incubation with primary antibody to detect actin

Monoclonal anti-actin antibody (Abcam 2Q1055) was diluted 1:1000 in 5% milk/TBS-Tween and applied to the nitrocellulose membrane. After incubation for 3 hours at room temperature with shaking, the membrane was washed in three changes of TBS-Tween over 25 min.

Incubation with secondary antibody and chemiluminescent detection Rabbit anti-Mouse IgG (FC) secondary antibody, AP (alkaline phosphatase) conjugate was diluted 1:15000 in 5% milk/TBS-Tween and applied to the nitrocellulose membranes for 1 hour at room temperature with shaking. The membranes were washed in four changes of TBS-Tween or TBS over 30 min and dried. The membranes were incubated with CDP-Star Chemiluminescent Substrate for 5 min at room temperature under gentle agitation. The nitrocellulose membranes were then exposed to Pierce Cl-x posure film to reveal Sam2p-GFP and actin signals, respectively. Bands were quantified with ImageJ 1.48 software.

Fluorescence microscopy analysis

CEN.PK 113-5D and BY4741 *SAM2*GFP strains were observed in a Nikon ECLIPSE 90i fluorescence microscope (Nikon) equipped with a 100X objective. Emission fluorescence due to GFP was detected by B-2A (EX 450–490 DM505 BA520) filter (Nikon). Digital images were acquired with a CoolSnap CCD camera (Photometrics) using MetaMorph 6.3 software (Molecular Devices).

Flow cytometric analysis

For identification of dead or severely compromised cells, cells were washed three times (Tris-HCl 50 mM, MgCl2 15 mM, pH 7.7) and resuspended in propidium iodide (PI) solution 0.23 mM. Samples were then analyzed using a CYTOMICS FC 500 flow cytometer (Beckman Coulter) equipped with a diode laser (excitation wavelength 488 nm). The fluorescence emission was measured through a 670 nm long pass filter (FL3 parameter) for PI signal. The sample flow rate during analysis did not exceed 600–700 cells/s. Threshold settings were adjusted so that the cell debris was excluded from the data acquisition; 25000 cells were measured for every sample. Data analysis was performed afterwards with Cyflogic 1.2.1 software (©Perttu Terho & ©CyFlo Ltd).

AXP extraction and quantification

ATP, ADP and AMP were extracted and quantified as described in [45]. Briefly, extraction was performed in 0.52 M TCA containing 17 mM EDTA. After centrifugation, supernatants were neutralized with 2 M Tris-base. Neutralized samples were then analyzed by HPLC with a Zorbax Eclipse XDB-C18 LC column (150 × 4.6 mm) (Agilent Technologies) kept at 20°C. Sample elution was carried out using a mobile phase consisting of acetonitrile and tetrabutylammonium buffer (0.005 M tetrabutylammonium hydrogensulfate, 0.01 M Na2HPO4) at pH 7.0, using a flow rate of 1 mL min^{-1}. A gradient was applied, where acetonitrile was increased from 6% to 25% and then back to 6%, as described in [45]. Adenonucleotides were detected with a photodiode array detector at 260 nm and peak identities were confirmed by co-elution with standards (Sigma-Aldrich). Concentrations were determined using calibration curves of standard solutions.

The energy charge (Ec) was calculated from the following equation:

$$E_c=([ATP]+0.5\times[ADP])/([ATP]+[ADP]+[AMP])$$

Extracellular metabolites and pH determination

Residual glucose and lactic acid produced were determined via high-performance liquid chromatography (HPLC, Model 1100, Agilent Technologies) using an Aminex HPX-87H ion exchange column 300 mm 7.8 mm (Bio-Rad) thermostated at 60°C. The mobile phase was 5 mM sulphuric acid with a flow of 0.6 ml/ min. Lactic acid was detected with an UV-detector at 210 nm. Glucose was detected with a RI detector, kept at 45°C.

The pH of the medium was measured with a pH-meter on fresh media or culture supernatants, after cells removal by centrifugation.

Statistical analysis

All statistical analysis, where *p*-values are indicated, was performed using a two-tails, unpaired, heteroscedastic Student's *t*-test.

REFERENCES

1. Datta R, Henry M: **Lactic acid: recent advances in products, processes and technologies — a review.** *J Chem Technol Biotechnol* 2006, **81**:1119–1129.

2. Wee Y-J, Kim J-N, Ryu H-W: **Biotechnological production of lactic acid and its recent applications.** *Food Technol Biotechnol* 2006, **44**:163–172.

3. Sauer M, Porro D, Mattanovich D, Branduardi P: **Microbial production of organic acids: expanding the markets.** *Trends Biotechnol* 2008, **26**:100–108.

4. Sauer M, Porro D, Mattanovich D, Branduardi P: **16 years research on lactic acid production with yeast - ready for the market?** *Biotechnol Genet Eng Rev* 2010, **27**:229–256.

5. Okano K, Tanaka T, Ogino C, Fukuda H, Kondo A: **Biotechnological production of enantiomeric pure lactic acid from renewable resources: recent achievements, perspectives, and limits.** *Appl Microbiol Biotechnol* 2010, **85**:413–423.

6. Dequin S, Barre P: **Mixed lactic acid-alcoholic fermentation by *Saccharomyces cerevisiae* expressing the *Lactobacillus casei* L (+)-LDH.** *Biotechnology (N Y)* 1994, **12**:173–177.

7. Porro D, Bianchi MM, Brambilla L, Menghini R, Bolzani D, Carrera V, Lievense J, Liu CL, Ranzi BM, Frontali L, Alberghina L: **Replacement of a metabolic pathway for large-scale production of lactic acid from**

engineered yeasts. *Appl Environ Microbiol* 1999, **65**:4211–4215.

8. Adachi E, Torigoe M, Sugiyama M, Nikawa J-I, Shimizu K: **Modification of metabolic pathways of *Saccharomyces cerevisiae* by the expression of lactate dehydrogenase and deletion of pyruvate decarboxylase genes for the lactic acid fermentation at low pH value.** *J Ferment Bioeng* 1998, **86**:284–289.

9. Ishida N, Saitoh S, Tokuhiro K, Nagamori E, Matsuyama T, Kitamoto K, Takahashi H: **Efficient production of L-Lactic acid by metabolically engineered *Saccharomyces cerevisiae* with a genome-integrated L-lactate dehydrogenase gene.** *Appl Environ Microbiol* 2005, **71**:1964–1970.

10. Branduardi P, Sauer M, De Gioia L, Zampella G, Valli M, Mattanovich D, Porro D: **Lactate production yield from engineered yeasts is dependent from the host background, the lactate dehydrogenase source and the lactate export.** *Microb Cell Fact* 2006, **5**:4.

11. Valli M, Sauer M, Branduardi P, Borth N, Porro D, Mattanovich D: **Improvement of lactic acid production in *Saccharomyces cerevisiae* by cell sorting for high intracellular pH**. *Appl Environ Microbiol* 2006, **72**:5492–5499.

12. Liu C, Lievense J: *Lactic Acid Producing Yeast*. U.S. patent application 2005, 0112737.

13. Rossi G, Sauer M, Porro D, Branduardi P: **Effect of *HXT1* and *HXT7* hexose transporter overexpression on wild-type and lactic acid producing *Saccharomyces cerevisiae* cells.** *Microb Cell Fact* 2010, **9**:15.

14. van Maris AJ, Winkler AA, Porro D, van Dijken JP, Pronk JT: **Homofermentative lactate production cannot sustain anaerobic growth of engineered *Saccharomyces cerevisiae*: possible consequence of energy-dependent lactate export.** *Appl Environ Microbiol* 2004, 70:2898–2905.

15. Miller C, Fosmer A, Rush B, McMullin T, Beacom D, Suominen P: **Industrial production of lactic acid.** In *Comprehensive Biotechnology*. Edited by Moo-Young Murray MB II, Colin W. Burlington: Elsevier; 2011:179–188.

16. Piper PW: **Resistance of yeasts to weak organic acid food preservatives.** *Adv Appl Microbiol* 2011, **77**:97–113.

17. Mira NP, Teixeira MC, Sá-Correia I: **Adaptive response and tolerance to weak acids in *Saccharomyces cerevisiae*: a genome-wide view**. *OMICS* 2010, **14**:525–540.

18. Piper P, Calderon CO, Hatzixanthis K, Mollapour M: **Weak acid adaptation: the stress response that confers yeasts with resistance to organic acid food preservatives.** *Microbiology* 2001, **147**:2635–2642.

19. Narendranath NV, Thomas KC, Ingledew WM: **Effects of acetic acid and lactic acid on the growth of *Saccharomyces cerevisiae* in a minimal medium.** *J Ind Microbiol Biotechnol* 2001, **26**:171–177.

20. Thomas KC, Hynes SH, Ingledew WM: **Influence of medium buffering capacity on inhibition of *Saccharomyces cerevisiae* growth by acetic and lactic acids.** *Appl Environ Microbiol* 2002, **68**:1616–1623.

21. Miller GE, Banerjee NC, Stowe CM: **Diffusion of certain weak**

organic acids and bases across the bovine mammary gland membrane after systemic administration. *J Pharmacol Exp Ther* 1967, **157**:245–253.

22. Bravim F, de Freitas JM, Fernandes AA, Fernandes PM: **High hydrostatic pressure and the cell membrane: stress response of *Saccharomyces cerevisiae.*** *Ann N Y Acad Sci* 2010, **1189**:127–132.

23. Ding J, Huang X, Zhang L, Zhao N, Yang D, Zhang K: **Tolerance and stress response to ethanol in the yeast *Saccharomyces cerevisiae.*** *Appl Microbiol Biotechnol* 2009, 85(2):253–263.

24. Folmer V, Pedroso N, Matias AC, Lopes SC, Antunes F, Cyrne L, Marinho HS: **H_2O_2 induces rapid biophysical and permeability changes in the plasma membrane of *Saccharomyces cerevisiae.*** *Biochim Biophys Acta* 2008, **1778**:1141–1147.

25. Simonin H, Beney L, Gervais P: **Cell death induced by mild physical perturbations could be related to transient plasma membrane modifications.** *J Membr Biol* 2007, **216**:37–47.

26. Simonin H, Beney L, Gervais P: **Controlling the membrane fluidity of yeasts during coupled thermal and osmotic treatments**. *Biotechnol Bioeng* 2008, 100:325–333.

27. Fu J, Wang Z, Chen T, Liu W, Shi T, Wang G, Tang YJ, Zhao X: **NADH plays the vital role for chiral pure D-(-)-2,3-butanediol production in *Bacillus subtilis* under limited oxygen conditions.** *Biotechnol Bioeng* 2014, **9999**:1–6.

28. Vemuri GN, Eiteman MA, McEwen JE, Olsson L, Nielsen J: **Increasing NADH oxidation reduces overflow metabolism in**

Saccharomyces cerevisiae. *Proc Natl Acad Sci U S A* 2007, **104**(7):2402–2407.

29. Thomas D, Surdin-Kerjan Y: **Metabolism of sulfur amino acids in *Saccharomyces cerevisiae.*** *Microbiol Mol Biol Rev* 1997, **61**:503–532.

30. Lieber CS, Packer L: **S-Adenosylmethionine: molecular, biological, and clinical aspects–an introduction.** *Am J Clin Nutr* 2002, **76**:1148S–1150S.

31. Malakar D, Dey A, Ghosh AK: **Protective role of S-adenosyl-L-methionine against hydrochloric acid stress in *Saccharomyces cerevisiae.*** *Biochim Biophys Acta* 2006, **1760**:1298–1303.

32. Malakar D, Dey A, Basu A, Ghosh AK: **Antiapoptotic role of S-adenosyl-l- methionine against hydrochloric acid induced cell death in *Saccharomyces cerevisiae.*** *Biochim Biophys Acta* 2008, **1780**:937–947.

33. Scheer M, Grote A, Chang A, Schomburg I, Munaretto C, Rother M, Söhngen C, Stelzer M, Thiele J, Schomburg D: **BRENDA, the enzyme information system in 2011**. *Nucleic Acids Res* 2011, **39**:D670–D676. D670-676.

34. Mudd S: **4 The Adenosyltransferases**. In *The Enzyme*, Volume 8. Edited by Boyer PD. New York: *Academic Press*; **1973**:121–154.

35. Lu SC: **S-Adenosylmethionine**. *Int J Biochem Cell Biol* 2000, **32**:391–395.

36. Cherest H, Surdin-Kerjan Y: **S-adenosyl methionine requiring mutants in *Saccharomyces cerevisiae*: evidences for the existence of**

two methionine adenosyl transferases. *Mol Gen Genet* 1978, **163**:153–167.

37. Thomas D, Rothstein R, Rosenberg N, Surdin-Kerjan Y: ***SAM2*** **encodes the second methionine S-adenosyl transferase in *Saccharomyces cerevisiae*: physiology and regulation of both enzymes.** *Mol Cell Biol* 1988, **8**:5132–5139.

38. Thomas D, Surdin-Kerjan Y: **The synthesis of the two S-adenosyl-methionine synthetases is differently regulated in *Saccharomyces cerevisiae.*** *Mol Gen Genet* 1991, **226**:224–232.

39. Kodaki T, Tsuji S, Otani N, Yamamoto D, Rao KS, Watanabe S, Tsukatsune M, Makino K: **Differential transcriptional regulation of two distinct S-adenosylmethionine synthetase genes (*SAM1* and *SAM2*) of *Saccharomyces cerevisiae.*** *Nucleic Acids Res Suppl* 2003, **3**:303–304.

40. Breker M, Gymrek M, Schuldiner M: **A novel single-cell screening platform reveals proteome plasticity during yeast stress responses**. *J Cell Biol* 2013, **200**:839–850.

41. Tkach JM, Yimit A, Lee AY, Riffle M, Costanzo M, Jaschob D, Hendry JA, Ou J, Moffat J, Boone C, Davis TN, Nislow C, Brown GW: **Dissecting DNA damage response pathways by analysing protein localization andabundance changes during DNA replication stress.** *Nat Cell Biol* 2012,**14**:966–976.

42. Huh WK, Falvo JV, Gerke LC, Carroll AS, Howson RW, Weissman JS, O'Shea EK: **Global analysis of protein localization in budding yeast.** *Nature* 2003, **425**:686–691.

43. Hu CK, Bai FW, An LJ: **Protein amino acid composition of plasma membranes affects membrane fluidity and thereby ethanol tolerance in a self-flocculating fusant of *Schizosaccharomyces pombe* and *Saccharomyces cerevisiae***. *Chinese Journal of Biotechinology* 2005, **21**(5):809-13.

44. Pronk JT: **Auxotrophic yeast strains in fundamental and applied research.** *Appl Environ Microbiol* 2002, **68**:2095–2100.

45. Ask M, Bettiga M, Mapelli V, Olsson L: **The influence of HMF and furfural on redox-balance and energy-state of xylose-utilizing *Saccharomyces cerevisiae.*** *Biotechnol Biofuels* 2013, **6**:22.

46. Wang Y, San KY, Bennett GN: **Cofactor engineering for advancing chemical biotechnology.** *Curr Opin Biotechnol* 2013, **24**(6):994–999.

47. Gietz RD, Woods RA: **Transformation of yeast by lithium acetate/single- stranded carrier DNA/polyethylene glycol method.** *Methods Enzymol* 2002, **350**:87–96.

48. Sambrook J, Fritsch EF, Maniatis T: *Molecular Cloning - A Laboratory Manual.* 2nd edition. New York: Cold Spring Harbor Laboratory; 1989.

49. Wach A, Brachat A, Pöhlmann R, Philippsen P: **New heterologous modules for classical or PCR-based gene disruptions in *Saccharomyces cerevisiae.*** *Yeast* 1994, **10**:1793–1808.

CHAPTER 2

An *in vivo* study on protein aggregation and membrane lipid in *Saccharomyces cerevisiae* strains exposed to lactic acid stress

(Berterame NM*, Ami D*, Porro D, Doglia SM, Branduardi P: "An *in vivo* study on protein aggregation and membrane lipid in *Saccharomyces cerevisiae* strains exposed to lactic acid stress". *Manuscript in preparation*. *equal contribution)

INTRODUCTION

The presence of high levels of lactic acid in its undissociated form imposes a high degree of stress to yeast cells, as discussed in the previous chapter. The lipophilic undissociated form of the acid (RCOOH) may permeate the plasma membrane by simple diffusion. Once in the near-neutral cytosol, the chemical dissociation of the weak acid occurs, leading to the release of protons (H^+) and of the respective counter-anion ($RCOO^-$). Due to their electric charge, these ions are not able to cross the hydrophobic lipid plasma membrane bilayer and accumulate within the cell. The accumulation of H^+ causes an intracellular acidification, causing a number of alterations, among which the decrease of DNA and RNA synthesis rate, the inhibition of metabolic activities and, in extreme cases, the disruption of the proton gradient across the plasma membrane. The accumulation of weak acid counter-anions, according to their specific characteristic, may lead to an increase in turgor pressure, oxidative stress, protein aggregation, lipid peroxidation, inhibition of membrane trafficking, and perturbation of plasma and vacuolar membranes spatial organization, reviewed in [1]. The loss of plasma membrane integrity increases cell permeability to other ions and other small metabolites, contributing to the alteration of internal pH and osmolite balance in weak acid-challenged cells and to the dissipation of the electrochemical potential maintained across this membrane, a driving force for active transports [2]. In literature is reported that the accumulation of lactate has a strong impact on the iron metabolism [3], has a pro-oxidant effect [4, 5], causes vacuolar fragmentation and impairs intracellular amino-acid homeostasis [6].

Therefore, the response to lactic acid stress was investigated in terms of effects on the major biomolecules classes of *S. cerevisiae* strains (BY4741

and two derived deleted strains) by Fourier transform infrared spectroscopy (FTIR) analysis.

The FTIR is in fact a non-invasive technique that allows rapid acquisition of the biochemical fingerprint of the sample under analysis, giving information on the content of the major biomolecules. This method is used not only to characterize the structural properties of isolated biomolecules, such as proteins, lipids, nucleic acids and carbohydrates [7, 8, 9, 10], but also to investigate complex biological systems including intact cells, tissues and whole model organisms [11]. Below, as an example it is shown a FTIR absorption spectrum of intact yeast cells (Figure 1).

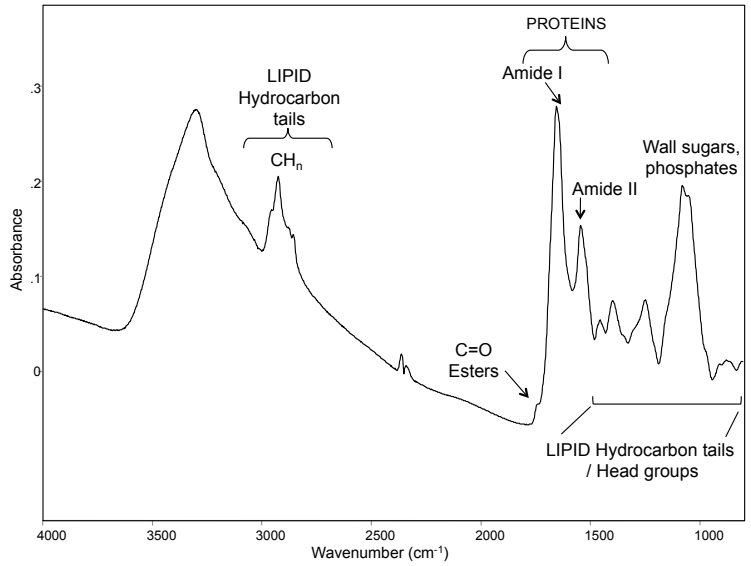

Figure 1: FTIR absorption spectrum of intact yeast cells (Ami D, unpublished data).

As shown, due to the absorption of the different classes of biomolecules, in the spectrum different regions are distinguishable.

In particular:

- from 3030 cm^{-1} to 2800 cm^{-1}: absorption mainly due to lipid hydrocarbon tails [7]
- ~1740 cm^{-1}: absorption of carbonyl group mainly from esters;
- from 1700 cm^{-1} to 1500 cm^{-1}: the spectrum is dominated by the amide I and amide II bands, respectively due to the C = O stretching and the NH bending of the peptide bond. In particular, the amide I band gives information on the protein secondary structure [10];
-from 1500 cm^{-1} to 1350 cm^{-1}**:** vibrational modes mainly due to lipid CH_2 and CH_3. The spectrum gives information about both lipid acyl chains and head group [7];
-from 1250 cm^{-1} to 1000 cm^{-1}: vibrational modes mainly due to the contribution of nucleic acid phosphodiester groups and phospholipids, as well as to the C-O absorption of carbohydrates [7, 8, 9];
- from 1000 cm^{-1} to 800 cm^{-1}: absorption of nucleic acid and lipid.

To resolve the overlapping components of the IR absorption bands, the second derivatives of the FTIR absorption spectra are also usually analysed [12], as in the present work. In particular, in the Result section the spectral range between 1700 cm^{-1} to 1600 cm^{-1} and between 1500 cm^{-1} and 1200 cm^{-1} are reported and commented, since proteins and lipids are the two classes of biomolecules that turned out to be more affected by lactic acid exposition. The effect of this organic acid on lipids was deeply investigated, evaluating the phenomenon of lipid peroxidation that might occur during weak acid stress, as reported above.

RESULTS

***Saccharomyces cerevisiae* BY4741 strain exposed or not to lactic acid: second derivatives analysis of the FTIR spectra**

The *S. cerevisiae* BY4741 strain was grown in minimal medium with 2% w/v glucose in the absence and in the presence of different concentration of lactic acid (pH3, with or without the addition of 40 g/L or 46 g/L lactic acid) and the cells were analysed by Fourier transform infrared (FTIR) analysis at 18 and 40 hours after the inoculation, respectively corresponding to the exponential and the stationary phase of growth.

Figure 2 shows the second derivatives of the FTIR absorption spectrum of intact cells, collected at 18 hours of growth, in the spectral range between 1700 cm^{-1} and 1600 cm^{-1} (panel A) and between 1500 cm^{-1} and 1200 cm^{-1} (panel B).

In the absence of the stressing agent (blue line, panel A), the proteins were in their native form: alpha-helices (~1657 cm^{-1}) and beta-sheets (~1639 cm^{-1}) [10]. When the cells were exposed to 40 g/L (green line) or 46 g/L of lactic acid at pH3 (red line) a shoulder or a well resolved peak at ~1629 cm^{-1}, representing intermolecular beta-sheets, typical of protein aggregates, appeared [13]. Therefore, lactic acid exposure correlates with protein aggregation and magnitude of this phenomenon seems to be lactic acid dose-dependent.

Observing the spectrum in the range of lipids response (panel B), it appears that the presence of the stressing agent resulted in decreased levels of phosphatidylcoline, as demonstrated by the decrease in the levels of its head group $N(CH_3)_3$ (~1440 cm^{-1}) [7]. Also the decrease of this membrane phospholipid seems to be lactic acid dose-dependent (see again the color code for lactic acid levels).

Therefore, it is possible to conclude that lactic acid exposure influences the biochemical fingerprint of yeast cells during the exponential phase of growth.

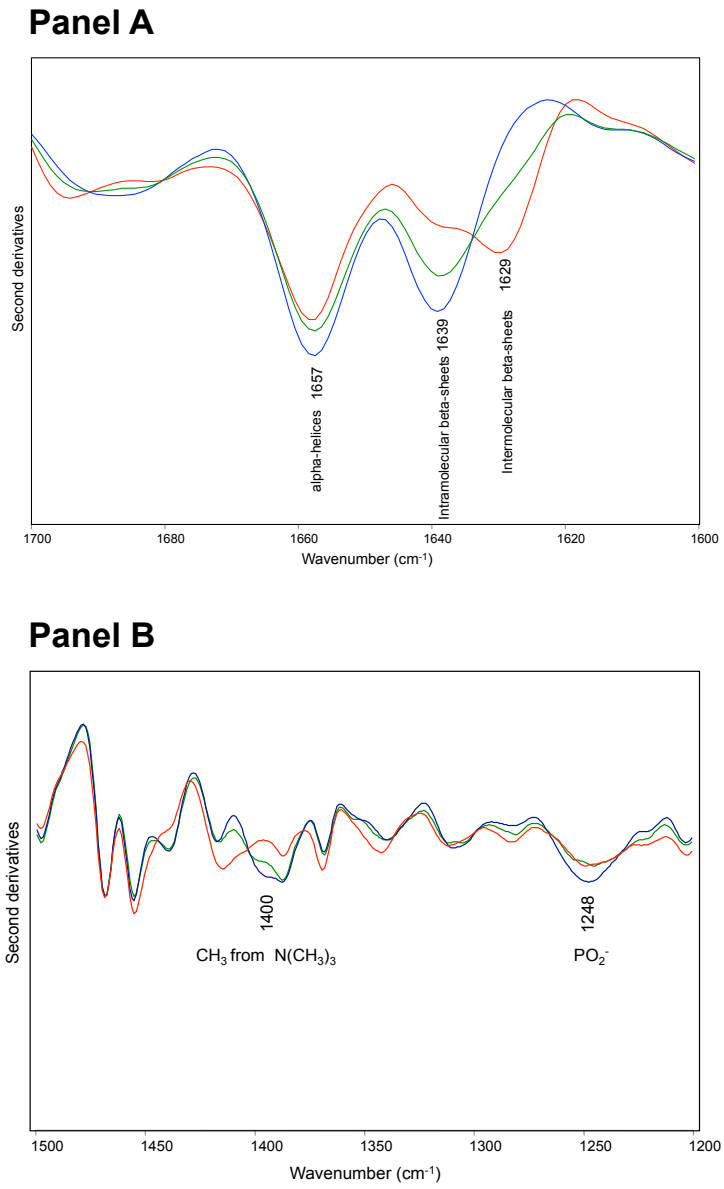

Figure 2: Second derivatives of FTIR absorption spectra of *S. cerevisiae* strain in the absence and in the presence of lactic acid. Cells were grown in shake flasks in minimal (YNB) medium with

2% w/v glucose in the absence and in the presence of different concentration of lactic acid: pH3 (blue line), 40 g/L lactic acid at pH3 (green line) and 46 g/L lactic acid at pH3 (red line). FTIR analysis was performed at 18 hours after the inoculation, corresponding the exponential growth phase. **Panel A**: Amide I band; **Panel B:** vibrational modes mainly due to lipid CH_2/CH_3 and to phosphate groups.

Remarkably, at 40 hours of growth the spectra measured in the presence and in the absence of the stressing agent were comparable. In particular the presence of lactic acid did not correlate with either decreased levels of phosphatidylcholine or with the formation of protein aggregates (data not shown).

Phosphatidylcholine, as well as being the most abundant membrane phospholipid, is the mainly responsible for the membrane fluidity [14]. Therefore, its decrease during the response to lactic acid exposure might be a strategy adopted by the cells in order to make the membrane more compact and, consequently, less permeable to the lactic acid influx.

Moreover, if the plasma membrane is considered not only as a barrier between the extracellular and the intracellular environments, but also as a stress sensor, changes in its composition may be a signal capable of inducing intracellular events, including protein aggregation. The growth delay observed when cells were exposed to the stressing agent might be therefore due to the phenomenon of protein aggregation (see Chapter 1, Results, Figure 7).

These hypotheses are supported by the fact that in the stationary phase of growth, when there were no differences between cells exposed or not to the lactic acid in terms of phosphatidylcholine levels and biomass accumulation, the phenomenon of intracellular protein aggregation was not observed.

Second derivatives analysis of the FTIR spectra of *Saccharomyces cerevisiae SAM2* deleted strain exposed or not to lactic acid

As discussed in the Chapter 1 in the paragraph "Effect of *SAM2* overexpression and deletion on lactic acid tolerance", the modulation of *SAM2* gene expression had effect during growth in the presence of lactic acid in the BY4741 background. In particular, the BY4741 *sam2Δ* strain turned out to be less sensitive to the stressing agent than its parental counterpart.

In order to evaluate whether the growth advantage observed in the *SAM2* deleted strain correlates with changes in the biochemical fingerprint, the BY4741 *sam2Δ* strain and the respective control strain were subjected to FTIR analysis. The yeast cells were grown in minimal medium with 2% w/v glucose in the absence or in the presence of 40 g/L lactic acid at pH3, and analysed at 18 hours after inoculation, where the growth advantage has been observed.

The spectra obtained for the BY4741 *sam2Δ* strain (Figure 3) show that the presence of lactic acid had a negligible effect in terms of intracellular protein aggregation (panel A); on the contrary, the exposure to this acid determined also in this case a clear reduction in phosphatidylcholine levels (panel B).

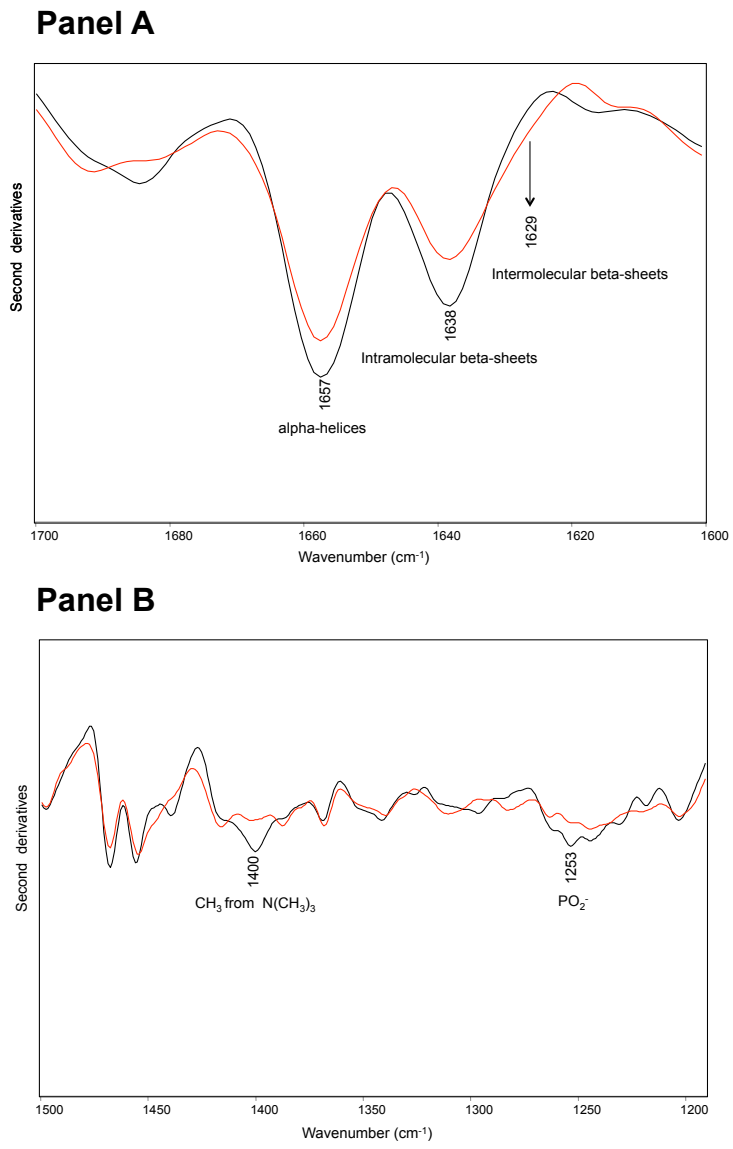

Figure 3: Second derivatives of FTIR absorption spectra of *S. cerevisiae* BY4741 *sam2Δ* strain in the absence and in the presence of lactic acid. Cells were grown in shake flasks in minimal (YNB) medium with 2% w/v glucose without (black line) or with (red line) 40 g/L lactic acid at pH3. FTIR analysis was performed at 18 hours after the inoculation, corresponding to the exponential

growth phase. **Panel A**: Amide I band; **Panel B:** vibrational modes mainly due to lipid CH_2/CH_3 and to phosphate groups.

BY4741 and BY4741 *sam2Δ* strains grown at pH3 have a quite comparable spectrum profile both in the region of proteins and lipids (data not shown). On the contrary, lactic acid exposure caused a strong aggregation of cell proteins in the parental strain, almost absent in the BY4741 *sam2Δ* (Figure 4, Panel A). The phosphatidylcholine levels, instead, were similar in both strains during lactic acid treatment (Figure 4, Panel B).

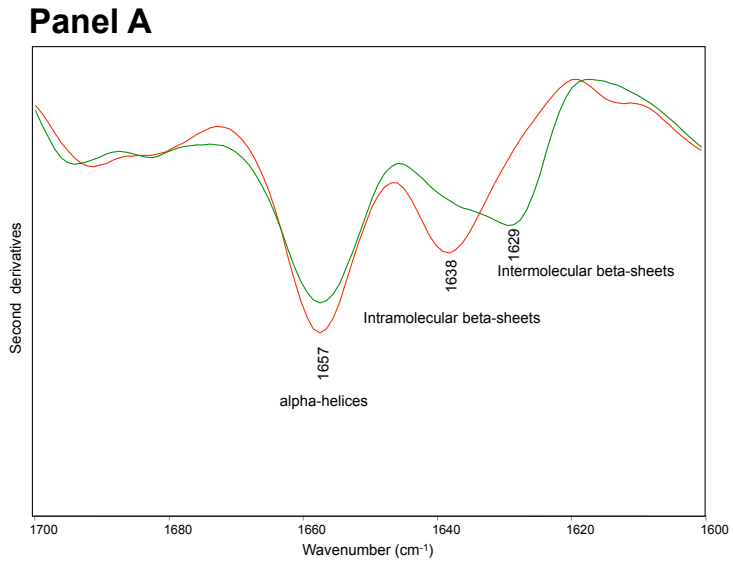

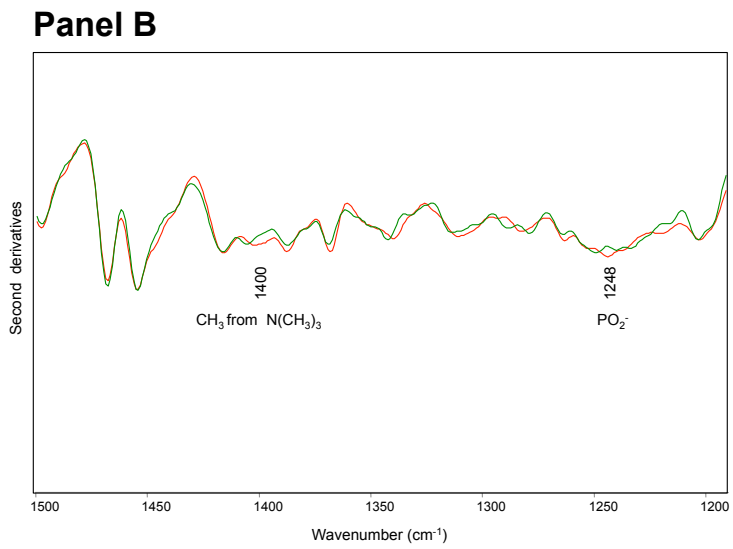

Figure 4: Second derivatives of FTIR absorption spectra of *S. cerevisiae* BY4741 and BY4741 *sam2Δ* strains in the presence of lactic acid. BY4741 (green line) and BY4741 *sam2Δ* (red line) parental strains were grown in shake flasks in minimal (YNB) medium with 2% w/v glucose with 40 g/L lactic acid at pH3. FTIR analysis was performed at 18 hours after the inoculation, corresponding to the exponential growth phase. **Panel A**: Amide I band; **Panel B:** vibrational modes mainly due to lipid CH_2/CH_3 and to phosphate groups.

Since the complementation of leucine auxotrophy made void the positive impact of *SAM2* deletion on cellular growth in the BY4741 background (Chapter 1, Results), it was examined if this complementation had also an effect on the major biomolecules. For this purpose, the BY4741 *sam2Δ* [pTEF-L] strain and the respective control strain were also subjected to FTIR analysis. The cells were grown in the same conditions described above and analysed at 18 hours after the inoculation.

Figure 5 shows the spectra obtained for the BY4741 *sam2Δ* [pTEF-L] strain grown in the absence and in the presence of the stressing agent. The same

biochemical fingerprint was obtained also for the control strain, BY4741 [pTEF-L] (data not shown).

As in the spectra of the leucine auxotrophic strains (BY4741 and BY4741 *sam2Δ*), previously shown, the presence of the organic acid determined also in this case a clear reduction in phosphatidylcholine levels (panel B). However, it is important to underline that the complementation of leucine auxotrophy, during lactic acid exposure, led to a strong protein aggregation even in the strain deleted in the *SAM2* gene (panel A).

This phenomenon is thus strain specific (Figure 4, panel A), but also dependent on the nutritional needs of the cell. Therefore, the growth advantage of the BY4741 *sam2Δ* strain, not detectable when the auxotrophy for leucine was genetically complemented, could be due, or at least correlates to the absence of the intracellular protein aggregation.

Panel A

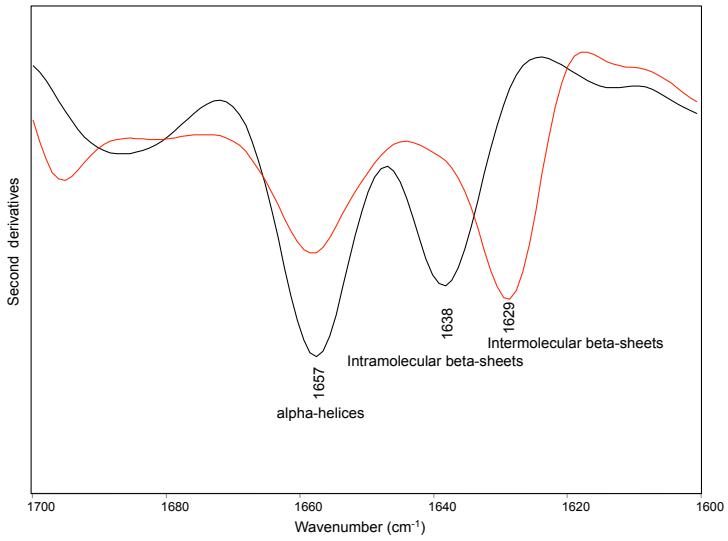

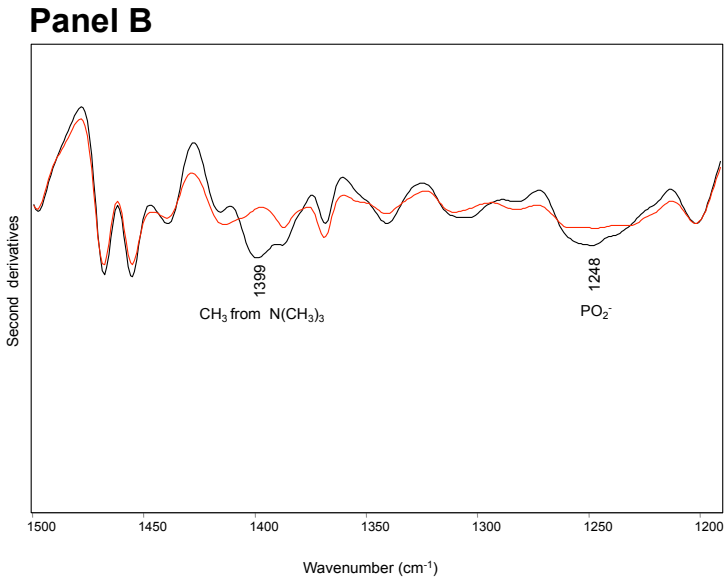

Figure 5: Second derivatives of FTIR absorption spectra of *S. cerevisiae* BY4741 *sam2Δ* [pTEF-L] strain in the absence and in the presence of lactic acid. Cells were grown in shake flasks in minimal (YNB) medium with 2% w/v glucose without (black line) or with (red line) 40 g/L lactic acid at pH3. FTIR analysis was performed at 18 hours after the inoculation, corresponding to the exponential growth phase. **Panel A**: Amide I band; **Panel B:** vibrational modes mainly due to lipid CH_2/CH_3 and to phosphate groups.

Effect of *OPI1* deletion on lactic acid tolerance

Opi1p is a transcription factor that acts as a repressor of the genes involved in the synthesis of phosphatidylcoline [15]. Opi1p activity is controlled by the presence of inositol that, together with phosphatidic acid, is necessary for the synthesis of phosphatidyl-inositol. In the absence of inositol, Opi1 binds to phosphatidic acid (precursor of membrane phospholipids) and by the interaction with Scs2p it is recruited to the endoplasmic reticulum. In the presence of inositol, phosphatidic acid levels decrease and Opi1 is released and it translocates into the nucleus where it inhibits the transcription of the

INO1 gene and the genes containing the UAS_{INO} sequence [16]. The activity of Opi1 is also regulated by protein kinase A and C (PKA, PKC) and casein kinase II phosphorylation [17]. Furthermore, Opi1 is target for the ubiquitin-dependent degradation [18].

As evidenced by the FTIR data, in all the strains under investigation a correlation between lactic acid exposure and a decrease in phosphatidylcoline levels exists. Consequently, the effect of *OPI1* deletion in the BY4741 strain was evaluated for growing cells challenged with different concentration of lactic acid. Figure 6 shows the results obtained by cultivating cells in minimal medium with 2% w/v glucose without or with lactic acid (46 g/L) at pH 3. No remarkable differences were observed between the control and the *OPI1* deleted strain during growth without lactic acid at low pH (left panel). Lactic acid had a clear negative effect on both strains, visible in terms of growth delay and biomass accumulation. Notably, in the stressed condition (right panel) a marked difference between the two strains was observed: the BY4741 *opi1Δ* turned out to be less sensitive to the stressing agent than the parental.

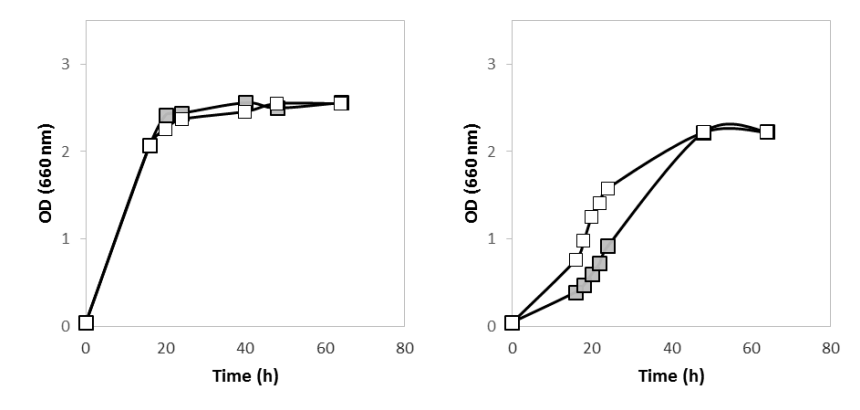

Figure 6: Growth of *S. cerevisiae* BY4741 and BY4741 *opi1Δ* strains in the absence and in the presence of lactic acid. Cells were grown in shake flasks in minimal (YNB) medium with 2% w/v

glucose without (**left panel**) or with (**right panel**) 46 g/L lactic acid at pH3. Growth was determined as OD at 660 nm. Light grey squares: BY4741 strain. White squares: BY4741 *opi1Δ* strain.

Second derivatives analysis of the FTIR spectra of *Saccharomyces cerevisiae OPI1* deleted strain exposed or not to lactic acid

The strain BY4741 *opi1Δ* and the respective control were grown under the same conditions described above for the growth kinetics, and examined at 18 hours after inoculation by FTIR analysis.

The lactic acid exposure on the BY4741 *opi1Δ* strain had not strong effects according to the recorded spectra. In the Amide I region there were no differences between cells challenged or not with the stressing agent, and just a slight decrease in phosphatidylcoline levels was observed (data not shown).

As shown in Figure 7, the phenomenon of protein aggregation typical of the BY4741 strain, when exposed to lactic acid, was completely absent in the mutant one (panel A). Moreover, the phosphatidylcholine levels were significantly higher in the BY4741 *opi1Δ* strain than those of the control strain, during lactic acid treatment (panel B). This result is in agreement with the biological role of *OPI1*, main repressor of genes involved in the phosphatidylcholine biosynthesis. Remarkably, despite a single gene deletion was operated, the effects under lactic acid stress condition are so pronounced to be detected by the spectroscopic analysis. The biochemical fingerprint of the two strains grown in the absence of lactic acid was comparable (data not shown).

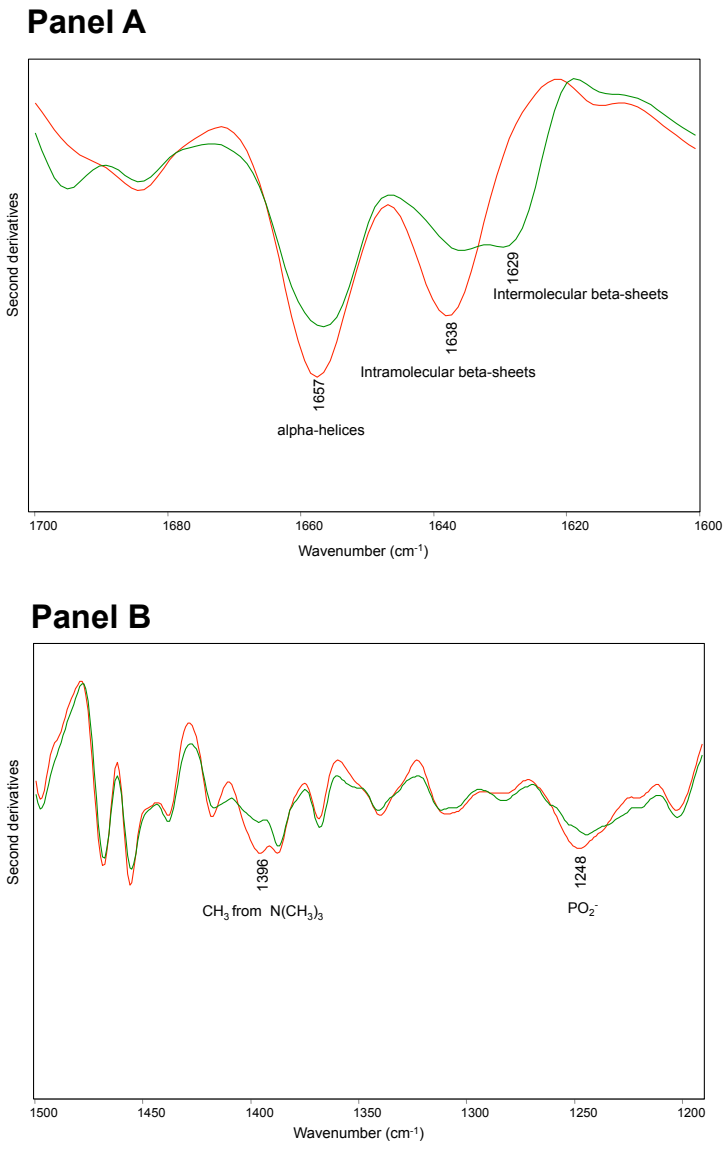

Figure 7: Second derivatives of FTIR absorption spectra of *S. cerevisiae* BY4741 and BY4741 *opi1Δ* strains in the presence of lactic acid. BY4741 (green line) and BY4741 *opi1Δ* (red line) parental strains were grown in shake flasks in minimal (YNB) medium with 2% w/v glucose with 46 g/L lactic acid at pH3. FTIR analysis was performed at 18 hours after the inoculation, corresponding

the exponential growth phase. **Panel A**: Amide I band; **Panel B:** vibrational modes mainly due to lipid CH_2/CH_3 and to phosphate groups.

Evaluation of Unfolded Protein Response (UPR) under lactic acid exposure

From FTIR analysis is therefore clear that, at biochemical level, the main difference between the BY4741 and the BY4741 *sam2Δ* or the BY4741 *opi1Δ* strains is the phenomenon of protein aggregation. For this reason the activation of the Unfolded Protein Response (UPR) was evaluated. This is indeed a cellular response triggered by the presence of protein aggregates, which involves a signal transduction cascade from the endoplasmic reticulum to the nucleus [19].

In particular, cells respond to the accumulation of unfolded proteins in the endoplasmic reticulum (RE) by increasing the transcription of genes encoding chaperones localized in this cellular compartment, such as BiP (Hsp70) and PDI (Protein Disulfide Isomerase), in order to accelerate the protein folding in the ER lumen. Moreover, the rate of degradation of misfolded proteins is increased by the action of ERAD (Endoplasmic Reticulum Associated Protein Degradation) and the protein synthesis is decreased [20].

HAC1 codifies for the transcription factor Hac1p that is supposed to be the controller of the UPR in yeast. Cox and Walter [21] have identified two different forms of *HAC1* mRNAs: the full length (969 base pairs), which is present in cells whether or not the UPR is induced; the shorter one that appears only when the UPR is induced, generated by the splicing of 251 base pairs from the full length mRNA form, by Ire1p. Only the mRNA mature form can be translated [22].

The UPR activation was therefore verified by evaluating the *HAC1* mRNAs. The BY4741, BY4741 *sam2Δ* and BY4741 *opi1Δ* strains were grown in

minimal medium with 2% w/v glucose in the absence and in the presence of lactic acid (46 g/L lactic acid at pH3). The RT-PCR experiment and the subsequent amplification of the cDNA, using specific primers for *HAC1*, were performed at 18 hours after the inoculation, during the exponential phase of growth. Figure 8 reports the result of a representative PCR obtained in the presence (panel A) and in the absence of the stressing agent (panel B).

In the presence of lactic acid the UPR was active in all the examined strains, while in the control condition, at pH3 without lactic acid, the UPR was active only in the deleted strains (the band of about 700 bp is present even though it is hardly visible). Therefore, the absence of intracellular protein aggregation in the BY4741 *sam2Δ* and BY4741 *opi1Δ* strains during lactic acid exposure (as shown in the FTIR analysis), might be explained by the fact that the cells are more prompt to face the stressing agent as the UPR is also active in non-stressful condition. On the contrary, the accumulation of protein aggregates in the parental strain might be due to the fact that UPR has to be *de novo* activated.

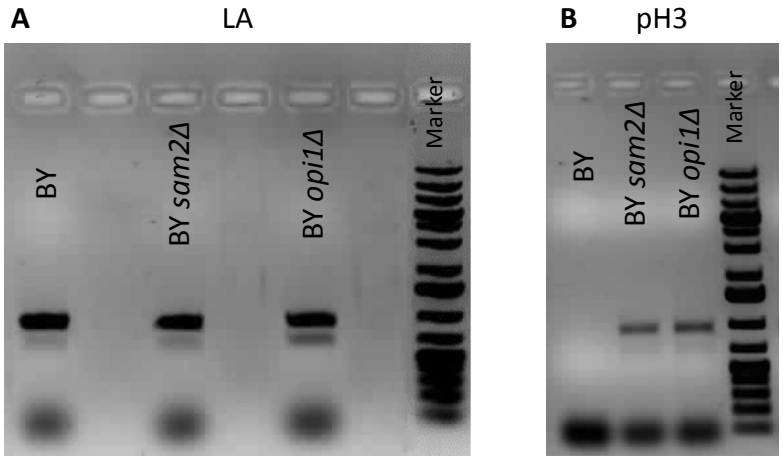

Figure 8: Evaluation of UPR in BY4741, BY4741 *sam2Δ* and BY4741 *opi1Δ*.
The *HAC1* mRNAs amplification was performed at 18 hours after the inoculation, corresponding to the exponential phase of growth, in the BY4741, BY4741 *sam2Δ* and BY4741 *opi1Δ* strains exposed (**panel A**) or not (**panel B**) to 46 g/L lactic acid at pH3.

Effect of lactic acid exposure on lipid peroxidation

Lipid peroxidation is one of the reported effects of the weak organic counter-anions on *S. cerevisiae* cells [2]. Lipid peroxidation starts with the attack of a radical Reactive Oxygen Species (ROS) to a double bond of a polyunsaturated fatty acid resulting in the formation of a radical polyunsaturated fatty acid. This species, due to its high reactivity, can lead to the formation of several products including malondialdehyde (MDA), which can therefore be used as an index of lipid peroxidation level (*R&D Systems* 1997. Minireviews-Reactive Oxygen Species (ROS)).

BY4741, BY4741 *sam2Δ* and BY4741 *opi1Δ* cells were grown in minimal medium until the exponential phase was reached and then they were treated with a pulse of lactic acid (40 g/L at pH 3), and without the stressing agent at

pH3 as control. After 30 minutes the cells were collected and the levels of MDA were evaluated (see Methods), (Figure 9).

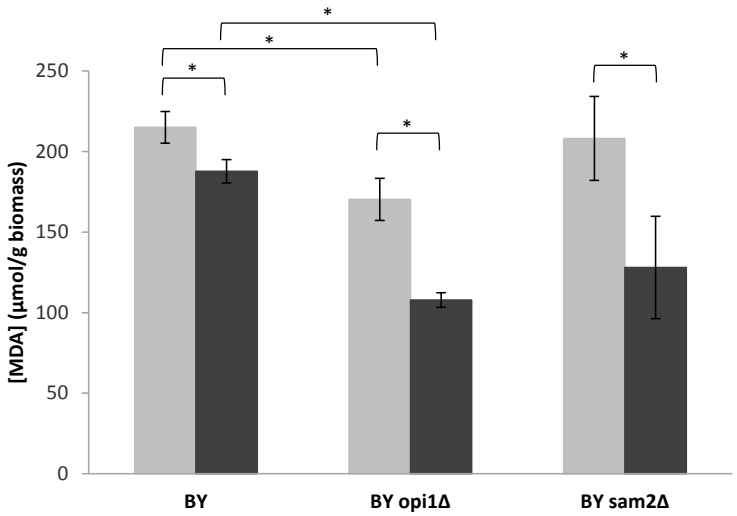

Figure 9: Evaluation of lipid peroxidation for cells stressed with lactic acid. Cells were grown in minimal medium until the exponential phase was reached and then they were treated or not with a pulse of lactic acid 40 g/L at pH 3. After 30 minutes the cells were collected and the levels of MDA were evaluated. Dark grey bars: cells shocked with lactic acid. Light grey bars: control. *$p \leq 0,05$ Student's *t*-test.

Surprisingly, the presence of lactic acid correlates with a statistically significant decrease in peroxidized lipid content, phenomenon particularly pronounced in the deleted strains (13%, 37% and 38% decrease for the BY4741, BY4741 *opi1Δ* and BY4741 *sam2Δ* strains, respectively). Moreover, *OPI1* deletion altered the lipid membrane peroxidation phenomenon. In particular, in both tested conditions (with or without lactic acid stress) the peroxidized lipid content was statistically significant lower in the BY4741 *opi1Δ* strain compared to the parental strain (21% and 43% decrease respectively at pH3 and at pH3 with lactic acid 40 g/L). It might be

concluded that the higher resistance to oxidative membrane damage and the absence of protein aggregation phenomenon (Figure 7, Panel A) are factors that contribute to the increased lactic acid tolerance shown in the BY4741 *opi1Δ* strain (Figure 6, Right Panel).

There were instead no significant differences between the BY4741 and BY4741 *sam2Δ* strains in terms of peroxidized lipid content. The growth advantage of this mutant strain during lactic acid stress might therefore mainly relate to the absence of protein aggregates.

DISCUSSION

This study was focused on the evaluation of *S. cerevisiae* response to lactic acid stress in terms of effects on the major biomolecules classes. In particular, BY4741 and derived *SAM2* and *OPI1* deleted strains were characterized.

The FTIR analysis showed that lactic acid exposure correlates with decreased levels of phosphatidylcholine during the exponential phase of growth. Since this phospholipid is the main responsible for membrane fluidity [22], its decrease might be a strategy adopted by the cell to diminish membrane permeability, and thus the lactic acid influx in the cytosol. Moreover, the decrease of phosphatidylcholine levels was more marked, and among them comparable, in the BY4741 and BY4741 *sam2Δ* strains compared to the BY4741 *opi1Δ* strain. This result is in agreement with the biological role played by Opi1p, the main repressor of the genes involved in the phosphatidylcholine biosynthetic pathway.

FTIR analysis also revealed a significant difference between the strains under investigation in the Amide I region. In particular, in the exponential phase of growth (T 18), the exposure to lactic acid correlates with the formation of intracellular protein aggregates in the parental strain, not visible in the BY4741 *sam2Δ* and BY4741 *opi1Δ* strains. The higher tolerance to lactic acid observed in the deleted strains compared to the parental strain might therefore be attributed to the absence of protein aggregation. It is indeed important to point out that when the leucine auxotrophy was complemented in the BY4741 *sam2Δ* strain, protein aggregates were observed and the positive impact of *SAM2* deletion on cellular growth was not significant (Chapter 1, Results).

Notably, it has been demonstrated that the leucyl-tRNA synthetase (LeuRS), the enzyme responsible for charging leucine to its cognate tRNA, functions as a sensor of leucine signaling to TORC1 [23]. In this case, the phenomenon of protein aggregation might be due to an increased activation of the TORC1 pathway.
It will be interesting to evaluate the effect of molecular chaperones overexpression in order to contrast the phenomenon of protein aggregation and determine whether this will result in a higher lactic acid tolerance.

The evaluation of the Unfolded Protein Response (UPR) led to the hypothesis that the absence of protein aggregates in the mutant strains might be due to the fact that these cells are more prompt to deal with stress. In fact, in the BY4741 *sam2Δ* and BY4741 *opi1Δ* strains, differently from the parental strain, the UPR was induced not only when cells were exposed to lactic acid but also in control condition (minimal medium at pH3).
It is important to underline that plasma membrane is not a simple barrier between the extracellular and the intracellular environment, but also an important stress sensor. Therefore, changes in its composition, such as the decrease of phosphatidylcholine levels, might trigger multiple reactions intracellularly [24], which could in turn lead to protein aggregation, a phenomenon potentially responsible for decreasing the growth rate of the parental strain. This hypothesis is supported by the fact that several proteins involved in the signaling cascades interact with the plasma membrane. For example, the activation of the enzyme adenylate cyclase Cyr1, responsible of the cyclic adenosine monophosphate (cAMP) synthesis, is dependent upon its peripheral association to the plasma membrane [25]. Therefore, changes in membrane fluidity could affect this interaction and consequently the enzymatic activity. In particular, a decreased Cyr1 activity leads to a

decrease in the intracellular levels of cAMP, resulting in pleiotropic phenotypes similar to nutrient starvation [25]. Thus, it will be interesting to determine whether the levels of this second messenger or the related PKA activity change when cells are exposed to lactic acid stress and if there are differences between the strains under investigation.

Furthermore, we might speculate that changes in membrane fluidity could also affect the activity of membrane proteins, among which transporters, immersed in the lipid bilayer. Consequently, differences in nutrients uptake could also affect signal transduction pathways [25].

However, if the membrane changes are not as pronounced as in the case of the BY4741 *opi1Δ* strain, it can be supposed that the cascade of reactions is not triggered, resulting in a higher (apparent) lactic acid tolerance.

In the BY4741 *sam2Δ* strain the absence of protein aggregates can not be related to a different composition of the plasma membrane, which is similar to that of the parental strain, but to pleiotropic effects consequent to *SAM2* deletion. Sam2p indeed catalyzes the formation of S-adenosyl methionine (SAM), a central coenzyme in the metabolism that participates to a very high number of reactions [26].

Since in literature is reported that weak organic acid counter-anions induce membrane lipids peroxidation [2], it was evaluated whether lactic acid is able to generate oxidative stress not only intracellularly, as suggested by Abbott [4], but also at the plasma membrane. Surprisingly, the exposure to the stressing agent correlated in all strains in analysis with a significant decrease in the amount of peroxidized lipids content. These results necessitate further analysis aimed to assess the saturation level of the membrane lipids. The reaction of lipid peroxidation is indeed generated by the attack of a Reactive Oxygen Species (ROS) to the double bond of a

polyunsaturated fatty acid. Whether the strategy adopted by the cell is aimed to reduce the membrane permeability, as previously discuss, it can be hypothesized that unsaturated membrane lipids decrease in favor of saturated ones, and consequently the peroxidized lipids content decreases.
This hypothesis is supported by data reported in literature regarding the exposure of *Zygosaccharomyces bailii* to acetic acid. This yeast is in fact able to induce profound rearrangements in the plasma membrane after acetic acid treatment. In particular, it is possible to observe a decrease of glycerophospholipids, specifically of phosphatidylcholine, in favor of sphingolipids and an increase in the degree of lipids saturation. These events make the membrane less fluid, more ordered and, hence, less permeable to acetic acid [27].

CONCLUSIONS

This study pointed out that the exposure to lactic acid in *S. cerevisiae* results in profound changes, never elucidated in literature, both at the plasma membrane, in terms of its composition and oxidative damage, and at intracellularly, in terms of protein aggregation.

Moreover, it was highlighted how the deletion of *OPI1* had pleiotropic effects. This gene engineering affected not only the phosphatidylcholine levels, direct gene target, but also the peroxidized lipid content and the accumulation of protein aggregates, factors that contribute to the increased robustness of the BY4741 *opi1Δ* strain in the presence of lactic acid.

METHODS

Yeast strains, media and cultivation

The BY4741 and the BY4741 *opi1Δ* strains were obtained from EUROSCARF, while the BY4741 *sam2Δ* strain has been obtained in our laboratory by target gene deletion on the BY4741 strain [28, and see also Chapter 1, Methods].

Yeast cultivations were performed in synthetic minimal medium (0.67% w/v YNB Biolife without amino acids) with 2% w/v D-glucose as carbon source, supplemented with leucine, uracil, methionine and histidine to a final concentration of 50 mg/L. Lactic acidic stress was imposed by adding the desired amount of L-lactic acid (Sigma-Aldrich) to the culture medium. The final media were prepared starting from 2 different stock solutions, one of 100 g/L lactic acid and one of synthetic minimal medium 2X, to obtain the desired lactic acid concentration. The pH of the lactic acid and the culture media were adjusted to 3 with pellets of KOH and HCl 1 M, respectively. Cell growth was monitored by measuring the OD at 660 nm at regular time intervals and cells were inoculated at an initial OD of 0.05. All cultures were incubated in shake flasks at 30°C and 160 rpm and the ratio of flask medium volume was 5/1. For the lipid peroxidation experiment, exponentially growing cells were collected and transferred in flasks containing lactic acid 40 g/L, adjusted to pH 3. The cells were incubated at 30°C and 160 rpm for 30 min.

FTIR microspectroscopy

Yeast cells from BY4741, BY4741 *sam2Δ* and BY4741 *opi1Δ S. cerevisiae* strains at 18 hours and 40 hours (for the BY4741 strain) of growth were washed three times in distilled water to eliminate medium contamination. Approximately 3 µl of the cell suspensions were then deposited onto an IR

transparent BaF2 support, and dried at room temperature for about 30 minutes to eliminate the excess water.

FTIR absorption spectra were acquired in transmission mode, between 4000 and 700 cm^{-1}, by means of a Varian 610-IR infrared microscope coupled to the Varian 670-IR FTIR spectrometer (both from Varian Australia Pty Ltd), equipped with a mercury cadmium telluride (MCT) nitrogen-cooled detector. The variable microscope aperture was adjusted from approximately 60 μm × 60 μm to 100 μm × 100 μm). Measurements were performed at 2 cm^{-1} spectral resolution; 25 KHz scan speed, triangular apodization, and by the accumulation of 512 scan co-additions.

Spectral analysis was conducted in the spectral range between 1700 cm^{-1} to 1600 cm^{-1} and between 1500 cm^{-1} and 1200 cm^{-1}. To this aim, second-derivatives spectra were obtained following the Savitsky-Golay method (third-grade polynomial, 9 smoothing points), after a binomial 13 smoothing points of the measured spectra [12], using the GRAMS/32 software (Galactic Industries Corporation, USA).

To verify the reproducibility and reliability of the spectral results, more than three independent preparations were analyzed.

Evaluation of UPR

RNA extraction

RNA was extracted from cells in exponential growth phase (T 18 h) by the AurumTM Total RNA Mini Kit (BIO-RAD), following manufacturer's instruction.

RT-PCR

RNA was reverse transcribed by iScript™ cDNA Synthesis Kit (BIO-RAD), following manufacturer's instruction.

HAC1 mRNAs amplification

The *S. cerevisiae HAC1* mRNAs sequences were amplified by PCR using as a template the cDNA. Phusion^{R} High-Fidelity DNA polymerase (NEB no. M0530) was used on a GeneAmp PCR System 9700 (PE Applied Biosystem, Inc.). Standard conditions used were 0.5 μM primers, 1 U of Phusion and 1.5 μL cDNA. The program used for amplification of mRNAs was as follows: after 30 sec at 98°C, 25 cycles (each cycle consisting of 7 sec at 98°C, 20 sec at 62.6°C and 30 sec at 72°C) were carried out, followed by 7 min at 72°C. Oligonucleotides pairs for *HAC1* were as follows: HAC1_fw (5′-ATGGAAATGACTGATTTTGAACTAACTAG-3′) and HAC1_rev (5′- TCATGAAGTGATGAAGAAATCATTCAATTC -3′).

Evaluation of lipid peroxidation

An estimation of lipid peroxidation was based on the level of malondialdehyde formed after lactic acid pulse stress of *S. cerevisiae* parental and mutant strains, as described in [29]. Briefly, after treatment with or without lactic acid the cells were collected, resuspended in 100 mM Tris pH 7.8 and broken by glass beads. After centrifugation the supernatant was collected and 250 μL of the extract were mixed with 500 μL of the mix TBARS (15% w/v trichloroacetic acid, 0.375% w/v thiobarbituric acid, 0.25 N hydrochloric acid). The solution was heated for 1 hour in a boiling water bath. The absorbance of the sample was determined at 535 nm against a blank that contained all the reagents except the extract. Results were expressed as micromoles of malondialdehyde per gram of wet weight biomass.

REFERENCES

1. Piper PW: **Resistance of yeasts to weak organic acid food preservatives.** *Adv Appl Microbiol* 2011, **77**:97–113.

2. Mira NP, Teixeira MC, Sa-Correia I: **Adaptive response and Tolerance to Weak Acids in *Saccharomyces cerevisiae*: A Genome-Wide View.** *OMICS A Journal of Integrative Biology* 2010, **14**(5):525-40.

3. Abbott DA, Suir E, van Maris A, Pronk JT: **Physiological and Transcriptional Responses to High Concentrations of Lactic Acid in Anaerobic Chemostat Cultures of *Saccharomyces cerevisiae.*** *Appl. Environ. Microbiol.* 2008, **74**(18):5759.

4. Abbott DA, Suir E, Duong GH, de Hulster E, Pronk JT, van Maris AJ: **Catalase overexpression reduces lactic acid-induced oxidative stress in *Saccharomyces cerevisiae*.** *Appl Environ Microbiol*. 2009, **75**(8):2320-5.

5. Branduardi P, Fossati T, Sauer M, Pagani R, Mattanovich D, Porro D: **Biosynthesis of vitamin C by yeast leads to increased stress resistance.** *PLOS ONE* 2007, **2**(10):e1092.

6. Suzuki T, Sugiyama M, Wakazono K, Kaneko Y, Harashima S: **Lactic-acid stress causes vacuolar fragmentation and impairs intracellular amino-acid homeostasis in *Saccharomyces cerevisiae*.** *J Biosci Bioeng*. 2012, **113**(4):421-30.

7. Casal HL, Mantsch HH: **Polymorphic phase behaviour of phospholipid membranes studied by infrared spectroscopy.** *Biochim Biophys Acta* 1984, **779**:381–401.

8. Kacuráková M, Mathlouthi M: **FTIR and laser-Raman spectra of oligosaccharides in water: caharacterization of the glycosydic bond.** *Carbohydr Res* 1996, **284**:145–157.

9. Banyay M, Sarkar M, Graslund A: **A library of IR bands of nucleic acids in solution.** *Biophys Chem* 2003, **104**:477–488.

10. Barth A: **Infrared spectroscopy of proteins.** *Biochim Biophys Acta* 2007, **1767**:1073–1101.

11. Ami D, Natalello A, Doglia SM: **Fourier transform infrared microspectroscopy of complex biological systems: from intact cells to whole organisms.** *Methods Mol Biol* 2012, **895**:85–100.

12. Susi H, Byler DM: **Resolution-enhanced Fourier transform infrared spectroscopy of enzymes.** *Methods Enzymol* 1986, **130**:290–311.

13. Seshadri S, Khurana R, Fink AL: **Fourier transform infrared spectroscopy in analysis of protein deposits.** *Methods Enzymol* 1999, **309**:559– 576.

14. Nagle JF, Tristram-Nagle S: **Structure of lipid bilayers.** *Biochim Biophys Acta* 2000, **1469**(3): 159-195.

15. Hickman MJ, Petti AA, Ho-Shing O, Silverman SJ, McIsaac RS, Lee TA, Botstein D: **Coordinated regulation of sulfur and phospholipid metabolism reflects the importance of methylation in the growth of yeast.** *Mol Biol Cell* 2011, **22**(21):4192-204.

16. Henry SA, Kohlwein SD, Carman GM: **Metabolism and Regulation of Glycerolipids in the Yeast *Saccharomyces cerevisiae*.** *Genetics* 2012, 190:317–349.

17. Chen M, Hancock LC, Lopes JM: **Transcriptional regulation of yeast phospholipid biosynthetic genes.** *Biochimica et Biophysica Acta* 2007, **1771**(3):310–321.

18. Cox JS, Chapman RE, Walter P: **The unfolded protein response coordinates the production of endoplasmic reticulum protein and endoplasmic reticulum membrane.** *Mol. Biol. Cell* 1997, **8**:1805–1814.

19. Shamu CE: **Signal Transduction: Splicing together the unfolded-protein response.** *Current Biology* 1997, **7**:R67-R70.

20. Liu CY, Kaufman RJ: **The unfolded protein response.** *J Cell Sci.* 2003, **116**(Pt 10):1861-2.

21. Cox JS, Walter P: **A novel mechanism for regulating activity of a transcription factor that controls the unfolded protein response**. *Cell* 1996, **87**:391-404.

22. Back SH, Schröder M, Lee K, Zhang K, Kaufman RJ: **ER stress signaling by regulated splicing: IRE1/HAC1/XBP1.** *Methods*. 2005, **35**(4):395-416.

23. Bonfils G, Jaquenoud M, Bontron S, Ostrowicz C, Ungermann C, De Virgilio C: **Leucyl-tRNA synthetase controls TORC1 via the EGO complex.** *Mol Cell* 2012, **46**:105–110.

24. Ziolkowska NE, Christiano R, Walther TC: **Organized living: formation mechanisms and functions of plasma membrane domains in yeast.** *Trends in Cell Biology* 2012, **22**(3):151-8.

25. Feldmann H**: Yeast: Molecular and Cell Biology. 2nd Completely Revised and Greatly Enlarged Edition.** *Wiley-Blackwell,* 2012.

26. Thomas D, Surdin-Kerjan Y: **Metabolism of sulfur amino acids in *Saccharomyces cerevisiae*.** *Microbiol Mol Biol Rev* 1997, **61**(4):503-32.

27. Lindberg L, Santos A, Riezman H, Olsson L, Bettiga M: **Lipidomic Profiling of *Saccharomyces cerevisiae* and *Zygosaccharomyces bailii* Reveals Critical Changes in Lipid Composition in Response to Acetic Acid Stress.** *PLOS ONE* 2013, **8**(9):e73936

28. Dato L, Berterame N, Ricci M, Paganoni P, Palmieri L, Porro D, Branduardi P: **Changes in *SAM2* expression affect lactic acid tolerance and lactic acid production in *Saccharomyces cerevisiae*.** *Microb Cell Fact*. 2014, **13**(1):147.

29. Fernandes AR, Prieto M, Sá-Correia I: **Modification of plasma membrane lipid order and H+-ATPase activity as part of the response of *Saccharomyces cerevisiae* to cultivation under mild and high copper stress.** *Arch Microbiol*. 2000, **173**(4):262-8.

CHAPTER 3

A novel pathway to produce butanol and isobutanol in *Saccharomyces cerevisiae*

INTRODUCTION

As discussed in the Introduction, butanol has superior liquid-fuel characteristics in respect to ethanol, similar properties to gasoline, and thus it has the potential to be used as a substitute for gasoline in currently running engines [1].

Clostridia are recognized as natural and good butanol producers and are employed in the industrial-scale production of solvents [2]. However, the complex metabolic characteristics and the difficulty of performing genetic manipulations on these bacteria fostered the exploitation of other well established cell factories. In recent years, *Escherichia coli* and *Saccharomyces cerevisiae* were engineered with the *Clostridia* butanol pathway [3,4]. While many optimizations have been successfully introduced in *E. coli* [5-8] reaching productions similar to that obtained in *Clostridia* [9], this was up to now not reported for the budding yeast. For an exhaustive view of the metabolic strategies applied for butanol and other fusel alcohol production see [10,11] and references therein. Remarkably, Liao *et al*. proposed that proteins, and thus the aminoacids released from proteins hydrolysis, can be used as a raw material for biorefining and so for biofuels production. Indeed, proteins are abundantly present as final waste of lignocellulose processing [12]. We focused our attention on the strategy which takes advantage of ketoacids as intermediates in amino acids biosynthesis and degradation metabolism to produce fusel alcohols in the yeast *S. cerevisiae*. While the pathway to isoketovalerate was better elucidated and recently successfully exploited for isobutanol formation in *S. cerevisiae* [13-17], butanol production from ketovalerate was never experimentally measured.

S. cerevisiae have one or more carrier systems specific for each aminoacid,

even if they are not all currently known. Among them, the general aminoacids permease, encoded by *GAP1* gene, is involved in glycine transport [18]. In the cytosol glycine can be catabolised in different ways, based on nutritional requirements. For example, it can be converted into serine through serine hydroxymethyltransferase enzyme (Shm2) [19] or into CO2 and NH3 through the enzymatic complex of glycine decarboxylase enzyme (GDC) [20].

Villas-Bôas and co-workers [21] have *in silico* proposed the generation of glyoxylate as a consequence of glycine deamination. Moreover, the authors described the formation of α-ketovalerate and α-isoketovalerate as intermediates of the same pathway through not identified reactions. Starting from these indications and knowing from literature that α-ketovalerate can be converted into butanol [22], and that α-isoketovalerate can be converted into isobutanol [23], in this study yeast cells were cultivated with glycine, observing the formation of both alcohols. By deeply investigating the literature, it was first (i) hypothesized and then (ii) biochemically demonstrated step by step the butanol and isobutanol production through the glycine degradation pathway via glyoxylate and α-ketoacids intermediates (Figure 1).

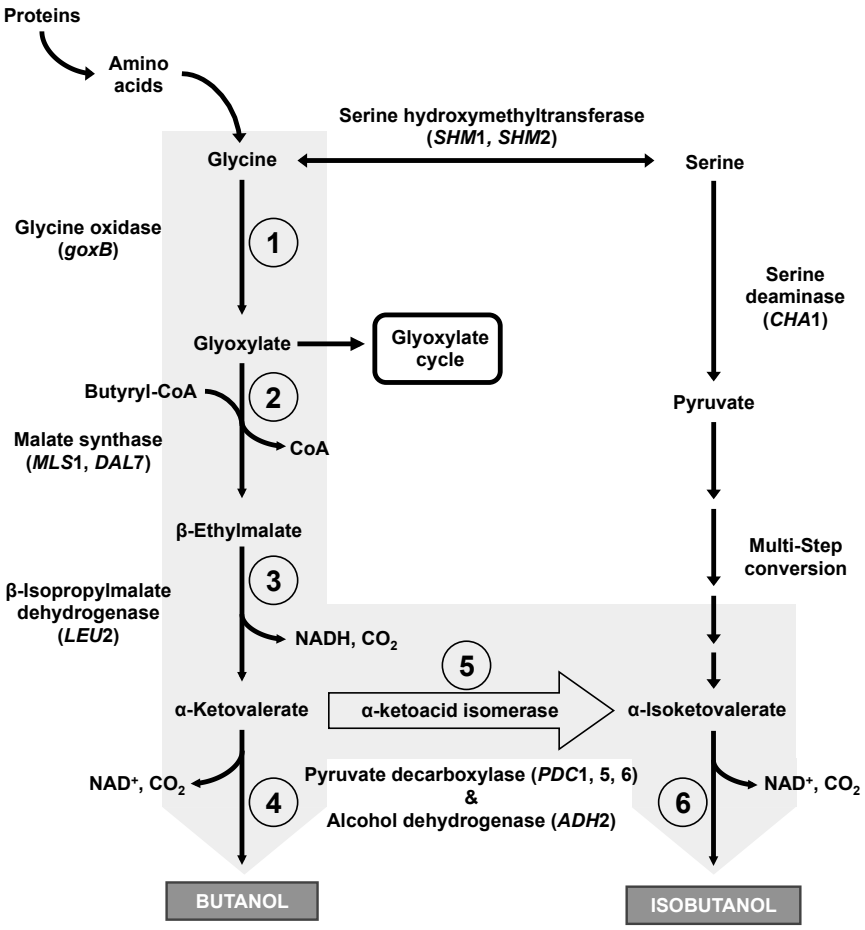

Figure 1: A novel pathway for butanol and isobutanol production. Metabolic pathway for butanol and isobutanol production from glycine in *S. cerevisiae* through the glyoxylate, β-ethylmalate and α-ketoacids intermediates (grey background arrows). The enzymatic activities involved and the associated gene(s) are also represented. Numbers inside circles indicates the steps of the pathway discussed in this study. The hypothesized isomerisation of α-ketovalerate into α-isoketovalerate is indicated by black arrow.

Additionally, at least one possible gene encoding for the enzymes responsible for butanol production was suggested.

Glycine deaminase has been hypothesized to catalyze the glycine conversion into glyoxylate [21], the first step of the pathway. In *S. cerevisiae* the gene encoding for this enzyme has not been annotated yet. However, *Bacillus subtilis* gene *goxB* [24] encodes for a glycine oxidase that can catalyze this conversion (Figure 1, circle 1). For the second step, similarly to what happens in *Pseudomonas aeruginosa* [25], the glyoxylate condensation with butyryl-CoA to yield the β-ethylmalate intermediate was hypothesized (Figure 1, circle 2). β-ethylmalate might be then converted into α-ketovalerate through a β-isopropylmalate dehydrogenase enzyme (Figure 1, circle 3), as described in *E. coli* [22]. The final step is well depicted by the Ehrlich pathway: the α-ketovalerate is converted into butanol through a reductive decarboxylation reaction [26] (Figure 1, circles 4 and 6).

Summarizing, the single steps of the proposed pathway have been already described in literature, even if in different pathways and from different microorganisms: moreover, in some cases indications were provided only as enzymatic reactions. In this work it was demonstrate that in the yeast *S. cerevisiae* thanks to these reactions glycine can be converted into butanol.

RESULTS

Butanol and isobutanol can be obtained from glycine

All the production experiments described here and in the next paragraphs were performed in two different *S. cerevisiae* genetic background, BY and CEN.PK (see Methods for further details), proving the production of butanol and isobutanol from glycine. Here butanol and isobutanol kinetics and titers related to the CEN.PK background are shown. It has to be underlined that the production levels obtained in the BY4741 background were consistent, but always lower. Because of the convenience of using single gene deletion mutants available from the Euroscarf collection, all the experiments related to the characterization of the enzymatic activities were performed using the BY4741 background. Yeast cells were grown in minimal defined medium and in the same medium but using glycine (15 g/L) instead of ammonium sulphate as nitrogen source (see Methods for details). The substitution was preferred to the addition to promote the glycine uptake, a poor nitrogen source if compared to ammonium sulphate, glutamine or glutamate [27]. Butanol and isobutanol accumulations were evaluated at different time point after the inoculum (Figure 2).

It was confirmed that butanol does not accumulate in minimal ammonium sulphate medium, while isobutanol does (Left panel diamond symbols, 46.5 mg/L) since it can derive from other pathways (see Figure 1). When glycine is added as substrate, both butanol and isobutanol accumulate over time, reaching a registered maximum of 92 and 58 mg/L with yields of 0.6% and 0.4%, respectively (Figure 2, Right panel), together with a glycine consumption.

The described experiment indicates therefore that (*i*) the butanol production

requires glycine as substrate and that (*ii*) the measured isobutanol might only partially derive from the glycine degradation pathway. As shown in the Figure 1, it can result partially from the serine degradation pathway. In fact, if serine (20 g/L) was used as substrate, almost 80 mg/L of isobutanol were obtained at 24 hours after the inoculation, while no butanol was detected (data not shown).

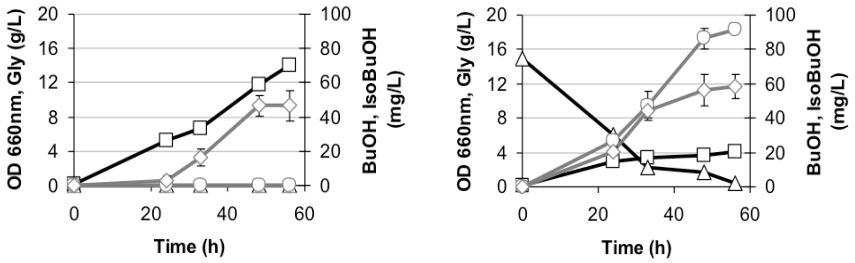

Figure 2: Butanol and isobutanol accumulation from glycine. Yeast cells were grown in Verduyn medium with ammonium sulphate (5 g/L, **left panel**) or glycine (15 g/L, **right panel**) as nitrogen source. Biomass accumulation (square), glycine consumption (triangle), butanol (circle) and isobutanol (diamond) productions are shown. The data presented here are representative of three independent experiments.

In the following sections the proposed pathway was characterize step by step. The substrates used are glycine, glyoxylate, α-ketovalerate and α-isoketovalerate. Unfortunately, the intermediate β-ethylmalate is not commercially available and for this reason a coupled enzymatic reaction starting from glyoxylate as initial substrate was planned to circumvent this problem.

The first reaction of the pathway: from glycine to glyoxylate

The first step is the conversion of glycine to glyoxylate, by a glycine deaminase activity [21]. Since no genes are annotated in yeast encoding for

this function and being the identification of a putative gene encoding for the desired function not trivial, a similar activity in other microorganisms was searched. It has been described that in *B. subtilis* the glycine conversion into glyoxylate is catalyzed by the glycine oxidase enzyme, encoded by *goxB* gene (Figure 3A). This enzyme catalyzes the primary amines oxidative deamination to yield the corresponding α-ketoacid, with concomitant ammonium and hydrogen peroxide production. The *B. subtilis* glycine oxidase is a homotetrameric flavoprotein which effectively catalyzes the oxidation of sarcosine (N-methylglycine), N-ethylglycine and glycine. Lower activities using D-alanine, D-valine, and D-proline as substrates were described although no activities were shown on L-amino acids and other D-amino acids [24]. Consequently, the *B. subtilis goxB* gene was synthesized with an optimized codon usage (see Additional file 1) for *S. cerevisiae* (*goxB* opt) and constitutively expressed in yeast. The heterologous enzymatic activity was tested using an in vitro assay for glycine oxidase (as described in the Methods section [28]), Figure 3B. As expected, in the control (transformed with the empty vector) as well as in the *goxB* opt overexpressing strains the assay revealed the desired activity, being 1.5 fold higher in the recombinant yeast. It has to be mentioned that overall the measured activities are quite low: however, it might be that the assay needs to be optimized. In fact, the activity measured in total protein extract from *E. coli* BL21 strain overexpressing the *B. subtilis goxB* gene was ~ 4.E-03 U/mg proteins (corresponding to ~ 0.004 U/mL), against 0.4 U/mL reported in literature for the purified enzyme [28].

The effect of glycine oxidase overexpression on butanol and isobutanol accumulation was preliminary tested in the two yeast genetic backgrounds, grown like described for Figure 2. In both cases, in the strains overexpressing the *goxB* opt gene we observed a higher butanol and

isobutanol accumulation, being about 30% and 15%, respectively (Figure 3, dark and pale gray columns, respectively). The data prove that an activity responsible for glycine conversion into glyoxylate is the first step leading to butanol accumulation, and it is also shown a first example of how to improve said activity (Figure 3, upper bars).

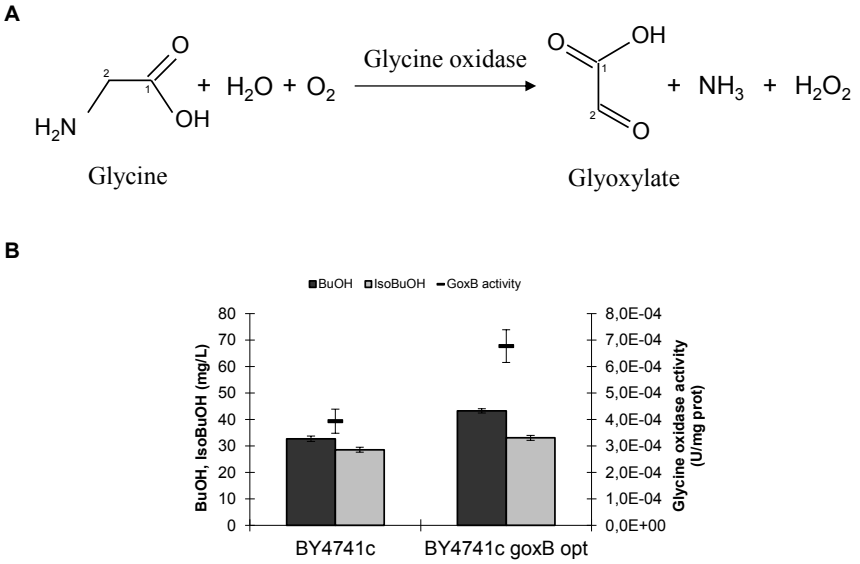

Figure 3: Glycine oxidase: reaction and enzymatic activity assay. (**A**) Reaction catalysed by glycine oxidase. The carbons of the molecules were numbered. (**B**) Glycine oxidase activity (upper bars), butanol (dark gray columns) and isobutanol (pale gray columns) for the wild type and modified yeast strains overexpressing the bacterial *goxB* gene optimized for the yeast codon usage. The data presented here are representative of three independent experiments.

The second reaction of the pathway: from glyoxylate to β-ethylmalate

In yeasts, no activity able to catalyze the condensation of glyoxylate with butyryl-CoA to form β-ethylmalate has been described yet. However, the malate synthase enzyme catalyzes a similar reaction: the glyoxylate condensation with acetyl-CoA to form malate [29]. In *S. cerevisiae* two

isoforms of malate synthase are described, encoded by *MLS1* and *DAL7* genes [29]. *MLS1* expression is repressed by glucose and induced when cells are growing on non-fermentable carbon sources, such as fatty acid, ethanol or acetate. *DAL7* encodes for an enzyme recycling the glyoxylate generated during allantoin degradation. Its expression is controlled by the nitrogen source present in the medium, resulting repressed in the presence of rich nitrogen sources, such as asparagine and ammonium, and derepressed in the presence of poor nitrogen sources, such as proline [29]. It was hypothesized first and then evaluated if butyryl-CoA could also be a substrate of malate synthase enzyme, considering the structural analogy with acetyl-CoA (Figure 4A).

BY4741c and BY4741c *mls1Δ* strains were grown in rich YPD medium and malate synthase activity was detected in the presence of butyryl-CoA as acyl-CoA donors, using a modified TNB-based assay (see Methods). YPD medium was used to have a cultural condition in which both Mls1 and Dal7 were present at similar level, as reported in literature [29]. Remarkably, when butyryl-CoA was added as acyl-CoA donor a malate synthase activity was detected, even if at lower value if compared to the activity measured in the presence of acetyl-CoA (1 U/mg proteins versus 2 U/mg proteins, respectively, data not shown). Based on our information, this is the first experimental evidence that a yeast malate synthase can accept butyryl-CoA as acyl-CoA donor. The *MLS1* deletion negatively affects the activity (about 25% of reduction, Figure 4B) and the same impairment is caused by *DAL7* deletion (data not shown), suggesting that the two enzymes might similarly contribute to the reaction of interest.

Moreover the capability of the yeast malate synthase to accept other acyl-CoA donor, such as exanoyl-CoA, octanoyl-CoA and decanoyl-CoA, was preliminary tested in the BY4741c wild type and *mls1Δ* strains (Figure 4B). A

malate synthase activity was detected for all of this cofactor in both strains and also in these cases the *MLS1* deletion led to a decreased activity.

If our hypothesis is correct, feeding the cells with glyoxylate should result in butanol and isobutanol accumulation. To determine favourable production conditions, yeast cells were grown in minimal medium in the absence or presence of different amount of glyoxylate (0.5, 1, 5 g/L) at different pH (2.5 and 5.5) values. Figure 4C confirms the butanol and isobutanol accumulation, not detectable if glyoxylate is absent (data not shown). In the reported example the production was obtained starting with 5 g/L of glyoxylate at pH 2.5. This pH value has been selected to facilitate the diffusion of undissociated glyoxylic acid inside the cells, since no carrier for this metabolite is reported in literature. In this condition the glyoxylate was almost totally consumed. Cells accumulated during the time about 20 and 30 mg/L of butanol and isobutanol, respectively. This confirms the involvement of glyoxylate as intermediate in the formation of the desired alcohols. At the moment we have no explanation for the higher isobutanol accumulation. One possibility could be that in case of high amount of glyoxylate, Agx1 [30] catalyzes its conversion into glycine, shifting the reaction trough serine formation (see Figure 1).

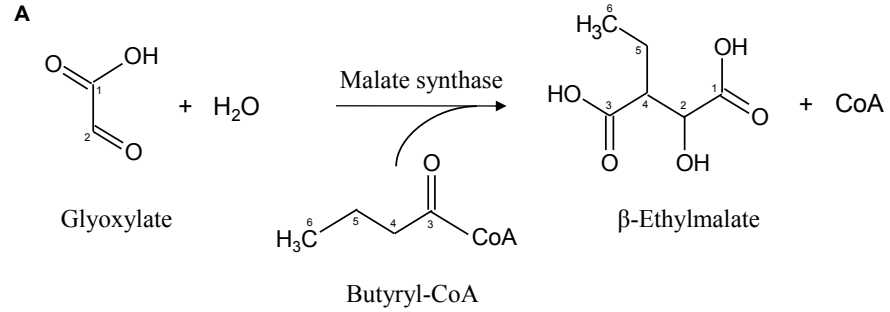

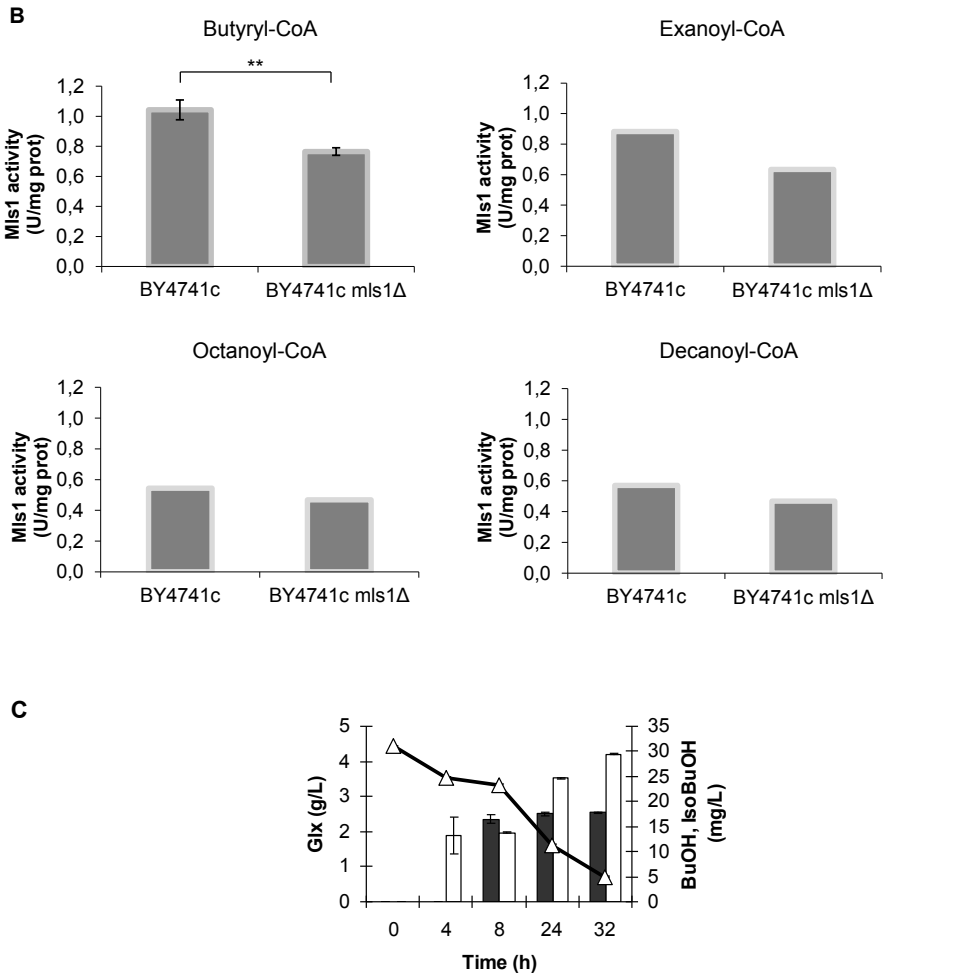

Figure 4: Malate synthase activity and glyoxylate bioconversion into butanol and isobutanol. (**A**) Glyoxylate conversion reaction performed by malate synthase enzyme in the presence of butyryl-CoA. The carbons of the molecules were numbered. (**B**) Malate synthase activity for the glyoxylate conversion into β-ethyl/propyl/butyl/pentyl malate. Malate synthase activity was assayed using butyryl-CoA, exanoyl-CoA, octanoyl-CoA and decanoyl-CoA as donor group in the BY4741c and BY4741c *mls1Δ* strains. The data regarding the experiment conduced in the presence of butyryl-CoA is representative of three independent experiments. $p \leq 0,01$ = ** (**C**) Glyoxylate bioconversion. Butanol (full columns) and isobutanol (empty columns) production as well as glyoxylate consumption (triangle) measured at different time point. The data presented here are representative of three independent experiments.

The third reaction of the pathway: from β-ethylmalate to α-ketovalerate

In *E. coli* the β-isopropylmalate dehydrogenase enzyme, encoded by the *leuB* gene, catalyzes the conversion of β-isopropylmalate into α-ketoisocaproate. Shen and Liao [22] have demonstrated the possibility to use this enzyme to additionally catalyze the conversion of β-ethylmalate into α-ketovalerate in *E. coli* cells (the reaction is depicted in Figure 5A). *LEU2* is the homologous of *leuB* in *S. cerevisiae* [31]. Therefore, by using the BY4741 strain (deleted in *LEU2*) and the same strain transformed with a *LEU2* multicopy plasmid, the contribution of the Leu2 activity in the novel pathway was tested. The activity assay was performed using two coupled reactions, since β-ethylmalate is not commercially available. In the first reaction, glyoxylate and butyryl-CoA should be converted into β-ethylmalate by the malate synthase activity, as described in the previous paragraph. The second coupled reaction, catalyzed by the Leu2 activity, utilizes the produced β-ethylmalate to generate α-ketovalerate and releasing NADH as reduced equivalent. Said cofactor can be spectrophotometrically measured to determine the activity. In the BY4741 *LEU2* overexpressing strain the activity was about 5 fold higher when compared to the BY4741 *leu2Δ* strain, being 0.1 and 0.02 U/mg proteins, respectively (Figure 5B).

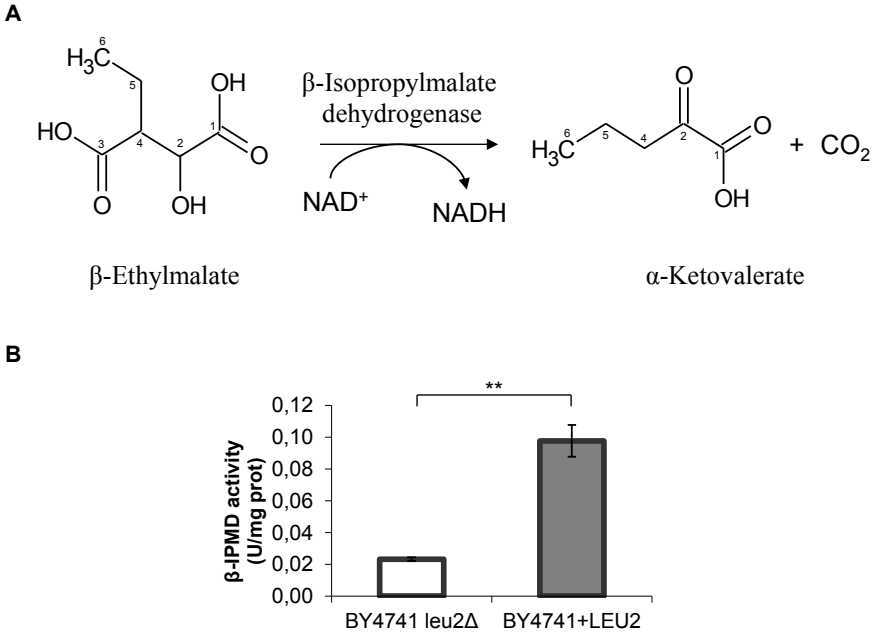

Figure 5: The β-isopropylmalate dehydrogenase involvement in the glycine degradation pathway. The β-isopropylmalate dehydrogenase activity was tested in a coupled reaction using glyoxylate as substrate instead of β-ethylmalate (not commercial available). The carbons of the molecules were numbered. (**A**) Reaction catalysed by the β-isopropylmalate dehydrogenase enzyme. (**B**) Activity of β-isopropylmalate dehydrogenase measured in yeast strain *leu2Δ* (empty column) and overexpressing *LEU2* gene (grey column). The data presented here are representative of three independent experiments. $p \leq 0,05$ = *; $p \leq 0,01$ = **; $p \leq 0,001$ = ***; $p > 0,05$ = n.s.

When *MLS1* or *DAL7* are deleted while Leu2 is present, the dehydrogenase activity significantly decreases, confirming that β-ethylmalate is the substrate of the reaction (Table 1). Table 1 reports all the combinations tested and the registered activities. Interestingly, the residual activity detected whenever *LEU2* is deleted suggests that other(s) activity(ies) might be responsible for β-ethylmalate conversion.

Concluding, these data indicate that the presence of *LEU2* coupled with malate synthase activity guarantees the glyoxylate conversion into

α-ketovalerate.

Gene			β-IPMD Activity (U/mg prot)
MLS1	***DAL7***	***LEU2***	
+	+	++	0.098 ± 0.010
+	+	-	0.023 ± 0.001
+	-	++	0.019 ± 0.002
+	-	-	0.016 ± 0.002
-	+	++	0.021 ± 0.002
-	+	-	0.018 ± 0.002

Table 1: β-Isopropylmalate dehydrogenase activity measured with assay coupling the reactions catalyzed by Mls1 and Leu2. The symbols "+" indicate the wild type copy or "++" the overexpression of the corresponding gene in the table. The symbol "-" indicate the deletion of the gene. The data presented here are representative of three independent experiments.

The last step: from α-ketoacids to butanol and isobutanol

The last step necessary in the glycine degradation to produce the desired alcohols is the reductive decarboxylation of α-ketovalerate into butanol and of α-isoketovalerate into isobutanol, Figure 6A.

The conversion of α-ketovalerate into α-isoketovalerate was proposed to occur through a dehydratation reaction, catalyzed by dihydroxyacid dehydratase enzyme [21]. However, at the best of our information, no experimental evidences are reported up to now. By looking at the chemical structure of the two ketoacids, this reaction might require an isomerization, like proposed in Figure 1.

The conversion of α-ketovalerate into butanol requires two reactions: in the first one α-ketovalerate decarboxylation generates the corresponding aldehyde; in the second one the aldehyde is reduced to alcohol, butanol in this case (Figure 6A, upper part). It was reported that in *S. cerevisiae* α-keto-β-methylvalerate, α-ketoisocaproate and α-isoketovalerate [32] can be decarboxylated to the α-ketoacids by pyruvate decarboxylases (Pdc). Going

one step forward, Brat *et al.* reported that through the α-isoketovalerate decarboxylation isobutanol can be produced [16], starting from valine as substrate. However, to avoid co-current pyruvate decarboxylation into ethanol, the authors replaced the *PDC* genes with the decarboxylase encoded by *ARO10* gene, which has no activity on pyruvate [16].

Yeast no data are available about a possible α-ketovalerate decarboxylation in yeast. When pyruvate, α-ketovalerate and α-isoketovalerate were used as substrates, the activities measured using an assay for Pdc activity were 722 ± 2.3, 1.75 ± 0.3 and 0.3 ± 0.05 U/mg proteins, respectively. The involvement of pyruvate decarboxylase in the last reaction was also demonstrated by measuring the butanol and isobutanol production in a *PDC1, 5, 6* deleted strain. In the presence of α-ketovalerate (1.1612 g/L, 10 mM) as substrate, the deletion of all three isoforms of pyruvate decarboxylase significantly decreases the butanol and isobutanol production, as shown in bioconversion experiment (Figure 6B). In particular, the butanol titer was 5 times lower than in wild type strain, 118 versus 583 mg/L respectively. By incubating the triple *PDC* deleted strain with α-isoketovalerate no isobutanol accumulation was observed (data not shown).

It is important to underline that in the presence of α-ketovalerate as substrate both butanol and isobutanol are produced (Figure 6C, Left panel) in the parental strain. Considering that more isobutanol is obtained when glycine is added to glucose minimal medium (Figure 2), we could hypothesize that α-isoketovalerate might partially derive from α-ketovalerate and that this reaction is probably irreversible, since in the presence of α-isoketovalerate only isobutanol accumulation was observed (Figure 6C, Right panel).

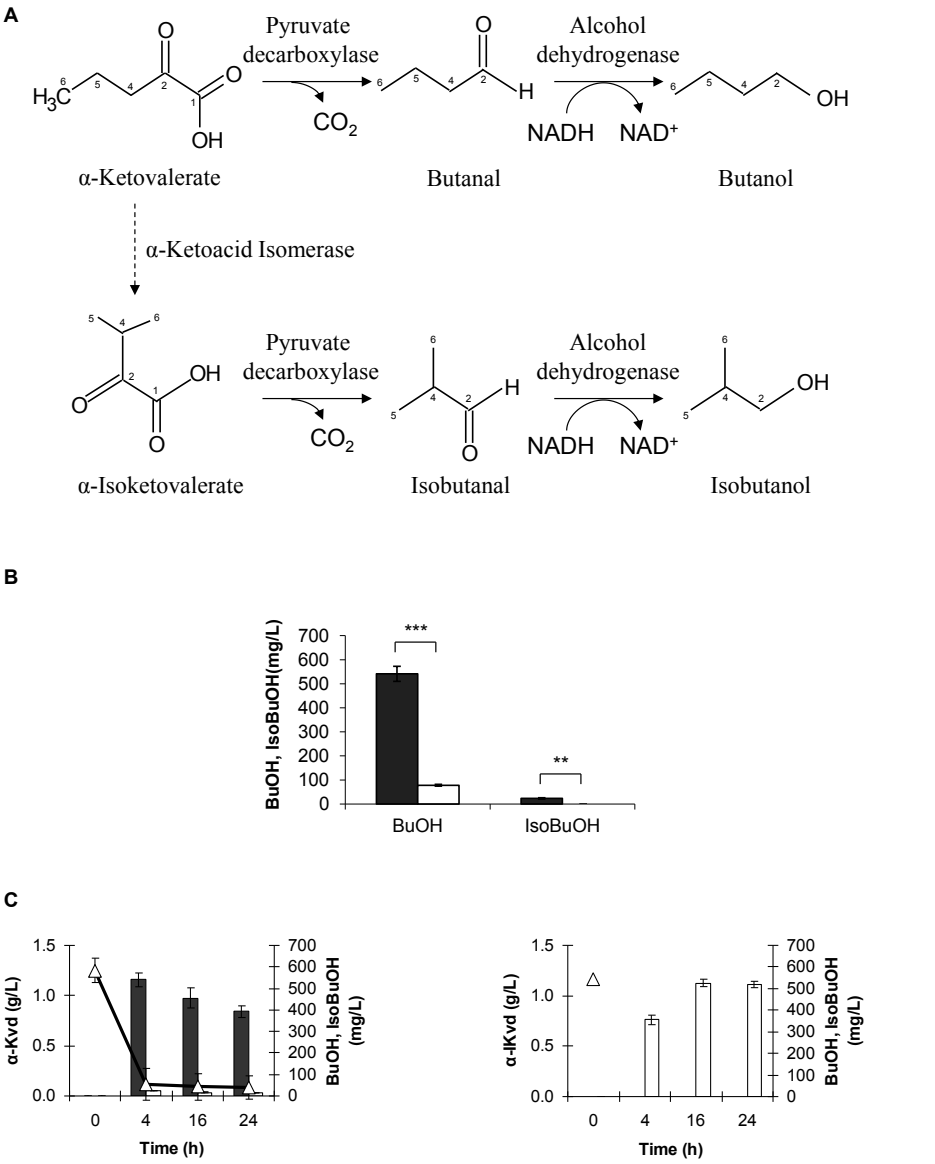

Figure 6: Pyruvate decarboxylase activity and α-ketoacids bioconversion into butanol and isobutanol. (**A**) α-ketovalerate and α-isoketovalerate conversion reaction performed by pyruvate decarboxylase enzyme. The carbons of the molecules were numbered. (**B**) Pyruvate decarboxylase deletion effect on butanol and isobutanol accumulation using α-ketovalerate as substrate. Parental (full column) and *PCD1, 5, 6* deleted strains (empty column). The data presented here are

representative of three independent experiments. $p \leq 0,05$ = *; $p \leq 0,01$ = **; $p \leq 0,001$ =***; $p > 0,05$ = n.s. (**C**) α-Ketovalerate (Left panel) and α-isoketovalerate (Right panel) bioconversion. Butanol (dark grey), isobutanol (white) and α-ketovalerate consumption (triangle) were reported. For α-isoketovalerate (triangle), the sole estimated initial concentration is given. The data presented here are representative of three independent experiments.

The glyoxylate conversion into butanol and isobutanol requires Mls1, Leu2 and Pdc(s) activities

To further prove the link between glycine and the fusel alcohols we developed an *in vitro* assay in which all reactions of the proposed pathway are coupled. To perform this assay we measured the pyruvate decarboxylase activity using glycine as substrate, monitoring the decrement of OD 340 nm since NADH is consumed during the last reaction. No data were obtained. We believe that this could be related to (*i*) a lower conversion of glycine to glyoxylate and/or to (*ii*) the very different physiochemical assay conditions required by glycine oxidase (the first enzyme of the pathway) in respect to all the other enzymes. Indeed, a Pdc activity was detected when glyoxylate was used as substrate, confirming the conversion of glyoxylate to the α-ketovalerate.

Figure 7 shows the complete panel of the Pdc activities measured in the different strains. The higher activity was registered in the wild type strain overxpressing the *LEU2* gene, the minimal (almost undetectable) in the double *MLS1*/*LEU2* deleted strain and an intermediate situation when only one of the two genes was deleted. To be more precise, the *LEU2* deletion affects more the activity, very likely because in the case of *MLS1* deletion, Dal7 is able to replace its function (and *vice versa*) [29].

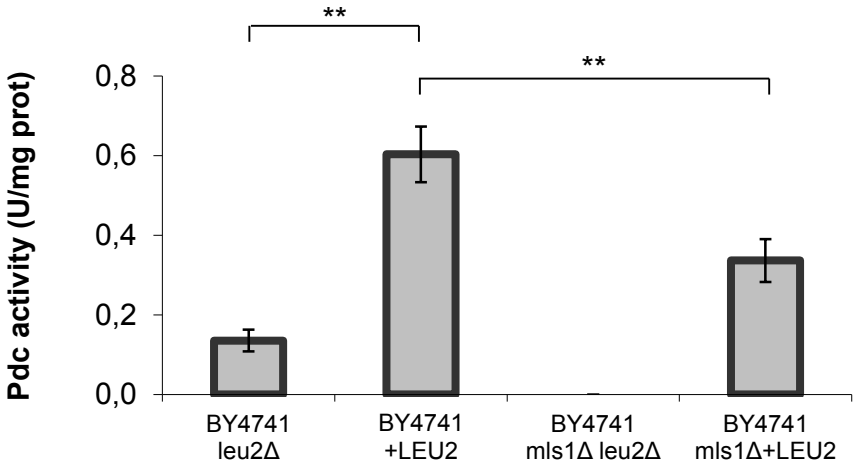

Figure 7: The evidence of glyoxylate degradation through the Mls, β-IPMD and Pdc(s) activities. The *MLS1* deletion effect was evaluated coupled with the *LEU2* deletion or overexpression. The data presented here are representative of three independent experiments. $p \leq 0,05$ = *; $p \leq 0,01$ = **; $p \leq 0,001$ = ***; $p > 0,05$ = n.s.

CONCLUSIONS

This study describes a novel pathway to produce butanol and isobutanol in the yeast *S. cerevisiae* through the glycine degradation pathway.

The entire pathway was characterized identifying for each step at least one enzymatic reaction with at least one relative gene for butanol production. 92 mg/L and 58 mg/L of butanol and isobutanol respectively were produced starting from 15 g/L of glycine as substrate.

It might be speculated that butanol derives from butyryl-CoA and that glycine is solely used to drive the flux. Remarkably, the proposed pathway implies catalytic reactions that justify how glycine is not simply burnt to carbon dioxide, but is an effective co-substrate for the butanol production, as highlighted by the numbered carbons (see Figures 3, 4, 5 and 6, panels A). Moreover, as reported by Villas-Boas (2005), when ^{13}C-labeled glycine was used as the sole nitrogen source a fraction of α-ketovalerate was labeled with two ^{13}C atoms [21]. Consequently, at least one of the two carbons of the glycine was incorporated into butanol. On the contrary, in the pathway recently proposed by [33] no carbon atoms from exogenous ^{13}C-labeled threonine were incorporated into butanol.

Despite the yield on glycine is still quite low, it is important to consider that the best butanol production reported for engineered *S. cerevisiae* was only 14.1 mg/L [34]. Diversely, the amount of isobutanol accumulated can not be simply compared with those reported in literature, 0.63 g/L, by engineered *S. cerevisiae* [16]. In fact, it does not represent the final main product in the proposed glycine degradation pathway, but it derives from the conversion of glycine or α-ketovalerate fractions. Moreover it should be underlined that butanol and isobutanol were obtained through endogenous activities which are in general involved in other reactions and specific for other substrates.

Therefore, it can be anticipated that there are many different possibilities for optimizing the pathway, considering every single enzyme involved, the pool of substrates and their compartmentalization.

Remarkably, here we demonstrated that the malate synthase is active in the presence of several acyl donors, including hexanoyl-CoA, octanoyl-CoA and decanoyl-CoA. These data are novel, and are potentially relevant in the view of a possible simultaneous production of higher alcohols with longer chains, despite they have not been measured yet by gas chromatography. A biofuel made of a mixture of higher alcohols would be highly desirable. From an economical point of view the production of higher alcohols starting from purified glycine cannot be considered as a sustainable process. Metabolic engineering and synthetic biology can then help in the construction of a yeast redirecting sugars to glycine production, and from there to optimize the sole butanol production, but this appears at the moment as a long way to run. However, an alternative seems closer to reality: a considerable fraction of proteins accumulate as waste product deriving from exhausted biomasses of different microbial productions and currently is not fully absorbed by the market [12]. It is then possible to imagine a side-stream process of production which is based on protein hydrolysates; the different aminoacids fed to a yeast strain optimized for desired fusel alcohol production could generate a blend with good properties as biofuel [12], adding value and completing the concept of biorefinery.

Considering the potentiality of *S. cerevisiae* as ethanol producer and considering the potentiality of the aminoacid degradation pathway for fusel alcohol productions [12], it really seems the right moment to intensify the effort in studying and improving yeast tolerance to a mixture of different organic solvents.

METHODS

Strains and growth conditions

The S. cerevisiae strains used in this study were CEN.PK 102-5B (MAT*a*,*ura3-52*, *his3-11*, *leu2-3/112*, *TRP1*, *MAL2-8c*, *SUC2* - Dr. P. Kötter, Institute of Microbiology, Johann Wolfgang Goethe-University, Frankfurt, Germany) [35] and BY4741 (MAT*a*, *ura3 Δ0*, *leu2 Δ0*, *met15 Δ0*, *his3 Δ1*) (EUROSCARF collection, Heidelberg, Germany). The strains BY4741 *mls1Δ* (*MATa*; *his3 Δ1*; *leu2 Δ0*; *met15 Δ0*;*ura3 Δ0*; *YNL117w::kanMX4*) and BY4741 *dal7Δ* (*MATa*; *his3 Δ1; leu2 Δ0; met15 Δ0; ura3 Δ0*; *YIR031c::kanMX4*) are provided by EUROSCARF deleted strain collection (EUROSCARF collection, Heidelberg, Germany). The strain deleted in all three isoform of pyruvate decarboxylase (*Δpdc1, 5, 6*) is CEN.PK RWB837 (*MATa; pdc1::loxP, pdc5::loxP, pdc6::loxP, ura3-52*) [36]. Strains designed with "c" correspond to the respective parental strain transformed with empty plasmid(s) (see below) to render them prototrophic. Strains designed with "*goxB* opt" are the corresponding parental strain transformed with plasmid pYX212 (see below) with the *B. subtilis goxB* coding sequence optimized for the *S. cerevisiae* codon usage. *goxB* opt gene was expressed under the control of the *S. cerevisiae TPI1* promoter. Yeast transformations were performed according to the LiAc/PEG/ss-DNA protocol [37]. All the parental and transformed strains are reported in the Table 2.

Parental strain	
Strain	**Genotype**
CEN.PK 102-5B	*MATa, ura3-52, his3-11, leu2-3/112, TRP1, MAL2-8c, SUC2*
CEN.PK RWB837	*MATa, pdc1::loxP, pdc5::loxP, pdc6::loxP, ura3-52*
BY4741	*MATa, ura3Δ0, leu2Δ0, met15Δ0, his 3Δ1*
BY4741 *mls1Δ*	*MATa; his3 Δ1; leu2 Δ0; met15 Δ0; ura3 Δ0; YNL117w::kanMX4*
BY4741 *dal7Δ*	*MATa; his3 Δ1; leu2 Δ0; met15 Δ0; ura3 Δ0; YIR031c::kanMX4*

Plasmid		
Expression plasmid	**Segregation**	**Markers, genes**
pYX212	multicopy (2μ derived)	*URA3*
pYX212*goxB* opt	multicopy (2μ derived)	*URA3*, optimised *goxB*
pYX022	integrative	*HIS3*
pYX242	multicopy (2μ derived)	*LEU2*

Transformed strain		
Strain	**Plasmids**	**Obtained strain**
CEN.PK 102-5B	pYX212, pYX022, pYX242	CEN.PKc
BY4741	pYX212, pYX022, pYX242	BY4741c
BY4741	pYX212*goxB* opt, pYX022, pYX242	BY4741c *goxB* opt
BY4741 *mls1Δ*	pYX212, pYX022, pYX242	BY4741c *mls1Δ*
BY4741 *mls1Δ*	pYX212*goxB* opt, pYX022, pYX242	BY4741c *mls1Δ* *goxB* opt
BY4741 *dal7Δ*	pYX212, pYX022, pYX242	BY4741c *dal7Δ*

Table 2: Strains and plasmids used in this work

Media composition for cell growth and bioconversion

Independent transformants and the respective control strains (at least three for each transformation) were cultivated in shake flasks with 5/1 ratio of flask volume/ medium in minimal synthetic medium with 20 g/L of glucose and supplemented with glycine, glyoxylate, α-ketovalerate or α-isoketovalerate, as specifically indicated in the experiments. YPD and YPGE (for the triple *PDC* deleted strains) media were prepared as follows: yeast extract 1% (w/v), tryptone 2% (w/v) and glucose 2% (w/v) for the YPD. In the YPGE the glucose was replaced with glycerol 1% (v/v) and ethanol 1% (v/v). All strains were grown at 30°C on orbital shaker at 160 rpm for 72 hours.

Kinetic experiment

The butanol and isobutanol production starting from glycine (Figure 2) was performed by growing the cells in Verduyn medium [38] with glucose 20 g/L and glycine 15 g/L as substrates.

Bioconversion experiment

The bioconversion experiments were performed in two phases: 1) cells were grown in YPD or YPGE (for the triple PDC deleted strains) medium until the stationary phase; 2) cells were collected by centrifugation (10 min at 4000 rpm) washed once with water and inoculated in appropriate medium to perform the bioconversion phase. The medium for glyoxylate bioconversion (Figure 4C) was minimal synthetic medium with glucose 20 g/L and glyoxylate 5 g/L at pH 2.5. The medium for α-ketovalerate (or α-isoketovalerate) bioconversion (Figure 6C) was minimal synthetic medium with glucose 20 g/L and α-ketovalerate (or α-isoketovalerate) 1.1612 g/L (corresponding to 10 mM).

Gene amplification and plasmids construction

The *B. subtilis goxB* gene was designed with codon usage adaptation for *S. cerevisiae* by Eurofins MWG Operon. In the Additional file 1 was reported the complete sequence of *goxB* synthesized. *goxB* opt gene was subcloned into the multicopy yeast expression plasmid pYX212 (R&D Systems, Inc., Wiesbaden, D, *URA3* marker), resulting in the plasmid pYX212*goxB* opt. The heterologous gene is under the control of the *S. cerevisiae TPI1* promoter. For the construction of the plasmid pYX212*goxB* opt, the recipient vector was EcoRI cut, blunted and dephosphorylated, while the insert was EcoRI blunt excised from the Eurofins plasmid. DNA manipulation, transformation and cultivation of *E. coli* (Novablue, Novagen) were performed following standard protocols [39]. All the restriction and modification enzymes utilised are from NEB (New England Biolabs, UK) or from Roche Diagnostics.

Cell growth and metabolites determination

The cellular growth was spectrophotometrically monitored at 660nm and was reported as variation of the optical density (OD) as a function of time (h). The amount of extracellular glucose, butanol, isobutanol, glyoxylate and α-ketovalerate were determined by HPLC based method using H_2SO_4 5 mM as mobile phase and Aminex HPX-87P column, 300 × 7.8 mm with a polystyrene divinylbenzene-based matrix (BioRad). The glycine quantification was performed using a previously described assay [40].

Determination of enzymatic activities

Exponentially growing cells were harvested by centrifugation at 4000 rpm for 10 min and washed with cold deionised water. The cell pellet was then re-suspended in 25 mM Tris-HCl pH 8.0 with protease inhibitor cocktail (Roche diagnostics, Cat. No. 04906837001) and 1 mM of phenylmethylsulfonyl

fluoride (PMSF) and mechanically disrupted using glass microbeads (600 µm, Sigma-Aldrich). Cells debris was removed by centrifugation at 14000 rpm for 10 min at 4°C and the clarified crude ex- tract was used for enzymatic analysis. The protein concentration in cell-free extracts was estimated according to Bradford [41] using bovine serum albumin as reference. Enzyme activities were measured on cell-free extracts by spectrophotometric assays. Activities were expressed as U/mg of total proteins.

Glycine oxidase activity

Glycine oxidase activity was assayed spectrophotometrically via determination of H_2O_2 with an enzyme-coupled assay using horseradish peroxidase and o-dianisidine, as previously described with some modifications [28]. The assay was performed on a final volume of 1 ml as follows: Tris-HCl 100 mM pH 8, phosphoric acid 10 mM, glycine 50 mM, o-dianisidine 1 mM, FAD 0.198 µM, horseradish peroxidase 14.72 U/mL, cell-free protein extract (0.5 mg/mL). The reaction was incubated at 37°C for 90 minutes and yellow colour, developed by o-dianisidine oxidation, was monitored at 530 nm. The glycine oxidase activity was expressed as U/mg of total proteins using the following equation:

Activity (U=mg prot tot)

=(((OD 530nm/min)/ε)·dilution factor)/mg prot tot

Were ε=8.3·1/(mM·cm)

One glycine oxidase unit is defined as the amount of enzyme that converts 1 mole of substrate (glycine) per minute at 25°C.

Malate synthase activity

The malate synthase activity was performed as described in Sigma-Aldrich protocol [42] using acetyl-CoA (or butyryl/exanoyl/octanoyl/decanoyl-CoA) + glyoxylate. The assay take into consideration that glyoxylate condensation with acetyl-CoA (or butyryl/exanoyl/octanoyl/decanoyl-CoA) produces malate (or β-ethyl/propyl/butyl/pentylmalate) and CoA. The free CoA can react with the Ellman reagent DTNB (5,5'-Dithio-bis(2-Nitrobenzoic Acid)) which reacts with free thiol groups, producing CoA-derivative and TNB (5-Thio-2-Nitrobenzoic Acid) [43]. The assay was performed on a final volume of 1 ml as follows: imidazole 50 mM pH 8, $MgCl_2$ 10 mM, acyl-CoA 0.125 mM, glyoxylate 5 mM, DTNB 0.05 µM, cell-free protein extract. The quantity of TNB produced is in stoichiometric ratio (1:1) with free thiol groups and was monitored spectrophotometrically at 412 nm. The malate synthase activity was expressed as U/mg of total proteins using the following equation:
Activity (U=mg prot tot)

=(((OD 412nm/min)/ε)·dilution factor)/mg prot tot

Were ε=13.6/(mM·cm)

β-isopropylmalate dehydrogenase activity (using glyoxylate and butyryl/exanoyl/octanoyl/decanoyl-CoA as substrates)

The β-isopropylmalate dehydrogenase enzyme catalyzes the NAD-dependent oxidation of the substrate with simultaneously conversion of NAD^+ to NADH. The activity was spectrophotometrically determined at 340 nm. The assay was performed on a final volume of 1 mL in cuvette with imidazole 50 mM pH 8, $MgCl_2$ 10 mM, acyl-CoA 0.125 mM, glyoxylate 0.5 mM, NAD^+ 1.575 mM. After incubation at 30°C for 10 min cell-free protein extract (0.6 mg/mL) were added and increasing of absorbance at 340 nm

was monitored for 10 min.

The β-isopropylmalate dehydrogenase activity was expressed as U/mg total proteins using the following equation:

Activity (U=mg prot tot)

$$=(\text{OD } 340\text{nm/min} \cdot \text{dilution factor}) / \varepsilon \cdot E_v$$

Were ε is the millimolar extinction coefficient of NADH at 340 nm (6.22 · 1/(mM · cm)) and Ev is the volume of cell extract used (expressed in millilitres).

Pyruvate decarboxylase activity (using glycine or glyoxylate and butyryl-CoA as substrates)

The pyruvate decarboxylase enzyme catalyzes the decarboxylation of ketoacid to form the derived aldehyde which is reduced by alcohol-dehydrogenase $NADH^-$ dependent activity. The conversion of NADH to NAD^+ is spectrophotometrically revealed at 340 nm.

The assay was performed based on pyruvate decarboxylase assay protocol of Sigma-Aldrich [42] with some modifications. When glycine was used as substrate Tris-HCl 100 mM pH 8, phosphoric acid 10 mM, glycine 50 mM, FAD 0.198 µM, $MgCl_2$ 10 mM, butyryl-CoA 0.125 mM and NADH 0.16 mM were added in cuvette in a final volume of 1 mL. After incubation at 37°C for 30 minutes, alcohol dehydrogenase enzymatic solution (200 U/mL) and 0.2 mg/mL of cell-free extract were added. The decrease of absorbance at 340 nm was monitored for 15–30 min.

When glyoxylate and butyryl-CoA were used as substrates imidazole buffer 35 mM, $MgCl_2$ 10 mM, butyryl- CoA 0.125 mM, glyoxylate 0.5 mM and NADH 0.16 mM were added in cuvette in a final volume of 1 mL. After

incubation at 30°C for 10 min 20 µL of alcohol dehydrogenase enzyme solution (200 U/mL) and 0.2 mg/mL of cell-free extract were added. The decrease of absorbance at 340 nm was monitored for 15 min.

The activity was expressed as U/mg total proteins using the following equation: Activity (U/mg prot tot) = (OD 340nm/min · dilution factor)/ ε · Ev.

Were ε is the millimolar extinction coefficient of NADH at 340 nm (6.22 · 1/(mM · cm)) and Ev is the volume of cell extract used (expressed in millilitres).

Additional file

Additional file 1 – Sequence of synthesized *goxB* gene with codone usage optimized for *Saccharomyces cerevisiae*

ATGAAGAAACACTACGACACTGCAGTTATAGGTGGAGGGATCATT
GGTTGTGCGATATCGTACGAATTGGCCAAAACTCAACAGAAGGTT
GTCCTGCTAGAAGCTGGAGAAGTAGGTAGAAAGACTACTAGTGCT
GCTGCTGGAATGCTTGGAGCTCATGCCGAATGCGAAAACAGGGAT
GCTTTCTTTGACTTTGCCATGCACTCACAAAGGCTTTATGAACCA
GCAGGGCAAGAATTGGAAGAAGCATGTGGTATTGATATTAGACGT
CATAATGGCGGAATGTTGAAGTTAGCCTATACGGAAGAGGATATT
GCCTGTTTAAGAAAGATGGATGATTTACCTAGCGTTACCTGGTTG
TCTGCTGAAGATGCATTGGAGAAGGAACCTTATGCATCGAAAGAC
ATACTAGGTGCATCCTTTATAAAAGATGATGTGCACGTAGAACCG
TATTATGTCTGCAAAGCCTACGCTAAAGGGGCTAGGAGATATGGT
GCTGACATTTACGAACACACACAAGTCACCTCAGTGAAAAGAATG
AACGGAGAGTATTGCATCACAACATCAGGTGGAGATGTTTATGCC
GACAAGGTTGCAGTTGCTTCTGGTGTATGGTCTGGTCGTTTCTTT
TCCCAGTTAGGTTTAGGTCAACCATTCTTTCCAGTAAAAGGCGAG
TGTTTGAGTGTTTGGAATGACGATACCCCATTAACCAAGACTCTT
TACCATGACCATTGTTACGTGGTTCCAAGAAAGTCCGGCAGATTG
GTCATTGGTGCCACTATGAAACATGGTGATTGGTCTGATACACCT
GACATTGGTGGCATTGAAGCTGTGATTGGTAAGGCGAAAACGATG
CTACCAGCAATTGAGCACATGAAAATCGATAGATTTTGGGCGGGT
TTAAGACCGGGAACAAGAGATGGCAAACCCTTCATTGGGAGACAT
CCCGAAGATAGCGGCATAATCTTTGCAGCCGGTCATTTCAGAAAT
GGCATACTGCTGGCTCCTGCAACAGCTGAAATGGTCAGAGACATG
ATCTTGGAACGTCAGATAAAACAAGAGTGGGAAGAGGCATTTAGG
ATCGATAGAAAAGAGGCGGTTCATATCTAA

REFERENCES

1. Savage N: Fuel options: **The ideal biofuel**. *Nature* 2011, **474**:S9–S11.

2. Dong H, Tao W, Dai Z, Yang L, Gong F, Zhang Y, Li Y: **Biobutanol.** *Adv Biochem Eng Biotechnol* 2012, **128**:85–100.

3. Atsumi S, Cann AF, Connor MR, Shen CR, Smith KM, Brynildsen MP, Chou KJ, Hanai T, Liao JC: **Metabolic engineering of *Escherichia coli* for 1-butanol production**. *Metab Eng* 2008, **10**:305–311.

4. Steen EJ, Chan R, Prasad N, Myers S, Petzold CJ, Redding A, Ouellet M, Keasling JD: **Metabolic engineering of *Saccharomyces cerevisiae* for the production of n-butanol**. *Microb Cell Fact* 2008, **7**:36.

5. Bond-Watts BB, Bellerose RJ, Chang MC: **Enzyme mechanism as a kinetic control element for designing synthetic biofuel pathways**. *Nat Chem Biol* 2011, **7**:222–227.

6. Trinh CT: **Elucidating and reprogramming *Escherichia coli* metabolisms for obligate anaerobic n-butanol and isobutanol production.** *Appl Microbiol Biotechnol* 2012, **95**:1083–1094.

7. McKee AE, Rutherford BJ, Chivian DC, Baidoo EK, Juminaga D, Kuo D, Benke PI, Dietrich JA, Ma SM, Arkin AP, et al: **Manipulation of the carbon storage regulator system for metabolite remodeling and biofuel production in *Escherichia coli.*** *Microb Cell Fact* 2012, **11**:79.

8. Ohno S, Furusawa C, Shimizu H: **In silico screening of triple reaction knockout *Escherichia coli* strains for overproduction of useful metabolites.** *J Biosci Bioeng* 2013, **115**:221–228.

9. Shen CR, Lan EI, Dekishima Y, Baez A, Cho KM, Liao JC: **Driving forces enable high-titer anaerobic 1-butanol synthesis in *Escherichia coli.*** *Appl Environ Microbiol* 2011, **77**:2905–2915.

10. Lan EI, Liao JC: **Microbial synthesis of n-butanol, isobutanol, and other higher alcohols from diverse resources.** *Bioresour Technol* 2013, **135**:339–349.

11. Dellomonaco C, Clomburg JM, Miller EN, Gonzalez R: **Engineered reversal of the β-oxidation cycle for the synthesis of fuels and chemicals**. *Nature* 2011, **476**:355–359.

12. Huo YX, Cho KM, Rivera JG, Monte E, Shen CR, Yan Y, Liao JC: **Conversion of proteins into biofuels by engineering nitrogen flux.** *Nat Biotechnol* 2011, **29**:346–351.

13. Chen X, Nielsen KF, Borodina I, Kielland-Brandt MC, Karhumaa K: **Increased isobutanol production in *Saccharomyces cerevisiae* by overexpression of genes in valine metabolism**. *Biotechnol Biofuels* 2011, **4**:21.

14. Kondo T, Tezuka H, Ishii J, Matsuda F, Ogino C, Kondo A: **Genetic engineering to enhance the Ehrlich pathway and alter carbon flux for increased isobutanol production from glucose by *Saccharomyces cerevisiae.*** *J Biotechnol* 2012, **159**:32–37.

15. Lee WH, Seo SO, Bae YH, Nan H, Jin YS, Seo JH: **Isobutanol production in engineered *Saccharomyces cerevisiae* by overexpression of 2- ketoisovalerate decarboxylase and valine biosynthetic enzymes.** *Bioprocess Biosyst Eng* 2012, **35**:1467–1475.

16. Brat D, Weber C, Lorenzen W, Bode HB, Boles E: **Cytosolic re-localization and optimization of valine synthesis and catabolism enables inseased isobutanol production with the yeast *Saccharomyces cerevisiae***. *Biotechnol Biofuels* 2012, **5**:65.

17. Brat D, Boles E: **Isobutanol production from d-xylose by recombinant *Saccharomyces cerevisiae.*** *FEMS Yeast Res* 2013, **13**:241–244.

18. Hofman-Bang J: **Nitrogen catabolite repression in *Saccharomyces cerevisiae.*** *Mol Biotechnol* 1999, **12**:35–73.

19. McNeil JB, McIntosh EM, Taylor BV, Zhang FR, Tang S, Bognar AL: **Cloning and molecular characterization of three genes, including two genes encoding serine hydroxymethyltransferases, whose inactivation is required to render yeast auxotrophic for glycine**. *J Biol Chem* 1994, **269**:9155–9165.

20. Sinclair DA, Dawes IW: **Genetics of the synthesis of serine from glycine and the utilization of glycine as sole nitrogen source by *Saccharomyces cerevisiae.*** *Genetics* 1995, **140**:1213–1222.

21. Villas-Bôas SG, Kesson M, Nielsen J: **Biosynthesis of glyoxylate from glycine in *Saccharomyces cerevisiae.*** *FEMS Yeast Res* 2005, **5**:703–709.

22. Shen CR, Liao JC: **Metabolic engineering of *Escherichia coli* for 1-butanol and 1-propanol production via the keto-acid pathways.** *Metab Eng* 2008, **10**:312–320.

23. Atsumi S, Hanai T, Liao JC: **Non-fermentative pathways for synthesis of branched-chain higher alcohols as biofuels.** *Nature* 2008, **451**:86–89.

24. Nishiya Y, Imanaka T: **Purification and characterization of a novel glycine oxidase from *Bacillus subtilis.*** *FEBS Lett* 1998, **438**:263–266.

25. Rabin R, Reeves HC, Ajl SJ: **Beta-ethylmalate synthetase.** *J Bacteriol* 1963, **86**:937–944.

26. Hazelwood LA, Daran JM, van Maris AJ, Pronk JT, Dickinson JR: **The Ehrlich pathway for fusel alcohol production: a century of research on *Saccharomyces cerevisiae* metabolism**. *Appl Environ Microbiol* 2008, **74**:2259–2266.

27. Piper MD, Hong SP, Eissing T, Sealey P, Dawes IW: **Regulation of the yeast glycine cleavage genes is responsive to the availability of multiple nutrients**. *FEMS Yeast Res* 2002, **2**:59–71.

28. Job V, Marcone GL, Pilone MS, Pollegioni L: **Glycine oxidase from *Bacillus subtilis*. Characterization of a new flavoprotein.** *J Biol Chem* 2002, **277**:6985–6993.

29. Hartig A, Simon MM, Schuster T, Daugherty JR, Yoo HS, Cooper TG: **Differentially regulated malate synthase genes participate in**

carbon and nitrogen metabolism of *S. cerevisiae.* *Nucleic Acids Res* 1992, **20**:5677–5686.

30. Schlösser T, Gätgens C, Weber U, Stahmann KP: **Alanine: glyoxylate aminotransferase of *Saccharomyces cerevisiae*-encoding gene *AGX1* and metabolic significance.** *Yeast* 2004, **21**:63–73.

31. Kohlhaw GB: **Beta-isopropylmalate dehydrogenase from yeast.** *Methods Enzymol* 1988, **166**:429–435.

32. ter Schure EG, Flikweert MT, van Dijken JP, Pronk JT, Verrips CT: **Pyruvate decarboxylase catalyzes decarboxylation of branched-chain 2-oxo acids but is not essential for fusel alcohol production by *Saccharomyces cerevisiae.*** *Appl Environ Microbiol* 1998, **64**:1303–1307.

33. Si T, Luo Y, Xiao H, Zhao H: **Utilizing an endogenous pathway for 1-butanol production in *Saccharomyces cerevisiae.*** *Metab Eng.* 2014, **22**:60-8.

34. Sakuragi H, Morisaka H, Kuroda K, Ueda M: **Enhanced butanol production by eukaryotic *Saccharomyces cerevisiae* engineered to contain an improved pathway**. *Biosci Biotechnol Biochem*. 2014, **28**:1-7.

35. van Dijken JP, Bauer J, Brambilla L, Duboc P, Francois JM, Gancedo C, Giuseppin ML, Heijnen JJ, Hoare M, Lange HC, et al: **An interlaboratory comparison of physiological and genetic properties of four *Saccharomyces cerevisiae* strains.** *Enzyme Microb Technol* 2000, **26**:706–714.

36. van Maris AJ, Winkler AA, Porro D, van Dijken JP, Pronk JT: **Homofermentative lactate production cannot sustain anaerobic growth of engineered *Saccharomyces cerevisiae*: possible consequence of energy-dependent lactate export.** *Appl Environ Microbiol* 2004, **70**:2898–2905.

37. Gietz RD, Woods RA: **Transformation of yeast by lithium acetate/single-stranded carrier DNA/polyethylene glycol method.** *Guide to Yeast Genetics and Molecular and Cell Biology*, *Pt B* 2002, **350**:87–96.

38. Verduyn C, Postma E, Scheffers W, Van Dijken J: **Effect of benzoic acid on metabolic fluxes in yeasts: a continuous-culture study on the regulation of respiration and alcoholic fermentation.** *Yeast* 1992, **8**:501–517.

39. Sambrook J, Maniatis T, Fritsch EF: **Molecular cloning: a laboratory manual.** 2nd edition. Cold Spring Harbor, N.Y.: *Cold Spring Harbor Laboratory*; 1989.

40. Stella CA, Sáenz DA, Chianelli MS, Kaminszczik S: **A simple protocol to evaluate nitrogen utilisation in *Saccharomyces cerevisiae.*** *Biochem Educ* 2000, **28**:169–170.

41. Bradford MM: **A rapid and sensitive method for the quantitation of microgram quantities of protein utilizing the principle of protein-dye binding.** *Anal Biochem* 1976, **72**:248–254.

42. Sigma L: URL: [http://www.sigmaaldrich.com].

43. Ellman GL: **Tissue sulfhydryl groups**. *Arch Biochem Biophys* 1959, **82**:70–77.

CONCLUSIONS

Production of biofuels, chemicals and energy from renewable feedstock is necessary in order to cope with economical and environmental issues due to the exploitation of fossil resource.

A crucial step in developing bio-industry is to create biorefineries capable of efficiently converting a broad range of biomass feedstock into low cost biofuels, biopower and other bioproducts. Therefore, the current research activities are focused on different relevant aspects for the implementation of biorefinery processes, such as optimization of the raw materials exploitation, valorisation of biomasses, the engineering of cell factories characterized by high rate of production, productivity and improved stress resistance and the improvement of the downstream phase in order to maximize yields and minimize costs.

The present study offered some examples about the utilization of different types of biomass feedstock and the tailoring of *Saccharomyces cerevisiae* as cell factory for the production of a relevant chemical and two promising biofuels. In particular, it was reported the use of glucose (representative of plant-derived sugars) and glycine (representative of aminoacids derived from industrial proteinaceous side stream) as renewable substrates for the respectively production of lactic acid and butanol and isobutanol.

In the Chapters 1 and 2 the tolerance to lactic acid and its production in *S. cerevisiae* laboratory and industrial strains, respectively, were discussed.

It is pointed out as the cofactor engineering has the potential to be used as an additional tool to achieve desired metabolic engineering goals and fits with current trends in systems biotechnology. In fact, the manipulation of SAM (S-adenosyl methionine, or AdoMet), a central cofactor of cell

metabolism, has a strong impact on tolerance and lactic acid production. In particular, the deletion of *SAM2*, gene codifying for the enzyme responsible for the synthesis of SAM, resulted in an increased lactic acid tolerance in the BY4741 genetic background, and in an increased lactic acid production (~69 g/L, approximately 5% more than in the parental strain) in the industrial omolactic strain m850.

Because of the results obtained with *SAM2* modulation and because we are highly interested in reprogramming cellular metabolism around the production of interest, an *in vivo* study on protein and membrane lipid in *S. cerevisiae* strains exposed to lactic acid stress was performed. Remarkably, an effect on protein aggregation triggered by the stressful condition was observed in the BY4741 parental strain. Moreover, an effect on the lipid composition, in particular a decrease in phosphatidylcholine level, was observed in BY4741 and BY4741 *sam2Δ* strains. Because of the central role of plasma membrane not only in physiological condition, but also and possibly even more during a process of production, the effect of the deletion of *OPI1* was examined. Its gene product is indeed involved in the biosynthetic pathway of phosphatidylcholine, the main membrane phospholipid.

This study pointed out that the exposure to lactic acid in *S. cerevisiae* results in profound changes, never elucidated in literature, both at the plasma membrane, in terms of its composition and oxidative damage, and at intracellularly, in terms of protein aggregation. Moreover, it was highlighted how the deletion of *OPI1* had pleiotropic effects. This gene engineering affected not only the phosphatidylcholine levels, direct gene target, but also the peroxidized lipid content and the accumulation of protein aggregates, factors that contribute to the increased robustness of the BY4741 *opi1Δ* strain in the presence of lactic acid.

Chapter 3 showed a possible valorization of the fraction of proteins that accumulates as a waste product in different microbial productions and currently is not totally absorbed by the market. The attention was indeed focused on the strategy, which takes advantage of ketoacids as intermediates in amino acids degradation metabolism to produce butanol and isobutanol in *S. cerevisiae*. In particular, by deeply investigating the literature, it was first hypothesized and then biochemically demonstrated step by step a novel pathway for the production of the two higher alcohols by the glycine degradation pathway via glyoxylate, β-ethylmalate and α-ketoacids intermediates. Additionally, at least one possible gene encoding for the enzymes responsible for butanol production was suggested. 92 mg/L and 58 mg/L of butanol and isobutanol respectively were produced starting from 15 g/L of glycine as substrate. Despite the yield on glycine is still quite low, it is important to consider that the best butanol production reported for engineered *S. cerevisiae* was only 14.1 mg/L. Therefore, considering the potentiality of *S. cerevisiae* as ethanol producer and considering the potentiality of the aminoacid degradation pathway for fusel alcohol productions, it really seems the right moment to intensify the effort in studying and improving yeast tolerance to a mixture of different organic solvents.

The versatility of the yeast *S. cerevisiae*, demonstrated both in terms of renewable feedstock used and bio-products obtained, confirms this microorganism as a key cell factory that can be employed together with other bio-based processes in the view of a true bioeconomical development. Further efforts will therefore be focused to increase the robustness of this

microorganism, in order to turn towards a biorefinery competitive with the processes currently available.

PUBLICATIONS

Dato L, Berterame NM, Ricci M, Paganoni P, Palmieri L, Porro D, Branduardi P: **Changes in *SAM2* expression affect lactic acid tolerance and lactic acid production in *Saccharomyces cerevisiae*.** *Microb Cell Fact*. 2014, **13**(1):147.

Branduardi P, Longo V, Berterame NM, Rossi G, Porro D: **A novel pathway to produce butanol and isobutanol in *Saccharomyces cerevisiae*.** *Biotechnol Biofuels.* 2013, **6**(1):68.

Dato et al. Microbial Cell Factories 2014, 13:147
http://www.microbialcellfactories.com/content/13/1/147

MICROBIAL CELL FACTORIES

RESEARCH Open Access

Changes in *SAM2* expression affect lactic acid tolerance and lactic acid production in *Saccharomyces cerevisiae*

Laura Dato[1†], Nadia Maria Berterame[1†], Maria Antonietta Ricci[2†], Paola Paganoni[1], Luigi Palmieri[2], Danilo Porro[1] and Paola Branduardi[1*]

Abstract

Background: The great interest in the production of highly pure lactic acid enantiomers comes from the application of polylactic acid (PLA) for the production of biodegradable plastics. Yeasts can be considered as alternative cell factories to lactic acid bacteria for lactic acid production, despite not being natural producers, since they can better tolerate acidic environments. We have previously described metabolically engineered *Saccharomyces cerevisiae* strains producing high amounts of L-lactic acid (>60 g/L) at low pH. The high product concentration represents the major limiting step of the process, mainly because of its toxic effects. Therefore, our goal was the identification of novel targets for strain improvement possibly involved in the yeast response to lactic acid stress.

Results: The enzyme *S*-adenosylmethionine (SAM) synthetase catalyses the only known reaction leading to the biosynthesis of SAM, an important cellular cofactor. SAM is involved in phospholipid biosynthesis and hence in membrane remodelling during acid stress. Since only the enzyme isoform 2 seems to be responsive to membrane related signals (*e.g.* myo-inositol), Sam2p was tagged with GFP to analyse its abundance and cellular localization under different stress conditions. Western blot analyses showed that lactic acid exposure correlates with an increase in protein levels. The *SAM2* gene was then overexpressed and deleted in laboratory strains. Remarkably, in the BY4741 strain its deletion conferred higher resistance to lactic acid, while its overexpression was detrimental. Therefore, *SAM2* was deleted in a strain previously engineered and evolved for industrial lactic acid production and tolerance, resulting in higher production.

Conclusions: Here we demonstrated that the modulation of *SAM2* can have different outcomes, from clear effects to no significant phenotypic responses, upon lactic acid stress in different genetic backgrounds, and that at least in one genetic background *SAM2* deletion led to an industrially relevant increase in lactic acid production. Further work is needed to elucidate the molecular basis of these observations, which underline once more that strain robustness relies on complex cellular mechanisms, involving regulatory genes and proteins. Our data confirm cofactor engineering as an important tool for cell factory improvement.

Keywords: Lactic acid production, Lactic acid stress, *Saccharomyces cerevisiae*, S-Adenosylmethionine (SAM), *SAM2*

* Correspondence: paola.branduardi@unimib.it
†Equal contributors
[1]Dipartimento di Biotecnologie e Bioscienze, Università degli Studi di Milano-Bicocca, Piazza della Scienza 2, 20126 Milan, Italy
Full list of author information is available at the end of the article

Background

Lactic acid and its production by lactic acid bacteria (LAB) have a long history in the food industry for its application as an acidulant, flavouring agent, pH buffering agent, or preservative [1-4]. Microbial processes for its production have been established early in the last century. However, the commercial production of the purified acid in large-scale by microorganisms is relatively new. The production and applications of its derivative polylactic acid (PLA) [5,6] currently elicited an increased interest in optically pure lactic acid. Furthermore, the presence of both carboxylic and hydroxyl groups in the lactic acid molecule enables its conversion into different technologically useful chemicals such as pyruvic acid, acrylic acid, 1,2-propanediol and lactate ester via chemical and biotechnological routes [2,3,7,8], making it a primary chemical platform.

Initially, the natural producers were the "bio-catalysts" of choice for industrial lactic acid fermentations [9,10]. However, LAB require complex nutrients and are inhibited by the product, especially at low pH. The most relevant bottleneck in production by LAB is in all likelihood related to the inhibitory effects of the low pH of the medium on cell growth, cell viability and in turn on lactic acid accumulation. Indeed, large amounts of $CaCO_3$ must be added during fermentation, to maintain a constant pH of the culture broth (at around 5) and sustain production. Under these conditions the final product is lactate, since the pK_a of lactic acid is 3.86. This in turn increases the operation costs for separation and purification of the desired product, which is actually the free acidic form [2,3,11], and therefore the acidification of the spent medium at the end of the fermentation becomes a required step.

The use of naturally low-pH tolerant organisms, such as yeasts, represents an alternative production route. In 1994 Dequin and Barre [12] first described a metabolically engineered *Saccharomyces cerevisiae* strain expressing a heterologous L-lactate dehydrogenase, obtaining a hetero-fermentative strain producing both ethanol and lactic acid. Since then, many improvements have been obtained along the years. Among them, (*i*) the deletion of pyruvate decarboxylase gene (s) to avoid ethanol production and increase production, productivity and yield of lactic acid [13-15], (*ii*) the increased yields due to the effect of different *S. cerevisiae* backgrounds and heterologous L-lactate dehydrogenases [16], (*iii*) the development of high-producing strains following classical selection methods, by direct exposure of the cells to the stressor, and indirect screenings by sorting the cells on the basis of tolerance-related traits like the capability to keep an higher intracellular pH [17,18], and (*iv*) the effect of overexpression of the hexose transporters (*e.g.* Hxt1p and Hxt7p) on glucose uptake and lactic acid productivity and production [19]. Metabolically engineered *S. cerevisiae* strains were also characterized for their energetic balance, showing that lactate production does not contribute to the net ATP production probably due to energy utilization for lactate export [20]. Recently, metabolically engineered yeast came on the market for lactic acid production (NatureWorks®) [21].

In spite of their ability to produce high levels of lactic acid at low pH, the presence of the undissociated weak acid in the growth medium imposes a high degree of stress to yeast cells [22-26]. The cell membrane is, in fact, selectively permeable to small polar and to hydrophobic molecules, like undissociated weak organic acids, which can cross it by passive diffusion following their gradient [27]. Because of the relatively high intracellular pH value, weak acids dissociate once into the cytoplasm, releasing H^+ and the corresponding anion. Accumulation of both species has detrimental effects on cells, ranging from lowering of intracellular pH and inhibition of metabolic activities, to interference with lipid organization and membrane permeability/functions and induction of oxidative stress and cell death (reviewed in [22,23]), among others. Therefore, during detoxification, the protons are expelled via the H^+-ATPase pump and the anions via active export systems (or metabolized), consuming huge amounts of energy. There is no surprise then in finding that membrane lipids and proteins are among the first targets of modification induced by some specific stresses [28-32].

Stress responses induce a complex cellular reprogramming. Classically, most metabolic engineering studies have focused on enzyme levels and on the effect of the amplification, addition, or deletion of a particular pathway directly linked with the product of interest. However, the current status of metabolic engineering is still hindered by the lack of our full understanding of cellular metabolism. Indeed, the complex aspects of integrated dynamics and overall control structure are the common obstacles for the optimal design of pathways to achieve a desired goal. Since cofactors are essential to a large number of biochemical reactions, their manipulation is expected to have large effects on metabolic networks. It is conceivable that cofactor availability and the proportion of cofactor in the active form may be critical in dictating the overall process yield. It has already been shown that cofactors play a major role in the production of different fermentation products (see, as example [33]). Furthermore, changes in cofactor pools induce changes at the transcriptional level as well as at the enzyme levels [34].

SAM (or AdoMet) is a central coenzyme in the metabolism that participates to a very high number of reactions [35]. In particular it functions as a donor of methyl groups to proteins, lipids, nucleic acids, vitamin B12 and others by SAM-dependent methyltransferases; it is also a precursor molecule in the aminopropylation and transulfuration pathways [36] and it regulates the

activities of various enzymes. SAM has a role in the modelling of the plasma membrane structure, since it donates three methyl groups during the synthesis of phosphatidylcholine (PC) from phosphatidylethanolamine (PE). Malakar *et al*. [37] demonstrated a protective role of externally added SAM in *S. cerevisiae* cells growing under inorganic acid (HCl) stress, which they associated to the measured increase in PC:PE ratio and to the higher activity of the proton pump Pma1p. Moreover, SAM displays an anti-apoptotic role, acting as an indirect scavenger of reactive oxygen species (ROS) via enhancement of glutathione biosynthesis [38].

We therefore focused our attention on SAM-synthetase which catalyses the only known reaction that, starting from L-methionine (Met) and ATP, leads to the biosynthesis of SAM [39-41]. Notably, *S. cerevisiae* has two distinct SAM-synthetase genes, named *SAM1* and *SAM2*, which arose from gene duplication [42,43] and share a high degree of similarity (83% identity in the ORF, 92% in the translated sequence) [43]. Although *SAM1* and *SAM2* have at least partially overlapping functions, their regulation is different. Both genes undergo feedback repression by SAM, like other genes of the sulfur aminoacids metabolism, but the expression of *SAM2* also increases during growth, in a Sam2p-dependent manner [44]. Remarkably, *SAM2* is repressed after the addition of myo-inositol and choline, suggesting that Sam2p, but not Sam1p, is involved in phospholipid biosynthesis [45]. It is very likely that Sam2p is concerned to this process also during lactic acid stress.

In this work, the expression and localization of Sam2p under lactic acid treatment were evaluated. To assess the role of this protein during lactic acid stress, *SAM2* was both overexpressed and deleted in *S. cerevisiae* laboratory strains. Moreover, when *SAM2* was deleted in the engineered and evolved lactic acid producing strain CEN.PK m850 [18], higher lactic acid productivity and production were obtained.

Results

Sam2p as a putative responsive element to lactic acid stress

Based on the reported beneficial effects of SAM during inorganic acid (HCl) stress [37] and its involvement in membrane remodelling, we evaluated the protein levels of Sam2p by western blot analysis during lactic acid exposure. A chromosomal tagging approach by which the GFP coding sequence was fused in frame to the C-terminal coding region of the endogenous copy of the *SAM2* gene has been applied (see Methods). The *SAM2*GFP strain was created in the CEN.PK 113-11C background, a robust *S. cerevisiae* reference strain, and also in the BY4741 background, commonly used for functional genetic studies (EUROSCARF collection http://web.uni-frankfurt.de/fb15/mikro/euroscarf/).

The BY4741 *SAM2*GFP and CEN.PK *SAM2*GFP strains were grown in minimal medium with 2% w/v glucose in the absence and in the presence of different concentrations of lactic acid (pH 5, pH 3, 12 g/L and 20 g/L lactic acid at pH 3) and Sam2p levels were estimated using an anti-GFP antibody at 16 and 40 hours after inoculation, respectively corresponding to the exponential and the early stationary phase of growth. The biomass accumulation and the growth phase among the different conditions within the same genetic background were similar, for each time point considered. As control, β-actin levels were also detected.

Two analyses were run in parallel: in the first, the total protein fraction was extracted with trichloroacetic acid (TCA); in the second, three sub-fractions resulting from sequential protein extraction were separated: the first containing only soluble proteins, the second containing insoluble proteins solubilized with urea, the third containing highly insoluble proteins excluded from the second fraction and solubilized with concentrated sodium dodecyl sulfate (SDS) (see Methods for details).

Figure 1 shows the western blots of the TCA extracts for CEN.PK (panel A) and BY (panel B) strains. Remarkably, in both strains the signal intensity of Sam2p-GFP increased in the presence of lactic acid, particularly in the BY strain (see panels B).

Noteworthy, Sam2p was found in all the three protein sub-fractions after sequential extraction. Additional file 1: Figure S1 shows the western blots obtained for CEN.PK. At 16 h, the signals detected in the soluble protein fractions were rather similar among the different conditions, thus the protein increase of the lactic acid samples was mainly ascribable to the highly insoluble protein fractions and to a lesser extent to the fractions solubilised with urea. This was also true for lactic acid samples collected at 40 h, when slight enrichments were also found in the native extracts (data not shown).

Overall, lactic acid determined an increase in the total amount of the Sam2p in both yeast backgrounds.

Sam2p localization under lactic acid exposure

The localization of Sam2p is still a matter of debate. In fact, while the *LoQate* database [46] and Tkach *et al.* [47] report a cytoplasmic localization, the *Yeast GFP Fusion Database* [48] reports it as ambiguous, the *OrganelleDB* (A. Kumar's Lab, Life Sciences Institute, University of Michigan; http://organelledb.lsi.umich.edu/) reports it as unknown and finally the *YPL$^+$ Database* (Oskolkova, Leitner and Kohlwein, personal communication) describes it as nuclear. Based on our previous data, therefore, the possible effects of lactic acid exposure on Sam2p-GFP fusion protein localization in the BY4741 *SAM2*GFP and CEN.PK *SAM2*GFP were investigated by fluorescence microscopy.

Yeast cells were grown in the same conditions described above and observed under epifocal microscope at 16 and

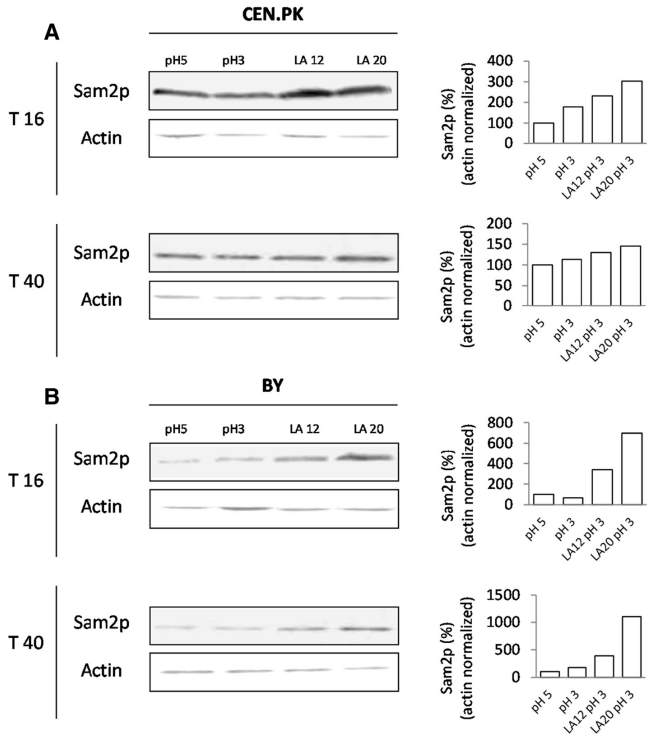

Figure 1 Western blot analysis of total Sam2p levels in cells grown in the absence and presence of lactic acid. CEN.PK 113-11C **(panel A)** and BY4741 *SAM2*GFP **(panel B)** cells were grown in shake flasks in minimal (YNB) medium with 2% w/v glucose without or with the addition of different concentrations of lactic acid (pH 5, pH 3, 12 g/L and 20 g/L lactic acid at pH3) and the Sam2p-GFP levels were evaluated after 16 and 40 hours after inoculation in the total protein fraction, extracted with TCA, using an anti-GFP antibody. Samples were normalised according to cell number. β-actin levels have been detected as control. Bands have been quantified by ImageJ 1.48 software. Histograms refer to the ratio (%) of Sam2p/Actin normalized to the values at pH 5. LA: lactic acid.

40 hours after inoculation. The images of Figure 2, depicting CEN.PK cells, show that the presence of lactic acid had no significant effects on Sam2p-GFP distribution. At 16 h (upper panels) the signal was diffused into the whole cell, with the exclusion of extended dark areas representing the vacuoles and nuclei (based on DAPI staining, not shown). Therefore, the localization appeared to be mainly cytoplasmatic, although a contingent association with membranes cannot be excluded. At 40 h (bottom panels), instead, discrete spots emerging from the diffused fluorescence signal were visible. A similar situation was observed in BY4741 cells (data not shown). The number and dimensions of these *foci* were highly variable in all cells, irrespective of whether lactic acid was present or not. Therefore the data reported do not allow additional speculations on their relevance to stress tolerance. The nature of the observed Sam2p *foci*, never reported in literature before, is still unknown, and its biological significance needs to be further investigated.

In conclusion, Sam2p distribution within the cytosol in both yeast strains appeared to change in correlation with the growth phase.

Effect of *SAM2* overexpression and deletion on lactic acid tolerance

The differential accumulation of Sam2p observed by the western blot analysis opens the question about a possible role of this protein during the cellular response to lactic

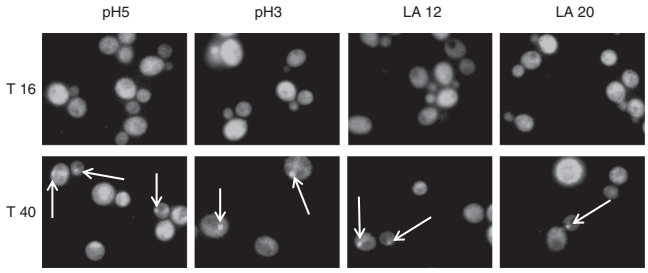

Figure 2 Sam2p-GFP fluorescence distribution during growth in the absence and presence of lactic acid. CEN.PK 113-11C *SAM2*GFP cells were grown in shake flasks in minimal (YNB) medium with 2% w/v glucose without or with the addition of different concentrations of lactic acid (pH 5, pH 3, 12 g/L and 20 g/L lactic acid at pH3). Epifocal microscope images were taken at 16 and 40 hours after inoculation, corresponding to exponential growth phase and early stationary phase, respectively. Pictures show Sam2p-GFP fluorescence in the green field. White arrows indicate Sam2p-GFP *foci*. LA: lactic acid.

acid stress at low pH. Consequently, the effect of *SAM2* overexpression was examined for growing cells challenged with different concentrations of the stressing agent. The wild type CEN.PK 102-3A and BY4741 strains were transformed with the pTEF-L-SAM2 multicopy plasmid (see Methods), carrying *SAM2* under the control of the strong constitutive *S. cerevisiae* TEF1 promoter. CEN.PK 102-3A and BY4741 cells transformed with the respective empty plasmid were used as controls.

Figure 3 shows the results obtained by cultivation in minimal medium with 2% w/v glucose without or with lactic acid (40 g/L) at pH 3. No remarkable differences were observed between the control and the *SAM2* overexpressing strains during growth without lactic acid at low pH, in both yeast backgrounds (Figure 3A). Lactic acid had a clear negative effect on the growth of all strains, visible in terms of growth delay and lower biomass accumulation (Figure 3B). However, while wild type and *SAM2* overexpressing cells grew similarly in the stressed condition for the CEN.PK background, in the BY background a marked difference between the two strains was observed, where surprisingly the *SAM2* overexpressing strain was much more affected compared to the control.

Since unexpectedly *SAM2* gene overexpression did not help improving lactic acid tolerance in the CEN.PK background and caused severe growth deficiencies in the BY4741 background, the effect of its deletion was also tested. *SAM2* was deleted in the CEN.PK 102-3A and BY4741 parental strains and in the same strains harbouring the pTEF-L plasmid (the backbone plasmid used for *SAM2* overexpression), complementing the leucine auxotrophy, to allow a direct comparison of all the data.

Figures 4 and 5 show the growth curves obtained, respectively for the parental strains and for the LEU^+ complemented strains. *SAM2* deletion had no effect, in all the tested strains, during growth in minimal medium at low pH (Figures 4A and 5A). When cells were stressed with lactic acid, once more no marked differences were observed in the CEN.PK background between the wild type and the deleted strain (Figures 4B and 5B). Interestingly, the BY4741 parental strain *sam2Δ* turned out to be less sensitive to the stressing agent than the wild type (Figure 4B): the specific growth rate in exponential phase was in fact 45% higher compared to control cells (0.11 ± 0.01 h^{-1} *vs* 0.16 ± 0.01 h^{-1}, mean and SD from three independent experiments). However, the complementation of leucine auxotrophy made void the positive impact of *SAM2* deletion on cellular growth (Figure 5B).

It has to be noticed that the final OD reached by the leu^- strains in the unstressed condition was lower compared to the values registered for LEU^+ complemented strains, possibly indicating that the standard amino acid supplementation (50 mg/L) was not sufficient in the case of leucine. This effect was stronger in the CEN.PK background (Figure 4A). Pronk [49] suggested complementation of the medium with 125 mg/L, 500 mg/L, 100 mg/L, 150 mg/L for histidine, leucine, methionine and uracil respectively. Accordingly, the growth experiments, in which the effect of *SAM2* modulation has been observed, were repeated in the presence of lactic acid at pH 3 with the supplemented relevant chemicals (Figure 6). While in this medium *SAM2* deletion did not affect the cellular growth in the presence of the stressing agent (panel A), *SAM2* overexpression was still detrimental to the cells (panel B). This confirms that Sam2p recombinant overproduction is not beneficial to improve the tolerance to this stress.

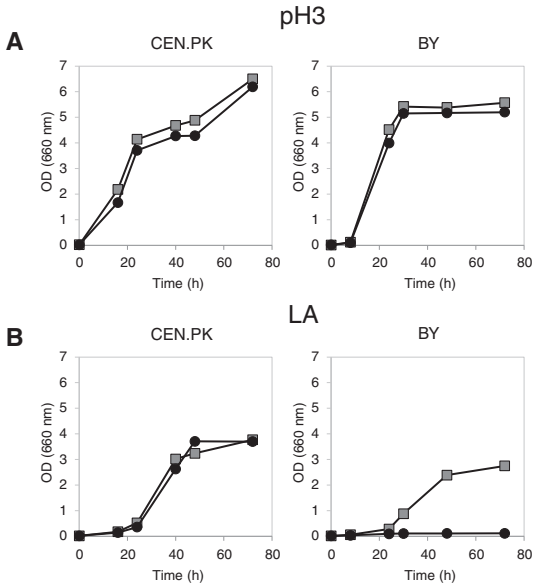

Figure 3 Growth of wild type and *SAM2* overexpressing cells in the absence and presence of lactic acid. Yeast cells were grown in shake flasks in minimal (YNB) medium with 2% w/v glucose at initial pH 3, without **(panel A)** or with **(panel B)** 40 g/l of lactic acid. Growth was determined as OD at 660 nm. Left panels: CEN.PK cells; right panels: BY cells. Dark grey squares: wild type control strains (CEN.PK 102-3A [pTEF-L], BY4741 [pTEF-L]). Black circles: cells overexpressing *SAM2* (CEN.PK 102-3A [pTEF-L-SAM2], BY4741 [pTEF-L-SAM2]).

Effect of lactic acid pulsed stress on cell viability

The effect of *SAM2* deletion and overexpression was also evaluated in terms of cellular viability in the aforementioned strains, *i.e.* CEN.PK 102-3A and BY4741 wt, *SAM2* overexpressing and *sam2Δ* (complemented or not for leucine auxotrophy). Cells were grown in minimal medium, until the exponential phase was reached, and then treated with a pulse of lactic acid at different concentrations (0, 25, 30, 35, 40 and 45 g/L at pH 3). After 30 minutes the cells were collected, stained with propidium iodide (PI) and analyzed by flow cytometry to identify dead and/or severely compromised cells. Figure 7 shows the histograms obtained for the BY4741 strains, where the left peak corresponds to intact (PI-negative) cells, while the right peak corresponds to the dead/damaged (PI-positive) cells (we currently do not have an interpretation for the bimodal distribution visible in the plots).

As for the growth experiments, also in this case the effects of *SAM2* gene modulation were observed only in the BY background. In particular, the parental *leu*$^-$ strain *sam2Δ* showed a percentage of dead/damaged cells consistently lower than the control strain (Figure 7A). When the leucine auxotrophy was complemented, however, the differences between the two strains were not significant (Figure 7B). On the contrary, and in agreement with what already observed in the kinetics of growth, the *SAM2* overexpressing strain showed an increased sensitivity to lactic acid stress, with a higher percentage of dead/damaged cells compared to the control (Figure 7B). It is worth to notice that for any tested lactic acid concentrations the BY *leu*$^-$ strains had a higher mortality compared to LEU$^+$ strains.

In the CEN.PK background, instead, the *SAM2* deletion and overexpression had no significant effect on cellular viability (data not shown).

Analysis of intracellular AXP levels

Our data indicate that the Sam2 protein levels respond to lactic acid in both the CEN.PK and BY4741 yeast strains, but the effects of *SAM2* gene deletion and overexpression, at least in terms of growth and cell viability, are only detectable in the BY background. We considered the hypothesis

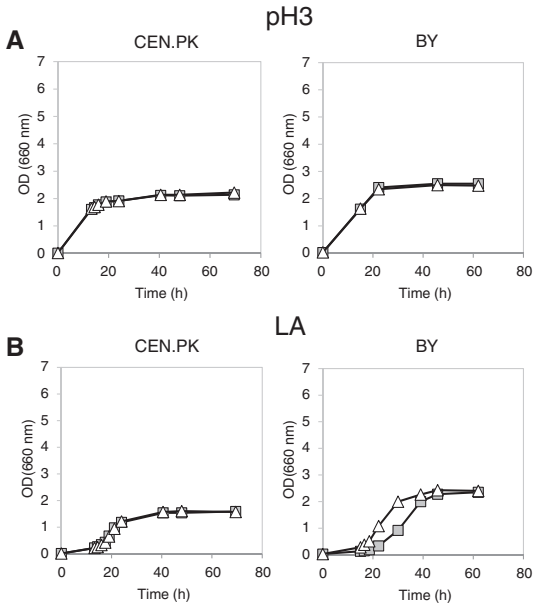

Figure 4 Growth of wild type and *sam2Δ* leucine nutritionally complemented strains in the absence and presence of lactic acid. Yeast cells were grown in shake flasks in minimal (YNB) medium with 2% w/v glucose and 50 mg/L of the necessary nutritional supplements at initial pH 3, without **(panel A)** or with **(panel B)** 34 and 38 g/l of lactic acid for CEN.PK (left panels) and BY (right panels), respectively. Growth was determined as OD at 660 nm. Light grey squares: parental wild type strains (CEN.PK 102-3A, BY4741). White triangles: *sam2Δ* cells (CEN.PK 102-3A *sam2Δ*, BY4741 *sam2Δ*).

that these differences might be correlated with different AXP pool composition. We therefore measured the adenine nucleotide content of CEN.PK 113-11C and BY4741 wt, *SAM2* overexpressing and *SAM2* deleted strains, complemented for leucine auxotrophy, during the exponential growth phase on minimal medium with 2% w/v glucose without or with lactic acid (samples were collected at OD ~1 if without and at OD ~0.3 if with lactic acid, respectively). The ATP, ADP and AMP (collectively referred as AXP) intracellular concentrations were determined by HPLC with the method from Ask *et al.* [50], as described in the Methods section. Data are reported in Figure 8, normalized for culture OD for consistency with the other data.

In the CEN.PK background (Figure 8A) similar levels of all the nucleotides were found in all the strains regardless the presence of lactic acid, and no differences were evident depending on *SAM2* expression levels. In the BY background, lower mean ATP levels were registered in the presence of lactic acid compared to control medium (Figure 8B), although again no specific differences were assessed in dependence on *SAM2* expression. Interestingly, a comparison of the data obtained for the two yeast backgrounds shows a lower mean ATP content in the BY strains compared to CEN.PK. The differences are statistically significant, with a Student's *t*-test *p*-value of 0.012 for the comparison at pH 3 and of 0.004 for the comparison in lactic acid at pH 3. Also the ADP and AMP mean concentrations were lower in the BY strain, especially in the presence of lactic acid, so that the calculated energy charge resulted conserved in all the strains, at physiological levels higher than 0.8 (data not shown).

Effect of *SAM2* deletion on lactic acid production by a *S. cerevisiae* strain engineered and evolved for the industrial process

Despite the fact that the mechanisms involved remain far from being elucidated, our data indicate that *SAM2* deletion might confer an advantage to cells exposed to lactic acid stress when the overall conditions are not

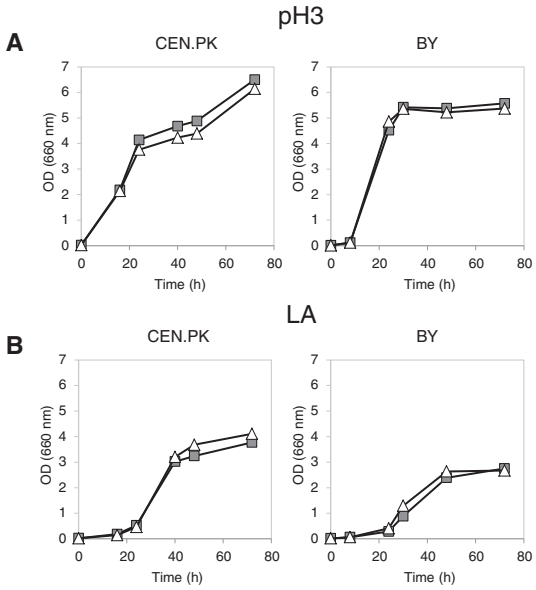

Figure 5 Growth of wild type and *sam2Δ LEU2* genetically complemented strains in the absence and presence of lactic acid. Yeast cells were grown in shake flasks in minimal (YNB) medium with 2% w/v glucose and 50 mg/L of the necessary nutritional supplements at initial pH 3, without **(panel A)** or with **(panel B)** 40 g/l of lactic acid. Growth was determined as OD at 660 nm. Left panels: CEN.PK cells; right panels: BY cells. Dark grey squares: wild type control strains (CEN.PK 102-3A [pTEF-L], BY4741 [pTEF-L]). White triangles: *sam2Δ* cells (CEN.PK 102-3A *sam2Δ* [pTEF-L], BY4741 *sam2Δ* [pTEF-L]).

optimal. Since the final goal of our studies is to find conditions that can bring advantages to lactic acid production, we tested the effects of *SAM2* deletion in the lactic acid producing strain during the production process. Indeed, even though the productive strain was originally derived from the robust CEN.PK background and does not bring any auxotrophies, still the production process puts it under extremely severe stress conditions.

The recombinant CEN.PK m850 strain is a homolactic fermenting cell factory able to produce up to 60 g/L in 60 h at pH values lower than 3. It was derived from the CEN.PK background via engineering steps that deleted all the pyruvate decarboxylase (*PDC*) genes and introduced the *L. plantarum* lactate dehydrogenase (LDH) activity, eliminating in this way all ethanol production in favour of lactic acid production from the free pyruvate. It furthermore underwent selection, following an adaptive laboratory evolution approach, for improved acid tolerance [18].

The *SAM2* gene was deleted in the CEN.PK m850 strain, and the performances of the parental and the *sam2Δ* strains were compared during the production of lactic acid in minimal medium in the presence of high amounts of initial glucose. Cells were first pre-cultivated for 24 hours in minimal medium with 10 g/L ethanol and 0.5 g/L glucose, to obtain the biomass, and then transferred to a fresh medium containing 5 g/L ethanol and 90 g/L glucose for the production phase (as previously described, [17]). Figure 9 reports the culture parameters monitored at time intervals throughout the production phase: cellular growth (panel A), residual glucose and produced lactic acid in the medium, measured by HPLC (panel B), cell viability as determined by flow cytometry (panel C) and culture medium pH (panel D).

No differences ($p > 0.05$ Student's *t*-test) were observed between the two strains in terms of biomass accumulation (Figure 9A) and cell viability, the latter assessed after staining with either PI (Figure 9C) or fluorescein diacetate (whose signal is linked to metabolically active cells; data not shown), and extracellular pH values were almost identical (Figure 9D). Instead, differences were measured for the glucose and lactic acid concentrations (Figure 9B),

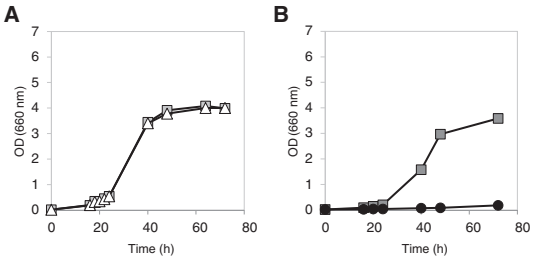

Figure 6 Growth of wild type, deleted or overexpressing *SAM2* BY strains in minimal supplemented medium with lactic acid. BY cells were grown in shake flasks in minimal (YNB) medium with 2% w/v glucose, 125 mg/L, 500 mg/L, 100 mg/L, 150 mg/L for histidine, leucine, methionine and uracil respectively, at initial pH 3, with 38 g/l of lactic acid. Growth was determined as OD at 660 nm. **Panel A**. Light grey squares: wild type control strain (BY4741) White triangles: *sam2Δ* cells (BY4741 *sam2Δ*). **Panel B**. Dark grey squares: wild type control strain (BY4741 [pTEF-L]) Black circles: cells overespressing *SAM2* (BY4741 [pTEF-L-SAM2]).

indicating higher specific lactic acid production rates for the CEN.PK m850 *sam2Δ* strain compared to the control.

A mean 5.4% increase in lactic acid production was observed in the *sam2Δ* strain at the end of the process (69.2 ± 0.6 *vs* 65.6 ± 0.9 g/L, average and SD of three independent experiments). Based on a two-tails, unpaired, heteroscedastic Student's *t*-test, the differences in production at the last two time points of the experiment are highly significant (*p*-values 0.0103 and 0.0087 respectively at 63 and 70 h). The 95% confidence intervals (CI) for lactic acid production throughout the process were also calculated (Additional file 2: Table S1), indicating statistical significance for the differences found from the 46 h time point onward. For both strains, the yields were similar (0.88 ± 0.01 and 0.87 ± 0.03 g of lactic acid per g of glucose consumed, respectively for the *sam2Δ* and the control strain). The differences observed between the two strains might be judged as small, but it must be considered that the cells were already pushed close to the theoretical limits (in terms of lactic acid yield) and in extreme conditions, therefore improvements of a high percentage cannot be expected.

To test if energetic balance might contribute to the observed differences, the intracellular AXP concentrations were determined in the control and *sam2Δ* strain during the process already described. Figure 10 shows the mean data and SD relative to cells analyzed immediately before inoculation (indicated as 0 h) and at 24 and 48 hours after the beginning of the production phase, respectively, in two independent experiments. At time 0 h, the ADP and AMP contents were lower whereas the ATP content was higher in the *sam2Δ* strain compared to the control, despite a high variability in the case of ATP. After inoculation, no differences were found between the two strains. At 24 h, the ADP and AMP concentrations increased in both strains compared to 0 h, while at 48 h all the three species decreased.

Accordingly, the calculated energy charge (Table 1) was higher in the *sam2Δ* strain immediately before the production phase (0 h), while there was no difference between the two strains later during production. Noteworthy, at all the time points and more pronouncedly during the production phase, the energy charge was below the physiological levels, differently from the laboratory strains, confirming the high stress experienced by the lactic acid producing strain.

Discussion

A hypothesis on the mechanism triggering Sam2p increase upon lactic acid stress

SAM has a role in the modelling of the plasma membrane structure, taking part to the PC synthesis starting from PE. Phospholipids represent a major portion of the dry weight of a cell, they are essential for many different cellular processes and their alteration leads to membrane dysfunction [51]. As well, they are reservoirs of secondary messengers, provide precursors for the synthesis of macromolecules, serve in the modification of membrane association, and function as molecular chaperons (reviewed in [52]). Since PC is the most abundant phospholipid species in yeast membranes, it is not surprising that the pathway responsible for SAM synthesis and the pathway responsible for PC synthesis are transcriptionally and metabolically coordinated. The key element of this coordination was shown to be the *SAM2* gene [53], since it is the only gene directly regulated by both Met4p and Opi1p transcriptional factors.

Moreover, PC is the major phospholipid species in the yeast mitochondrial membranes [54], and it is required for mitochondrial respiratory functions [55]. Therefore, we could speculate that a signal inducing the increase of Sam2p in response to the toxic effects of lactic acid

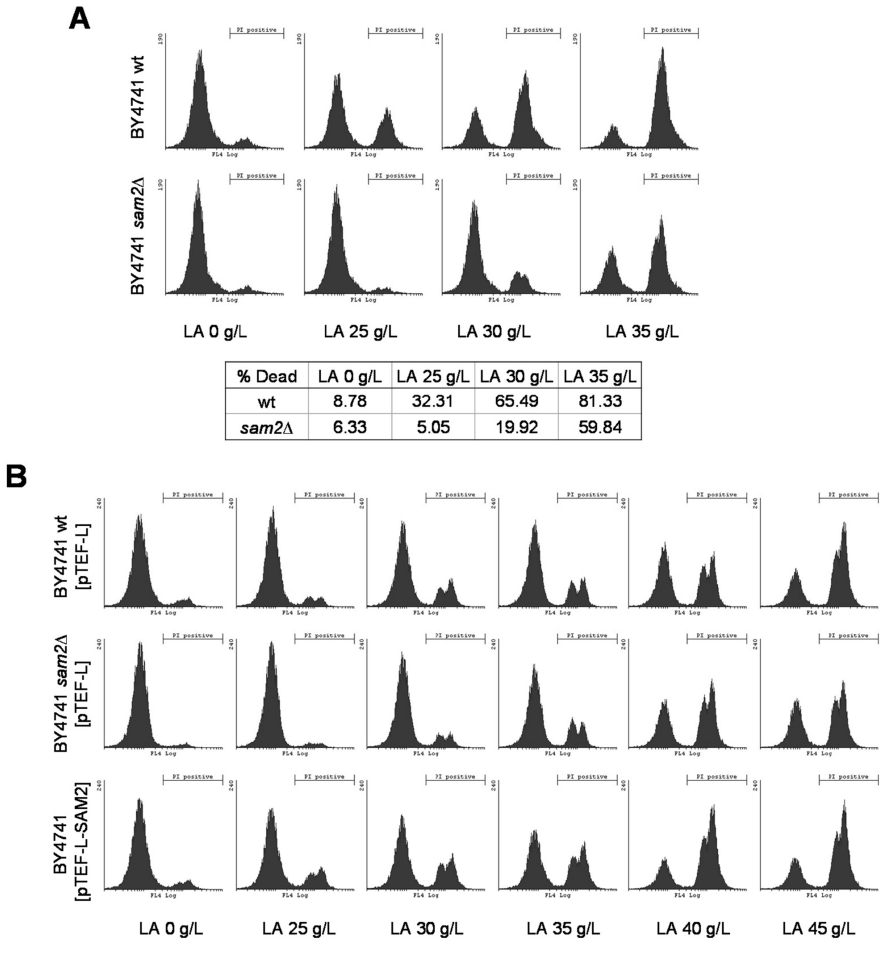

% Dead	LA 0 g/L	LA 25 g/L	LA 30 g/L	LA 35 g/L
wt	8.78	32.31	65.49	81.33
*sam2*Δ	6.33	5.05	19.92	59.84

% Dead	LA 0 g/L	LA 25 g/L	LA 30 g/L	LA 35 g/L	LA 40 g/L	LA 45 g/L
wt pTEF-L	7.94	10.71	24.24	26.6	45.75	71.62
*sam2*Δ pTEF-L	3.42	4.93	14.97	26.67	56.62	55.94
pTEF-L-SAM2	9.36	22.33	33.97	44.59	73.19	71.62

Figure 7 Viability determination for cells stressed with lactic lacid. Cells were grown in minimal medium until the exponential phase and then treated with a pulse of lactic acid. After 30 min of incubation, cells were collected and stained with propidium iodide (PI) to detect dead and/or severely damaged cells by flow cytometry. The fluorescence emission was measured through a 670 nm long pass filter (FL3 parameter). For each sample, 25000 cells were analysed. The bar indicates the PI positive subpopulation. **Panel A**: BY4741 and BY4741 *sam2Δ*. **Panel B**: BY4741 [pTEF-L], BY4741 *sam2Δ* [pTEF-L] and BY4741 [pTEF-L-SAM2].

(shown in the western blot analysis) might be triggered by the increased need of PC synthesis.

An apparent inconsistency

We initially hypothesized that *SAM2* overexpression might have a positive effect on cellular fitness. The reported antioxidant properties of SAM in mammals as well as in yeast [38,56,57] would have supported this hypothesis. The results presented demonstrated that in the BY4741 strain this was not the case, and instead the deletion of *SAM2* had a positive effect. Such an unexpected outcome has been described before for different gene products: for example, the expression of the gene encoding for the cell wall mannoprotein Sed1p was induced by exposure of *S. cerevisiae* cells to lactic acid, but its deletion conferred more resistance to the same stressor [58]. Moreover, *SED1* deletion in combination with the deletion of three genes (*DSE2*, *SCW11*, *EAF3*) identified after a screening for lactic acid resistance resulted in enhancement of the resistant phenotype of the single deleted mutants [59]. These findings might support the role of *SAM2* as stress-mediator, similarly to other stress-induced genes.

Localization, distribution and abundance of Sam2p

The protein Sam2p has a predicted globular structure, with no transmembrane regions or signal peptide [60], like its homolog Sam1p; it is therefore predicted to be soluble. Its cellular localization in this work was shown by fluorescence microscopy to be mainly cytoplasmic during exponential growth phase, and then to change during the early stationary phase, showing scattered (cytoplasmic) *foci*. This might also explain the decreased solubility. To test a possible interaction with other proteins in complex (es) eventually associated to the membranes, we analysed plasma membrane enriched fractions (PMEF) of the strain CEN.PK, finding a statistically non significant (i.e. present in two out of three replicates) enrichment of a spot corresponding to Sam2p (our unpublished results). This might reflect its association in (homo or hetero) protein complexes, and a co-sedimentation with plasma membrane proteins during the extraction protocols. Overall, the data suggest that Sam2p is probably relocated in a different way in response to diverse stimuli, presumably requiring its function in different and specific pathways, which need to be further investigated. Co-immunoprecipitation and co-localization experiments will be very helpful to shed some light on this aspect.

The outcomes of manipulating *SAM2* expression

If the observed increase in Sam2p levels is a cellular mechanism triggered to cope with lactic acid stress, why does the deletion of the corresponding gene determine higher lactic acid production in the m850 background?

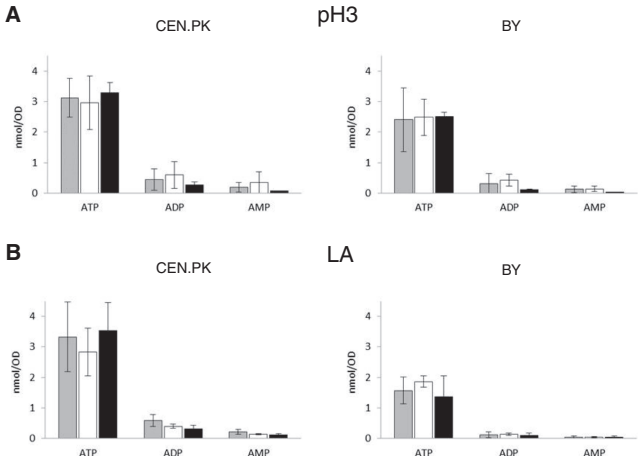

Figure 8 Intracellular adenine nucleotides concentrations in the absence and presence of lactic acid. Yeast cells were grown in shake flasks in minimal (YNB) medium with 2% w/v glucose at initial pH 3, without **(panel A)** or with **(panel B)** 40 g/l of lactic acid. ATP, ADP and AMP were extracted from samples collected during the exponential growth phase and determined by HPLC. Concentrations are expressed per OD of cell culture. The mean and SD for two independent experiments is reported. Left panels: CEN.PK cells; right panels: BY cells; Grey bars: CEN.PK 102-3A [pTEF-L], BY4741 [pTEF-L]; white bars: CEN.PK 102-3A *sam2Δ* [pTEF-L], BY4741 *sam2Δ* [pTEF-L]; black bars: CEN.PK [pTEF-L-SAM2], BY4741 [pTEF-L-SAM2].

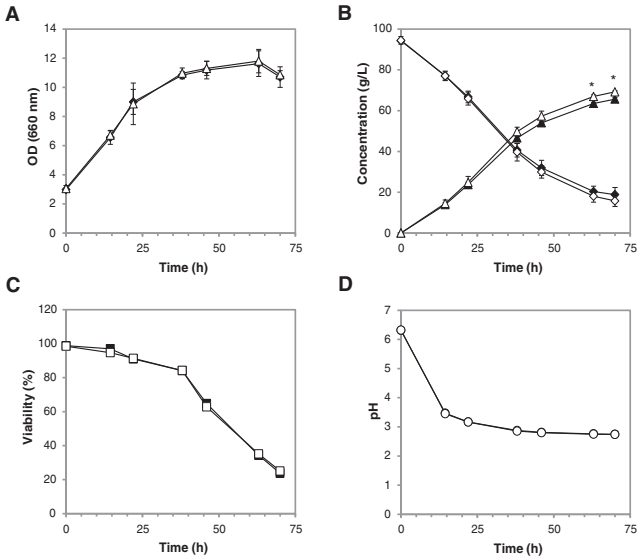

Figure 9 Batch lactic acid production in wt and *sam2Δ* strains. Fermentation profiles for CEN.PK m850 (filled symbols) and CEN.PK m850 *sam2Δ* (open symbols) pre-grown in shake flasks and then transferred in new flasks in minimal medium containing 90 g/L of glucose for the lactic acid production phase. **(A)** Biomass formation (OD at 660 nm). **(B)** Residual glucose (diamonds) and produced lactic acid (triangles). **(C)** Cellular viability was determined by PI staining followed by flow cytometry. **(D)** Culture medium pH. **Panel A** and **B** report the mean and SD for three independent experiments (*$p \leq 0.01$; Student's *t*-test; for supplementary details see Additional file 2: Table S1); **Panel C** and **D** report data from a single representative experiment.

Our data on AXP concentrations suggest that the energetic balance might have a role. In fact, the higher ATP concentration found in the CEN.PK m850 *sam2Δ* strain before starting the lactic acid production phase, together with a higher energy charge value, might account for the superior performance of this strain compared to the CEN.PK m850 parental strain. Probably, a higher biosynthetic potential endows the cells with a larger pool of beneficial metabolites and/or better sustain the activity of energy-consuming detoxifying systems. As it was previously demonstrated that lactic acid production in engineered *S. cerevisiae* is limited by ATP availability [20], the fact that no ATP or energetic differences were detected later on during production is not surprising, since it is highly probable that in such a dynamic situation any ATP excess would be readily used by the cells. In the laboratory strains, the different auxotrophies might also contribute to the different ATP levels, due to the energetic cost of amino acid intake. The substantially lower percentages of dead cells in the genetically complemented BY clearly indicate that prototrophy gives a substantial advantage during lactic acid stress. Besides that, other mechanisms might as well be involved in the different outcomes of *SAM2* expression in the two laboratory strains. More specifically, in the case of the BY4741 background *SAM2* overexpression caused severe growth deficiencies and increase cell death even if no specific differences in ATP levels were assessed in dependence on *SAM2* modulation. Furthermore, the positive impact of *SAM2* deletion was not significant when the leucine auxotrophy was complemented. Notably, it has been demonstrated that the leucyl-tRNA synthetase (LeuRS) triggers TORC1 activation [61], therefore promoting cell growth. The resulting biosynthetic pathways stimulation might cover the positive effect of Sam2p absence postulated in our hypothesis and might also account for cellular growth in more severe stress conditions (40 g/l of lactic acid). Despite more experimental evidences are necessary before further speculations can be proposed, the differences between/among

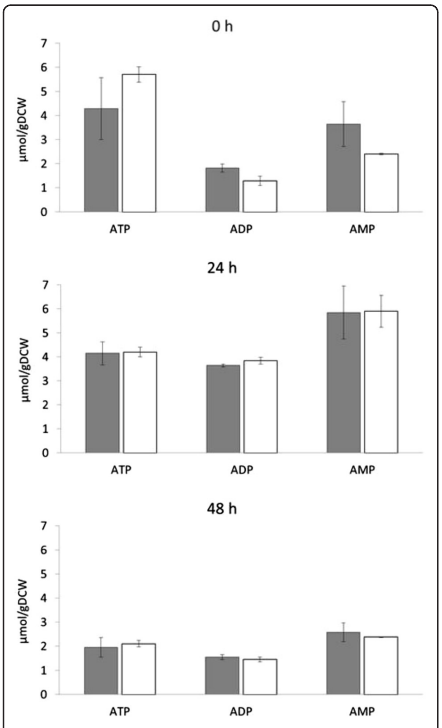

Figure 10 Intracellular adenine nucleotides concentrations in the lactic acid producing strains. CEN.PK m850 (grey bars) and CEN.PK m850 *sam2Δ* (white bars) were pre-grown in shake flasks and then transferred in new flasks in minimal medium containing 90 g/L of glucose for the lactic acid production phase. ATP, ADP and AMP were extracted and determined by HPLC, immediately before (0 h) or after the transfer in the production medium, at the indicated times (24 h and 48 h). Nucleotide concentrations are expressed per gram of dry cell weight (DCW). The mean and SD for two independent experiments is reported.

genetic backgrounds are possibly ascribable to other pathways in which SAM is involved. For example, SAM is also consumed in the synthesis of ergosterol, and CEN.PK was shown to have a different regulation of the ergosterol biosynthesis pathway and different ergosterol contents compared to S288c (the progenitor of BY, [62]). Our data to date seem to suggest that the connection between lactic acid stress and Sam2p function is interconnected with many specific pathways, and it is not only ascribable to energy availability or auxotrophic requirement.

Conclusions

Cofactor engineering, *i.e.* the manipulation of cofactor levels, as exemplified by SAM in this work, in addition to providing means to study cellular metabolism has the potential to be used as an additional tool to achieve desired metabolic engineering goals and fits with current trends in systems biotechnology. Our findings confirm the potential of cofactor-engineering strategies for industrial application [63].

Summarizing, at least four are the most relevant observations deriving from the current work. First of all, (*i*) lactic acid addition at low pH determines an increase of Sam2p in the cell. This increase was mainly associated to the insoluble protein fraction. In parallel, the fluorescence microscopy data highlighted the presence of protein aggregates appearing in stationary phase cells (Figure 2), whose further investigation might lead to novel insights on the dynamics of Sam2p (and Sam1p) interactions with other partners for the accomplishment of specific functions. This work hence added useful information on the cellular distribution of an enzyme of high importance for cell metabolism, whose localization is still reported as ambiguous.

Then, (*ii*) the overexpression of *SAM2* reduces the fitness of the laboratory strain BY4741 during lactic acid stress, while it has no obvious effects on the intrinsically more stress resistant laboratory strain CEN.PK 113-5D. On the contrary, (*iii*) the deletion of *SAM2* confers a growth advantage and a higher viability to BY4741 cells under lactic acid stress in a leucine auxothrophic strain, while again it has no obvious effects on the strain CEN. PK 113-5D.

Finally (*iv*) the deletion of *SAM2* allows a better production (g/L) and productivity (g/L h) of lactic acid from a previously engineered and evolved yeast strain.

All together, these data indicate Sam2p as a responsive element to lactic acid stress and suggest its modulation for lactic acid production improvement. Clarifying the nature of Sam2p interactions with other cellular components and their role in response to lactic acid stress might lead, in the future, to even higher resistance properties and productions via engineering of other interactors.

Methods

Yeast strains, transformation, media and cultivation

The *S. cerevisiae* parental and derived strains used in this study are listed in Table 2. Strain CEN.PK 102-3A was used for overexpression/deletion studies and CEN.PK 113-11C for GFP fusion. BY4741 (obtained from EUROSCARF) was used for overexpression/deletion studies and GFP fusion. The m850 lactic strain has been previously described [17,18], obtained starting from a *PDC1*, *PDC5*, *PDC6* triple deleted CEN.PK strain [20], and was here deleted in *SAM2*.

Table 1 Energy charge values in the lactic acid producing strains

Time (h)	m850		m850 *sam2Δ*	
0	0.53	±0.11	0.68	±0.01
24	0.44	±0.02	0.44	±0.03
48	0.45	±0.07	0.48	±0.01

The mean and SD for two independent experiments are reported.

Yeast transformations were performed according to the LiAc/PEG/ss-DNA protocol [64] and the strains were transformed with the constructs described below, in parallel with the corresponding empty plasmids. Integration of the constructs was confirmed by PCR analysis. For each set of transformation at least three independent transformants were initially tested, showing no significant differences among them.

Yeast cultures were performed in synthetic minimal medium (0.67% w/v YNB Biolife without amino acids) with 2% w/v D-glucose as carbon source. When required, supplements such as leucine, uracil, methionine and histidine were added to a final concentration of 50 mg/L, or to 125 mg/L, 500 mg/L, 100 mg/L, 150 mg/L for histidine, leucine, methionine and uracil respectively for the experiment shown in Figure 6, while the antibiotic G418 (Roche Diagnostics) was added to a final concentration of 200 mg/L. Lactic acidic stress was imposed by adding the desired amount of L-lactic acid (Sigma-Aldrich) to the culture medium. The final media have been prepared starting from 2 different stock solutions, one of 100 g/L lactic acid and one of synthetic minimal medium 2X, in order to obtain the desired lactic acid concentration. The pH of the lactic acid and the culture media were adjusted to 3 with pellets of KOH and HCl 1 M, respectively. Cell growth was monitored by measuring the OD at 660 nm at regular time intervals and cells were inoculated at an initial OD of 0.02 for growth kinetics experiments and at an initial OD of 0.005 for western blot and fluorescence microscopy experiments. All cultures were incubated in shake flasks at 30°C and 160 r.p.m. and the ratio of flask/medium volume was 5/1.

For the lactic acid pulsed stress experiment, aliquots of exponentially growing cultures were transferred in tubes containing the desired amount of lactic acid, adjusted to pH 3, at a final OD of 0.1. The cells were incubated at 30°C and 160 r.p.m. for 30 min.

The producing strain CEN.PK m850 and the derived transformants were cultivated as previously described [17]. Briefly, after a first batch growth phase, cells were collected by centrifugation and resuspended in fresh medium at a final OD of 3; lactic acid production kinetics were then performed by incubating at 32°C and 185 r.p.m. in 250-mL quadruple baffled shake flasks in minimal medium containing 2.78 g/L $CaCO_3$, 1.7 g/L YNB without amino acids and without $(NH4)_2SO_4$, 1 g/L urea, 5 ml/L ethanol, and with different glucose concentration (70, 80, 90 g/L) as carbon source. Each experiment was repeated at least three times.

Gene amplification and plasmids construction

The *S. cerevisiae SAM2* gene sequence was amplified by PCR using as a template the genomic DNA from CEN.PK strain, extracted by standard methods [65]. Pwo DNA polymerase (Roche catalogue no. 11 644 955 001) was used on a GeneAmp PCR System 9700 (PE Applied Biosystem, Inc.). Standard conditions used were 0.2 mM primers, 1.5 U of Pwo and 3 μL of genomic DNA. The program used for amplification of gene was as follows: after 5 min at 94°C, 30 cycles (each cycle consisting of 45 sec at 94°C, 30 sec at 58°C and 1 min 30 sec at 72°C) were carried out, followed by 7 min at 72°C. Oligonucleotides pairs for *SAM2* were as follows: SAM2_fw (5′-AATCATGTCCAAGAGCAAAACTTTCTTAT-3′) and SAM2_rev (5′-CATGGGAAAAACCAAAGAAATTGGAATTTTAA -3′). The amplified fragment was sub-cloned using the Perfectly Blunt Cloning kit (Novagen) into the *Escherichia coli* vector pSTBlue-1 obtaining the plasmid pSTBlue-SAM2. The insert was sequenced and it resulted identical to the deposited *S. cerevisiae* target sequence (*SAM2*, GeneID: 852113). This coding sequence was used for the construction of the multicopy expression plasmid pTEF-L-SAM2. This plasmid was derived from the commercial yeast multicopy expression plasmid p427-TEF (Dualsystems Biotechnology, CH), upon substitution of the selective marker Kan-MX with *LEU2* as follows: p427-TEF was *Nco*I digested, blunted and *Dra*III digested. The *LEU2* marker was excised from pYX042 (R & D Systems, Inc., Wiesbaden, D) by digestion with *Not*I, followed by blunting, and *Dra*III digestion, and then ligated to the recipient vector. The obtained vector pTEF-L was linearized with *Eco*RI and ligated to the *SAM2* ORF, excised with *Eco*RI from pSTBlue-SAM2.

The disruption of *SAM2* was performed using a standard recombination approach. pSTBlue-SAM2 was *Nco*I digested, blunted and *Eco*RV digested in the *SAM2* ORF. The excided fragment of about 200 nt was replaced with Kan-MX. The Kan marker was obtained from pFA6A-KanMX4 [66] digested with *Eco*RV and *Bam*HI. The deletion cassette *SAM2*sx-KanMX-*SAM2*dx was excised from the resulting plasmid by cutting with *Nde*I and *Pvu*II and used directly for yeast transformations. The obtained clones were screened by PCR using the following conditions: 5 min at 94°C, 30 cycles (45 sec at 94°C, 45 sec at 58°C and 2 min at 72°C) and 7 min at 72°C. The control primers, SAM2_fw_gen (5′-CGACGTCAAATCTTCATATGCAAGG-3′) and Kan_fw (5′-AACGTGAGTCTTTTCCTTACCCAT-3′), were designed upstream of the ATG

Table 2 Yeast strains used and created in this study

Strain	Relevant genotype	Plasmid	Reference
CEN.PK 113-11C	*MATa, ura3-52, his3-Δ1*	-	P. Kotter[1]
CEN.PK 102-3A	*MATa, ura3-52, leu2-3,112*	-	P. Kotter[1]
CEN.PK [pTEF-L]	CEN.PK 102-3A	pTEF-L, multicopy (*Sc*TEF1, *LEU2*)	This work
CEN.PK [pTEF-L-SAM2]	CEN.PK 102-3A	pTEF-L-SAM2 (*Sc*TEF1, *ScSAM2*, *LEU2*)	This work
CEN.PK *sam2Δ*	CEN.PK 102-3A *sam2::KanMX4*	-	This work
CEN.PK *sam2Δ* [pTEF-L]	CEN.PK 102-3A *sam2Δ*	pTEF-L (*Sc*TEF1, *LEU2*)	This work
CEN.PK *SAM2*GFP	CEN.PK 113-11C *SAM2:: SAM2*GFP-*HIS3*	-	This work
CEN.PK m850	*MATa, pdc1(-6,-2)::loxP, pdc5(-6,-2)::loxP, pdc6 (-6,-2)::loxP, ura3-52, acid tolerant*	YEpLpLDH (*Sc*TPI, *Lp*LDH, *URA3*)	[18]
CEN.PK m850 *sam2Δ*	CEN.PKm850 *sam2::KanMX4*	YEpLpLDH (*Sc*TPI, *Lp*LDH, *URA3*)	This work
BY4741	*MATa, his3-Δ1, leu2-Δ0, met15-Δ0, ura3-Δ0*	-	EUROSCARF[2]
BY4741[pTEF-L]	BY4741	pTEF-L (*Sc*TEF1, *LEU2*)	This work
BY4741[pTEF-L-SAM2]	BY4741	pTEF-L-SAM2 (*Sc*TEF1, *ScSAM2*, *LEU2*)	This work
BY4741 *sam2Δ*	BY4741 *sam2::kanMX4*	-	This work
BY4741 *sam2Δ* [pTEF-L]	BY4741 *sam2Δ*	pTEF-L (*Sc*TEF1, *LEU2*)	This work
BY4741 *SAM2*GFP	BY4741 *SAM2:: SAM2*GFP-*HIS3*	-	This work

[1]Institut fur Mikrobiologie der Johann Wolfgang Goethe Universitat, Frankfurt, Germany.
[2]http://web.uni-frankfurt.de/fb15/mikro/euroscarf/.

and in the KanMX marker cassette. The DyNAzyme™ II DNA Polymerase (Finnzymes Reagents) was utilized for those reactions. DNA manipulation, transformation and cultivation of *E. coli* (Novablue, Novagen) were performed following standard protocols [65]. All the restriction and modification enzymes utilised are from NEB (New England Bio- labs, UK) or from Roche Diagnostics.

The substitution of *SAM2* endogenous ORF with the construct *SAM2*GFP was performed using a standard recombination approach. The construct was obtained by PCR using as template the Longtine plasmid pFA6a-GFP (S65T)-His3MX6. Standard conditions used were 0.2 mM primers, 1.5 U of Pwo and 0.3 μL of plasmid DNA. The program used for amplification of construct was as follows: 5 min at 94°C, 5 cycles (45 sec at 94°C, 30 sec at 50° C and 2 min at 72°C) and 7 min at 72°C, then 20 cycles (45 sec at 94°C, 30 sec at 65°C and 2 min at 72°C) and 7 min at 72°C. Oligonucleotides pairs for *SAM2*GFP were as follows: SAM2_Fw_longtine (5′-TCAAGAGTACTCATGGGAAAAACCAAAGAAATTGGAATTTCGGATCCCCGGGTTAATTAA-3′) and SAM2_Rev_longtine (5′-TATAAAAATCAAAATAAAACATTTATTGTCTAAATGTTTAGAATTCGAGCTCGTTTAAAC-3′). The amplified fragment was used directly for yeast transformation.

The obtained clones were screened by PCR using the following conditions: 5 min at 94°C, 30 cycles (45 sec at 94°C, 45 sec at 57.5°C and 1 min 30 sec at 72°C) and 7 min. the control primers were as follows: SAM2_fw_gen (5′-CGACGTCAAATCTTCATATGCAAGG-3′) and Gfp_Rev (5′-AAGAATTGGGACAACTCCAGTGA-3′). The DyNAzyme™ II DNA Polymerase (Finnzymes Reagents) was utilized for those reactions.

Protein extractions for western blot analysis

Total protein extraction

10^8 cells were broken by glass beads in 20% TCA. After centrifugation, the pellet was resuspended in the Laemmli buffer system and in 1 M Tris, pH 7. The sample was boiled for 3 min and after centrifugation the supernatant was collected for the western blot analysis.

Tris-Urea-SDS sequential extraction

10^8 cells were resuspended in Tris buffer (50 mM Tris pH 8.7, 150 mM NaCl, 1 mM EDTA, 1 mM protease inhibitor cocktail, 1 mM PMSF) and broken by glass beads. After centrifugation the supernatant was collected (soluble fraction) and the pellet was resuspended in urea buffer (50 mM Tris pH 8.7, 150 mM NaCl, 1 mM EDTA, 1 mM protease inhibitor cocktail, 1 mM PMSF, 8 M urea). The sample was centrifuged and the supernatant was collected (urea fraction) while the pellet was resuspended in SDS buffer (SDS 10%, 1 mM protease inhibitor cocktail, 1 mM PMSF; SDS fraction).

SDS-PAGE and western blot analysis

The samples were boiled for 3 min in the Laemmli buffer system and then were loaded on a 12% poly-acrylamide analytical SDS gel. Electrophoresis in the separating gel was conducted at 30 mA for 5 hours. After the stacking gel was removed, transfer of proteins from SDS gels to 0.45 μM Protran Nitrocellulose Transfer Membrane was done for 1 hour at 250 mA.

Blocking and incubation with primary antibody to detect Sam2p-GFP

The nitrocellulose paper was then incubated in 5% milk made in TBS-Tween over night at 4°C with shaking. Monoclonal anti-GFP antibody (Living Colors A.v JL-8, Diatech Labline) was diluted 1:1000 in 5% milk/TBS-Tween and applied to the nitrocellulose membrane. After incubation for 2 hours at room temperature with shaking, the membrane was washed in three changes of TBS-Tween over 25 min.

Blocking and incubation with primary antibody to detect actin

Monoclonal anti-actin antibody (Abcam 2Q1055) was diluted 1:1000 in 5% milk/TBS-Tween and applied to the nitrocellulose membrane. After incubation for 3 hours at room temperature with shaking, the membrane was washed in three changes of TBS-Tween over 25 min.

Incubation with secondary antibody and chemiluminescent detection

Rabbit anti-Mouse IgG (FC) secondary antibody, AP (alkaline phosphatase) conjugate was diluted 1:15000 in 5% milk/TBS-Tween and applied to the nitrocellulose membranes for 1 hour at room temperature with shaking. The membranes were washed in four changes of TBS-Tween or TBS over 30 min and dried. The membranes were incubated with CDP-Star Chemiluminescent Substrate for 5 min at room temperature under gentle agitation. The nitrocellulose membranes were then exposed to Pierce Cl-x posure film to reveal Sam2p-GFP and actin signals, respectively. Bands were quantified with ImageJ 1.48 software.

Fluorescence microscopy analysis

CEN.PK 113-5D and BY4741 *SAM2*GFP strains were observed in a Nikon ECLIPSE 90i fluorescence microscope (Nikon) equipped with a 100X objective. Emission fluorescence due to GFP was detected by B-2A (EX 450–490 DM505 BA520) filter (Nikon). Digital images were acquired with a CoolSnap CCD camera (Photometrics) using MetaMorph 6.3 software (Molecular Devices).

Flow cytometric analysis

For identification of dead or severely compromised cells, cells were washed three times (Tris-HCl 50 mM, $MgCl_2$ 15 mM, pH 7.7) and resuspended in propidium iodide (PI) solution 0.23 mM. Samples were then analyzed using a CYTOMICS FC 500 flow cytometer (Beckman Coulter) equipped with a diode laser (excitation wavelength 488 nm). The fluorescence emission was measured through a 670 nm long pass filter (FL3 parameter) for PI signal. The sample flow rate during analysis did not exceed 600–700 cells/s. Threshold settings were adjusted so that the cell debris was excluded from the data acquisition; 25000 cells were measured for every sample. Data analysis was performed afterwards with Cyflogic 1.2.1 software (©Perttu Terho & ©CyFlo Ltd).

AXP extraction and quantification

ATP, ADP and AMP were extracted and quantified as described in [50]. Briefly, extraction was performed in 0.52 M TCA containing 17 mM EDTA. After centrifugation, supernatants were neutralized with 2 M Tris-base. Neutralized samples were then analyzed by HPLC with a Zorbax Eclipse XDB-C18 LC column (150 × 4.6 mm) (Agilent Technologies) kept at 20°C. Sample elution was carried out using a mobile phase consisting of acetonitrile and tetrabutylammonium buffer (0.005 M tetrabutylammonium hydrogensulfate, 0.01 M Na2HPO4) at pH 7.0, using a flow rate of 1 mL min^{-1}. A gradient was applied, where acetonitrile was increased from 6% to 25% and then back to 6%, as described in [50]. Adenonucleotides were detected with a photodiode array detector at 260 nm and peak identities were confirmed by co-elution with standards (Sigma-Aldrich). Concentrations were determined using calibration curves of standard solutions. The energy charge (E_c) was calculated from the following equation:

$$E_c = ([ATP] + 0.5 \times [ADP])/([ATP] + [ADP] + [AMP])$$

Extracellular metabolites and pH determination

Residual glucose and lactic acid produced were determined via high-performance liquid chromatography (HPLC, Model 1100, Agilent Technologies) using an

Aminex HPX-87H ion exchange column 300 mm × 7.8 mm (Bio-Rad) thermostated at 60°C. The mobile phase was 5 mM sulphuric acid with a flow of 0.6 ml/min. Lactic acid was detected with an UV-detector at 210 nm. Glucose was detected with a RI detector, kept at 45°C.

The pH of the medium was measured with a pH-meter on fresh media or culture supernatants, after cells removal by centrifugation.

Statistical analysis

All statistical analysis, where *p*-values are indicated, was performed using a two-tails, unpaired, heteroscedastic Student's *t*-test.

Additional files

Additional file 1: Figure S1. Western blot analysis of the fractions obtained from sequential protein extraction for the strain CEN.PK 113-11C *SAM2*GFP. Cells were grown in shake flasks in minimal (YNB) medium with 2% w/v glucose without or with the addition of different concentrations of lactic acid (pH 5, pH 3, 12 g/L and 20 g/L lactic acid at pH3) and then three protein sub-fractions were obtained after sequential extraction in Tris buffer (Native, **A**), 8 M urea **(B)** and 10% SDS **(C)**. The Sam2p-GFP levels were evaluated after 16 hours after inoculation using an anti-GFP antibody. Samples were normalised according to cell number. β-actin levels have been detected as control. Bands have been quantified by ImageJ 1.48 software. Histograms refer to the ratio (%) of Sam2p/Actin normalized to the values at pH 5. LA: lactic acid.

Additional file 2: Table S1. Statistical evaluation of differences in lactic acid production.

Competing interests

The authors declare that they have no competing interests.

Authors' contributions

LD, NMB and MAR carried out the experiments, participated in the design of the study, data interpretation and in writing the manuscript. PP carried out the initial setting of the differential growth kinetics and analyses. LP contributed to the data interpretation and manuscript revision. DP and PB conceived the study, participated in its design, data interpretation and in writing the manuscript. All the authors have read and approved the final manuscript.

Acknowledgements

The authors would like to thank Maria del Pilar Larosa and Giusy Adamo for technical contribution, Simone Passolunghi for technical contribution with the flow cytometric analysis, and Valeria Mapelli from Chalmers University of Technology (Sweden) for kindly providing the protocol for AXP extraction and quantification. P.B. and D.P. acknowledge the support by FAR (Fondo di Ateneo per la Ricerca) of the University of Milano-Bicocca. L.D. acknowledges the Post doctoral fellowship of the University of Milano Bicocca. The research leading to these results has also received funding from the European Community's Seventh Framework Programme (FP7/2007-2013) under the project entitled "Systems Biology as a Driver for Industrial Biotechnology" (SYSINBIO, Grant agreement no. KBBE-212766).

Author details

[1]Dipartimento di Biotecnologie e Bioscienze, Università degli Studi di Milano-Bicocca, Piazza della Scienza 2, 20126 Milan, Italy. [2]Dipartimento di Bioscienze, Biotecnologie e Biofarmaceutica, Università degli Studi di Bari Aldo Moro, Via Orabona 4, 70125 Bari, Italy.

Received: 9 June 2014 Accepted: 8 October 2014
Published online: 30 October 2014

References

1. Vickroy T: **Lactic Acid.** In *Comprehensive Biotechnology*, Volume 3. Edited by Moo-Young M. Oxford: Pergamon Press; 1985.
2. Sauer M, Porro D, Mattanovich D, Branduardi P: **Microbial production of organic acids: expanding the markets.** *Trends Biotechnol* 2008, **26:**100–108.
3. Sauer M, Porro D, Mattanovich D, Branduardi P: **16 years research on lactic acid production with yeast - ready for the market?** *Biotechnol Genet Eng Rev* 2010, **27:**229–256.
4. Porro D, Gasser B, Fossati T, Maurer M, Branduardi P, Sauer M, Mattanovich D: **Production of recombinant proteins and metabolites in yeasts: when are these systems better than bacterial production systems?** *Appl Microbiol Biotechnol* 2011, **89:**939–948.
5. Madhavan Nampoothiri K, Nair NR, John RP: **An overview of the recent developments in polylactide (PLA) research.** *Bioresour Technol* 2010, **101:**8493–8501.
6. John RP, Nampoothiri KM, Pandey A: **Fermentative production of lactic acid from biomass: an overview on process developments and future perspectives.** *Appl Microbiol Biotechnol* 2007, **74:**524–534.
7. Gao C, Ma C, Xu P: **Biotechnological routes based on lactic acid production from biomass.** *Biotechnol Adv* 2011, **29:**930–939.
8. Fan Y, Zhou C, Zhu X: **Selective catalysis of lactic acid to produce commodity chemicals.** *Catal Rev* 2009, **51:**293–324.
9. Datta R, Henry M: **Lactic acid: recent advances in products, processes and technologies — a review.** *J Chem Technol Biotechnol* 2006, **81:**1119–1129.
10. Wee Y-J, Kim J-N, Ryu H-W: **Biotechnological production of lactic acid and its recent applications.** *Food Technol Biotechnol* 2006, **44:**163–172.
11. Okano K, Tanaka T, Ogino C, Fukuda H, Kondo A: **Biotechnological production of enantiomeric pure lactic acid from renewable resources: recent achievements, perspectives, and limits.** *Appl Microbiol Biotechnol* 2010, **85:**413–423.
12. Dequin S, Barre P: **Mixed lactic acid-alcoholic fermentation by *Saccharomyces cerevisiae* expressing the *Lactobacillus casei* L (+)-LDH.** *Biotechnology (N Y)* 1994, **12:**173–177.
13. Porro D, Bianchi MM, Brambilla L, Menghini R, Bolzani D, Carrera V, Lievense J, Liu CL, Ranzi BM, Frontali L, Alberghina L: **Replacement of a metabolic pathway for large-scale production of lactic acid from engineered yeasts.** *Appl Environ Microbiol* 1999, **65:**4211–4215.
14. Adachi E, Torigoe M, Sugiyama M, Nikawa J-I, Shimizu K: **Modification of metabolic pathways of *Saccharomyces cerevisiae* by the expression of lactate dehydrogenase and deletion of pyruvate decarboxylase genes for the lactic acid fermentation at low pH value.** *J Ferment Bioeng* 1998, **86:**284–289.
15. Ishida N, Saitoh S, Tokuhiro K, Nagamori E, Matsuyama T, Kitamoto K, Takahashi H: **Efficient production of L-Lactic acid by metabolically engineered *Saccharomyces cerevisiae* with a genome-integrated L-lactate dehydrogenase gene.** *Appl Environ Microbiol* 2005, **71:**1964–1970.
16. Branduardi P, Sauer M, De Gioia L, Zampella G, Valli M, Mattanovich D, Porro D: **Lactate production yield from engineered yeasts is dependent from the host background, the lactate dehydrogenase source and the lactate export.** *Microb Cell Fact* 2006, **5:**4.
17. Valli M, Sauer M, Branduardi P, Borth N, Porro D, Mattanovich D: **Improvement of lactic acid production in *Saccharomyces cerevisiae* by cell sorting for high intracellular pH.** *Appl Environ Microbiol* 2006, **72:**5492–5499.
18. Liu C, Lievense J: *Lactic Acid Producing Yeast.* U.S. patent application 2005, 0112737.
19. Rossi G, Sauer M, Porro D, Branduardi P: **Effect of *HXT1* and *HXT7* hexose transporter overexpression on wild-type and lactic acid producing *Saccharomyces cerevisiae* cells.** *Microb Cell Fact* 2010, **9:**15.
20. van Maris AJ, Winkler AA, Porro D, van Dijken JP, Pronk JT: **Homofermentative lactate production cannot sustain anaerobic growth of engineered *Saccharomyces cerevisiae*: possible consequence of energy-dependent lactate export.** *Appl Environ Microbiol* 2004, **70:**2898–2905.
21. Miller C, Fosmer A, Rush B, McMullin T, Beacom D, Suominen P: **Industrial production of lactic acid.** In *Comprehensive Biotechnology.* Edited by Moo-Young Murray MB II, Colin W. Burlington: Elsevier; 2011:179–188.
22. Piper PW: **Resistance of yeasts to weak organic acid food preservatives.** *Adv Appl Microbiol* 2011, **77:**97–113.
23. Mira NP, Teixeira MC, Sá-Correia I: **Adaptive response and tolerance to weak acids in *Saccharomyces cerevisiae*: a genome-wide view.** *OMICS* 2010, **14:**525–540.

24. Piper P, Calderon CO, Hatzixanthis K, Mollapour M: **Weak acid adaptation: the stress response that confers yeasts with resistance to organic acid food preservatives.** *Microbiology* 2001, **147:**2635–2642.
25. Narendranath NV, Thomas KC, Ingledew WM: **Effects of acetic acid and lactic acid on the growth of *Saccharomyces cerevisiae* in a minimal medium.** *J Ind Microbiol Biotechnol* 2001, **26:**171–177.
26. Thomas KC, Hynes SH, Ingledew WM: **Influence of medium buffering capacity on inhibition of *Saccharomyces cerevisiae* growth by acetic and lactic acids.** *Appl Environ Microbiol* 2002, **68:**1616–1623.
27. Miller GE, Banerjee NC, Stowe CM: **Diffusion of certain weak organic acids and bases across the bovine mammary gland membrane after systemic administration.** *J Pharmacol Exp Ther* 1967, **157:**245–253.
28. Bravim F, de Freitas JM, Fernandes AA, Fernandes PM: **High hydrostatic pressure and the cell membrane: stress response of *Saccharomyces cerevisiae*.** *Ann N Y Acad Sci* 2010, **1189:**127–132.
29. Ding J, Huang X, Zhang L, Zhao N, Yang D, Zhang K: **Tolerance and stress response to ethanol in the yeast *Saccharomyces cerevisiae*.** *Appl Microbiol Biotechnol* 2009, **85**(2):253–263.
30. Folmer V, Pedroso N, Matias AC, Lopes SC, Antunes F, Cyrne L, Marinho HS: **H_2O_2 induces rapid biophysical and permeability changes in the plasma membrane of *Saccharomyces cerevisiae*.** *Biochim Biophys Acta* 2008, **1778:**1141–1147.
31. Simonin H, Beney L, Gervais P: **Cell death induced by mild physical perturbations could be related to transient plasma membrane modifications.** *J Membr Biol* 2007, **216:**37–47.
32. Simonin H, Beney L, Gervais P: **Controlling the membrane fluidity of yeasts during coupled thermal and osmotic treatments.** *Biotechnol Bioeng* 2008, **100:**325–333.
33. Fu J, Wang Z, Chen T, Liu W, Shi T, Wang G, Tang YJ, Zhao X: **NADH plays the vital role for chiral pure D-(−)-2,3-butanediol production in *Bacillus subtilis* under limited oxygen conditions.** *Biotechnol Bioeng* 2014, **9999:**1–6.
34. Vemuri GN, Eiteman MA, McEwen JE, Olsson L, Nielsen J: **Increasing NADH oxidation reduces overflow metabolism in *Saccharomyces cerevisiae*.** *Proc Natl Acad Sci U S A* 2007, **104**(7):2402–2407.
35. Thomas D, Surdin-Kerjan Y: **Metabolism of sulfur amino acids in *Saccharomyces cerevisiae*.** *Microbiol Mol Biol Rev* 1997, **61:**503–532.
36. Lieber CS, Packer L: **S-Adenosylmethionine: molecular, biological, and clinical aspects–an introduction.** *Am J Clin Nutr* 2002, **76:**1148S–1150S.
37. Malakar D, Dey A, Ghosh AK: **Protective role of S-adenosyl-L-methionine against hydrochloric acid stress in *Saccharomyces cerevisiae*.** *Biochim Biophys Acta* 2006, **1760:**1298–1303.
38. Malakar D, Dey A, Basu A, Ghosh AK: **Antiapoptotic role of S-adenosyl-l-methionine against hydrochloric acid induced cell death in *Saccharomyces cerevisiae*.** *Biochim Biophys Acta* 2008, **1780:**937–947.
39. Scheer M, Grote A, Chang A, Schomburg I, Munaretto C, Rother M, Söhngen C, Stelzer M, Thiele J, Schomburg D: **BRENDA, the enzyme information system in 2011.** *Nucleic Acids Res* 2011, **39:**D670–D676. D670-676.
40. Mudd S: **4 The Adenosyltransferases.** In *The Enzyme*, Volume 8. Edited by Boyer PD. New York: Academic Press; 1973:121–154.
41. Lu SC: **S-Adenosylmethionine.** *Int J Biochem Cell Biol* 2000, **32:**391–395.
42. Cherest H, Surdin-Kerjan Y: **S-adenosyl methionine requiring mutants in *Saccharomyces cerevisiae*: evidences for the existence of two methionine adenosyl transferases.** *Mol Gen Genet* 1978, **163:**153–167.
43. Thomas D, Rothstein R, Rosenberg N, Surdin-Kerjan Y: ***SAM2* encodes the second methionine S-adenosyl transferase in *Saccharomyces cerevisiae*: physiology and regulation of both enzymes.** *Mol Cell Biol* 1988, **8:**5132–5139.
44. Thomas D, Surdin-Kerjan Y: **The synthesis of the two S-adenosyl-methionine synthetases is differently regulated in *Saccharomyces cerevisiae*.** *Mol Gen Genet* 1991, **226:**224–232.
45. Kodaki T, Tsuji S, Otani N, Yamamoto D, Rao KS, Watanabe S, Tsukatsune M, Makino K: **Differential transcriptional regulation of two distinct S-adenosylmethionine synthetase genes (*SAM1* and *SAM2*) of *Saccharomyces cerevisiae*.** *Nucleic Acids Res Suppl* 2003, **3:**303–304.
46. Breker M, Gymrek M, Schuldiner M: **A novel single-cell screening platform reveals proteome plasticity during yeast stress responses.** *J Cell Biol* 2013, **200:**839–850.
47. Tkach JM, Yimit A, Lee AY, Riffle M, Costanzo M, Jaschob D, Hendry JA, Ou J, Moffat J, Boone C, Davis TN, Nislow C, Brown GW: **Dissecting DNA damage response pathways by analysing protein localization and abundance changes during DNA replication stress.** *Nat Cell Biol* 2012, **14:**966–976.
48. Huh WK, Falvo JV, Gerke LC, Carroll AS, Howson RW, Weissman JS, O'Shea EK: **Global analysis of protein localization in budding yeast.** *Nature* 2003, **425:**686–691.
49. Pronk JT: **Auxotrophic yeast strains in fundamental and applied research.** *Appl Environ Microbiol* 2002, **68:**2095–2100.
50. Ask M, Bettiga M, Mapelli V, Olsson L: **The influence of HMF and furfural on redox-balance and energy-state of xylose-utilizing Saccharomyces cerevisiae.** *Biotechnol Biofuels* 2013, **6:**22.
51. Ghosh AK, Ramakrishnan G, Rajasekharan R: **YLR099C (*ICT1*) encodes a soluble Acyl-CoA-dependent lysophosphatidic acid acyltransferase responsible for enhanced phospholipid synthesis on organic solvent stress in *Saccharomyces cerevisiae*.** *J Biol Chem* 2008, **283:**9768–9775.
52. Carman GM, Han GS: **Regulation of phospholipid synthesis in the yeast *Saccharomyces cerevisiae*.** *Annu Rev Biochem* 2011, **80:**859–883.
53. Hickman MJ, Petti AA, Ho-Shing O, Silverman SJ, McIsaac RS, Lee TA, Botstein D: **Coordinated regulation of sulfur and phospholipid metabolism reflects the importance of methylation in the growth of yeast.** *Mol Biol Cell* 2011, **22:**4192–4204.
54. Zinser E, Sperka-Gottlieb CD, Fasch EV, Kohlwein SD, Paltauf F, Daum G: **Phospholipid synthesis and lipid composition of subcellular membranes in the unicellular eukaryote *Saccharomyces cerevisiae*.** *J Bacteriol* 1991, **173:**2026–2034.
55. Griac P, Swede MJ, Henry SA: **The role of phosphatidylcholine biosynthesis in the regulation of the *INO1* gene of yeast.** *J Biol Chem* 1996, **271:**25692–25698.
56. Evans PJ, Whiteman M, Tredger JM, Halliwell B: **Antioxidant properties of S-adenosyl-L-methionine: a proposed addition to organ storage fluids.** *Free Radic Biol Med* 1997, **23:**1002–1008.
57. Webb CB, Twedt DC, Fettman MJ, Mason G: **S-adenosylmethionine (SAMe) in a feline acetaminophen model of oxidative injury.** *J Feline Med Surg* 2003, **5:**69–75.
58. Kawahata M, Masaki K, Fujii T, Iefuji H: **Yeast genes involved in response to lactic acid and acetic acid: acidic conditions caused by the organic acids in *Saccharomyces cerevisiae* cultures induce expression of intracellular metal metabolism genes regulated by Aft1p.** *FEMS Yeast Res* 2006, **6:**924–936.
59. Suzuki T, Sakamoto T, Sugiyama M, Ishida N, Kambe H, Obata S, Kaneko Y, Takahashi H, Harashima S: **Disruption of multiple genes whose deletion causes lactic-acid resistance improves lactic-acid resistance and productivity in *Saccharomyces cerevisiae*.** *J Biosci Bioeng* 2013, **115:**467–474.
60. Reynolds SM, Käll L, Riffle ME, Bilmes JA, Noble WS: **Transmembrane topology and signal peptide prediction using dynamic bayesian networks.** *PLoS Comput Biol* 2008, **4:**e1000213.
61. Bonfils G, Jaquenoud M, Bontron S, Ostrowicz C, Ungermann C, De Virgilio C: **Leucyl-tRNA synthetase controls TORC1 via the EGO complex.** *Mol Cell* 2012, **46:**105–110.
62. Otero JM, Vongsangnak W, Asadollahi MA, Olivares-Hernandes R, Maury J, Farinelli L, Barlocher L, Osterås M, Schalk M, Clark A, Nielsen J: **Whole genome sequencing of *Saccharomyces cerevisiae*: from genotype to phenotype for improved metabolic engineering applications.** *BMC Genomics* 2010, **11:**723.
63. Wang Y, San KY, Bennett GN: **Cofactor engineering for advancing chemical biotechnology.** *Curr Opin Biotechnol* 2013, **24**(6):994–999.
64. Gietz RD, Woods RA: **Transformation of yeast by lithium acetate/single-stranded carrier DNA/polyethylene glycol method.** *Methods Enzymol* 2002, **350:**87–96.
65. Sambrook J, Fritsch EF, Maniatis T: *Molecular Cloning - A Laboratory Manual.* 2nd edition. New York: Cold Spring Harbor Laboratory; 1989.
66. Wach A, Brachat A, Pöhlmann R, Philippsen P: **New heterologous modules for classical or PCR-based gene disruptions in *Saccharomyces cerevisiae*.** *Yeast* 1994, **10:**1793–1808.

doi:10.1186/s12934-014-0147-7
Cite this article as: Dato *et al.*: Changes in *SAM2* expression affect lactic acid tolerance and lactic acid production in *Saccharomyces cerevisiae*. *Microbial Cell Factories* 2014 **13**:147.

Additional files

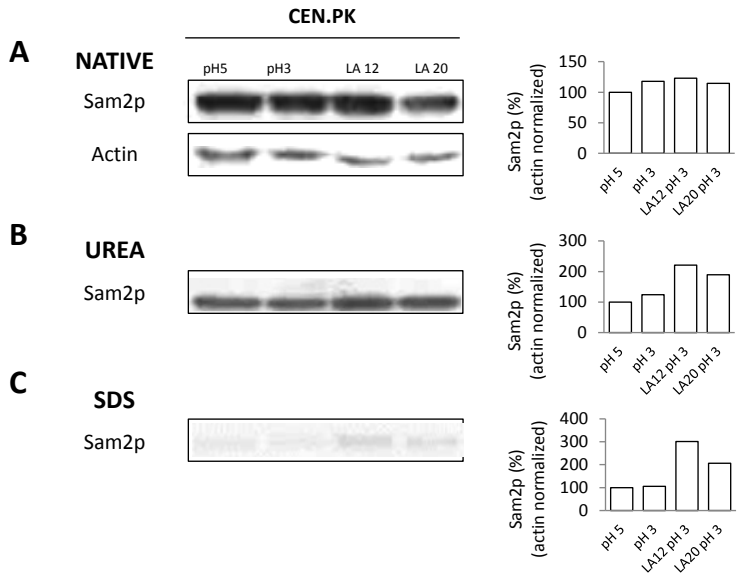

Figure S1: Western blot analysis of the fractions obtained from sequential protein extraction for the strain CEN.PK 113-11C SAM2GFP. Cells were grown in shake flasks in minimal (YNB) medium with 2% w/v glucose without or with the addition of different concentrations of lactic acid (pH 5, pH 3, 12 g/L and 20 g/L lactic acid at pH3) and then three protein sub-fractions were obtained after sequential extraction in Tris buffer (Native, **A**), 8 M urea (**B**) and 10% SDS (**C**). The Sam2p-GFP levels were evaluated after 16 hours after inoculation using an anti-GFP antibody. Samples were normalised according to cell number. à-actin levels have been detected as control. Bands have been quantified by ImageJ 1.48 software. Histograms refer to the ratio (%) of Sam2p/Actin normalized to the values at pH 5. LA: lactic acid.

Table S1 – Statistical evaluation of differences in lactic acid production

	95% CI[1] (*z* low and *z* up[2], g/L)				*t*-test *p*-values
Time (h)	**m850**		**m850 *sam2Δ***		**m850 *vs* m850 *sam2Δ***
14,5	12.85	15	12.72	16.38	0.5997
22	22.41	25.06	21.56	28.18	0.5833
38	45.42	47.8	47.25	52.18	0.1167
46	53.71	54.29	54.55	60.11	0.1423
63	63.17	63.88	66.04	67.89	0.0103
70	64.58	66.7	68.57	69.82	0.0087

Data for three independent experiments are reported.
[1] Confidence Interval
[2] Lower and upper endpoints of the CI

Branduardi et al. Biotechnology for Biofuels 2013, 6:68
http://www.biotechnologyforbiofuels.com/content/6/1/68

Biotechnology for Biofuels

RESEARCH Open Access

A novel pathway to produce butanol and isobutanol in *Saccharomyces cerevisiae*

Paola Branduardi[1*†], Valeria Longo[1†], Nadia Maria Berterame[1], Giorgia Rossi[2] and Danilo Porro[1]

Abstract

Background: The sustainable production of biofuels remains one of the major issues of the upcoming years. Among the number of most desirable molecules to be produced, butanol and isobutanol deserve a prominent place. They have superior liquid-fuel features in respect to ethanol. Particularly, butanol has similar properties to gasoline and thus it has the potential to be used as a substitute for gasoline in currently running engines. *Clostridia* are recognized as natural and good butanol producers and are employed in the industrial-scale production of solvents. Due to their complex metabolic characteristics and to the difficulty of performing genetic manipulations, in recent years the *Clostridia* butanol pathway was expressed in other microorganisms such as *Escherichia coli* and *Saccharomyces cerevisiae*, but in yeast the obtained results were not so promising. An alternative way for producing fusel alcohol is to exploit the degradation pathway of aminoacids released from protein hydrolysis, where proteins derive from exhausted microbial biomasses at the end of the fermentation processes.

Results: It is known that wine yeasts can, at the end of the fermentation process, accumulate fusel alcohols, and butanol is among them. Despite it was quite obvious to correlate said production with aminoacid degradation, a putative native pathway was never proposed. Starting from literature data and combining information about different organisms, here we demonstrate how glycine can be the substrate for butanol and isobutanol production, individuating at least one gene encoding for the necessary activities leading to butanol accumulation. During a kinetic of growth using glycine as substrate, butanol and isobutanol accumulate in the medium up to 92 and 58 mg/L, respectively.

Conclusions: Here for the first time we demonstrate an alternative metabolic pathway for butanol and isobutanol production in the yeast *S. cerevisiae*, using glycine as a substrate. Doors are now opened for a number of optimizations, also considering that starting from an aminoacid mixture as a side stream process, a fusel alcohol blend can be generated.

Keywords: Butanol, Isobutanol, Glycine, *Saccharomyces cerevisiae*

Background

The production of biofuels from renewable biomasses is one of the answers to help solving the problems associated with limited fossil resources and climate changes. Butanol has superior liquid-fuel characteristics in respect to ethanol, similar properties to gasoline, and thus it has the potential to be used as a substitute for gasoline in currently running engines [1].

Clostridia are recognized as natural and good butanol producers and are employed in the industrial-scale production of solvents [2]. However, the complex metabolic characteristics and the difficulty of performing genetic manipulations on these bacteria fostered the exploitation of other well established cell factories. In recent years, *Escherichia coli* and *Saccharomyces cerevisiae* were engineered with the *Clostridia* butanol pathway [3,4]. While many optimizations have been successfully introduced in *E. coli* [5-8] reaching productions similar to that obtained in *Clostridia* [9], this was up to now not reported for the budding yeast. For an exhaustive view of the metabolic strategies applied for butanol and other fusel alcohol production see [10,11] and references therein. Remarkably, *Liao et al.* proposed that proteins, and thus the aminoacids released from proteins hydrolysis,

* Correspondence: paola.branduardi@unimib.it
†Equal contributors
[1]University of Milano Bicocca, Piazza della Scienza 2, 20126, Milano, Italy
Full list of author information is available at the end of the article

can be used as a raw material for biorefining and so for biofuels production. Indeed, proteins are abundantly present as final waste of lignocellulose processing [12]. We focused our attention on the strategy which takes advantage of ketoacids as intermediates in amino acids biosynthesis and degradation metabolism to produce fusel alcohols in the yeast *S. cerevisiae*. While the pathway to isoketovalerate was better elucidated and recently successfully exploited for isobutanol formation in *S. cerevisiae* [13-17], butanol production from ketovalerate was never experimentally measured.

S. cerevisiae have one or more carrier systems specific for each aminoacid, even if they are not all currently known. Among them, the general aminoacids permease, encoded by *GAP*1 gene, is involved in glycine transport [18]. In the cytosol glycine can be catabolised in different ways, based on nutritional requirements. For example, it can be converted into serine through serine hydroxymethyltransferase enzyme (Shm2) [19] or into CO_2 and NH_3 through the enzymatic complex of glycine decarboxylase enzyme (GDC) [20].

Villas-Bôas and co-workers [21] have *in silico* proposed the generation of glyoxylate as a consequence of glycine deamination. Moreover, the authors described the formation of α-ketovalerate and α-isoketovalerate as intermediates of the same pathway through not identified reactions. Starting from these indications and knowing from literature that α-ketovalerate can be converted into butanol [22], and that α-isoketovalerate can be converted into isobutanol [23], we cultivated yeast cells with glycine, observing the formation of both alcohols. By deeply investigating the literature, we have first (*i*) hypothesized and then (*ii*) biochemically demonstrated step by step the butanol and isobutanol production through the glycine degradation pathway via glyoxylate and α-ketoacids intermediates (Figure 1). Additionally, we suggest at least one

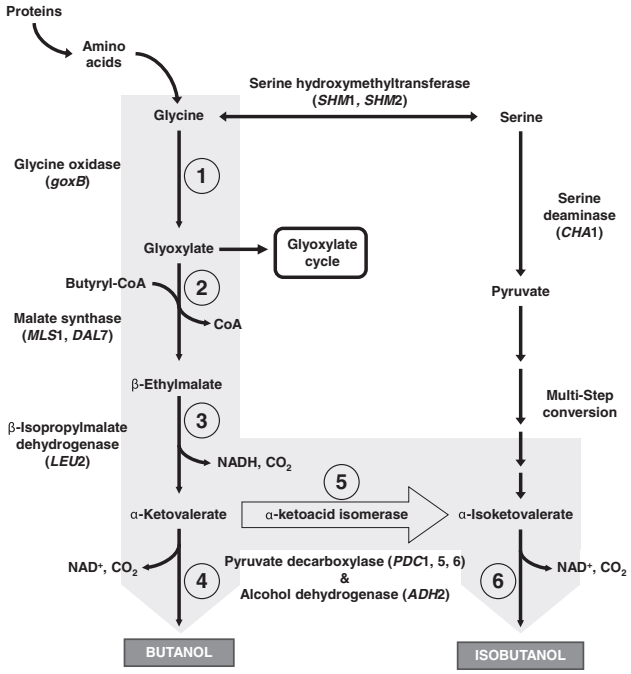

Figure 1 A novel pathway for butanol and isobutanol production. Metabolic pathway for butanol and isobutanol production from glycine in *S. cerevisiae* through the glyoxylate, β-ethylmalate and α-ketoacids intermediates (grey background arrows). The enzymatic activities involved and the associated gene(s) are also represented. Numbers inside circles indicates the steps of the pathway discussed in this study. The hypothesized isomerisation of α-ketovalerate into α-isoketovalerate is indicated by black arrow.

possible gene encoding for the enzymes responsible for butanol production.

Glycine deaminase has been hypothesized to catalyze the glycine conversion into glyoxylate [21], the first step of the pathway. In *S. cerevisiae* the gene encoding for this enzyme has not been annotated yet. However, *Bacillus subtilis* gene *goxB* [24] encodes for a glycine oxidase that can catalyze this conversion (Figure 1, circle 1). For the second step, similarly to what happens in *Pseudomonas aeruginosa* [25], we hypothesized the glyoxylate condensation with butyryl-CoA to yield the β-ethylmalate intermediate (Figure 1, circle 2). β-ethylmalate might be then converted into α-ketovalerate through a β-isopropylmalate dehydrogenase enzyme (Figure 1, circle 3), as described in *E. coli* [22]. The final step is well depicted by the Ehrlich pathway: the α-ketovalerate is converted into butanol through a reductive decarboxylation reaction [26] (Figure 1, circles 4 and 6).

Summarizing, the single steps of the proposed pathway have been already described in literature, even if in different pathways and from different microorganisms: moreover, in some cases indications were provided only as enzymatic reactions. In this work we demonstrate that in the yeast *S. cerevisiae* thanks to these reactions glycine can be converted into butanol.

Results and discussion

Butanol and isobutanol can be obtained from glycine

All the production experiments described here and in the next paragraphs were performed in two different *S. cerevisiae* genetic background, BY and CEN.PK (see Methods for further details), proving the production of butanol and isobutanol from glycine. Here we show butanol and isobutanol kinetics and titers related to the CEN.PK background. It has to be underlined that the production levels obtained in the BY4741 background were consistent, but always lower. Because of the convenience of using single gene deletion mutants available from the Euroscarf collection, all the experiments related to the characterization of the enzymatic activities were performed using the BY4741 background.

Yeast cells were grown in minimal defined medium and in the same medium but using glycine (15 g/L) instead of ammonium sulphate as nitrogen source (see Methods for details). The substitution was preferred to the addition to promote the glycine uptake, a poor nitrogen source if compared to ammonium sulphate, glutamine or glutamate [27]. Butanol and isobutanol accumulations were evaluated at different time point after the inoculum (Figure 2). We confirmed that butanol does not accumulate in minimal ammonium sulphate medium, while isobutanol does (left panel diamond symbols, 46.5 mg/L), since it can derive from other pathways (see Figure 1). When glycine is added as substrate, both butanol and isobutanol accumulate over time, reaching a registered maximum of 92 and 58 mg/L, respectively (Figure 2, right panel), together with a glycine consumption. The described experiment indicates therefore that *(i)* the butanol production requires glycine as substrate and that *(ii)* the measured isobutanol might only partially derive from the glycine degradation pathway.

In the following sections we characterize the proposed pathway step by step. The substrates used are glycine, glyoxylate, α-ketovalerate and α-isoketovalerate. Unfortunately, the intermediate β-ethylmalate is not commercially available and for this reason a coupled enzymatic reaction starting from glyoxylate as initial substrate was planned to circumvent this problem.

The first reaction of the pathway: from glycine to glyoxylate

The first step is the conversion of glycine to glyoxylate, by a glycine deaminase activity [21]. Since no genes are annotated in yeast encoding for this function and being the identification of a putative gene encoding for the desired function not trivial, we searched for a similar activity in other microorganisms. It has been described that in *B. subtilis* the glycine conversion into glyoxylate is catalyzed by the glycine oxidase enzyme, encoded by *goxB* gene, Figure 3A. This enzyme catalyzes the primary amines oxidative deamination to yield the corresponding α-ketoacid, with concomitant ammonium and hydrogen

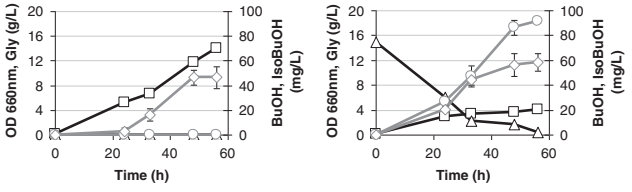

Figure 2 Butanol and isobutanol accumulation from glycine. Yeast cells were grown in Verduyn medium with ammonium sulphate (5 g/L, left panel) or glycine (15 g/L, right panel) as nitrogen source. Biomass accumulation (square), glycine consumption (triangle), butanol (circle) and isobutanol (diamond) productions are shown. The data presented here are representative of three independent experiments.

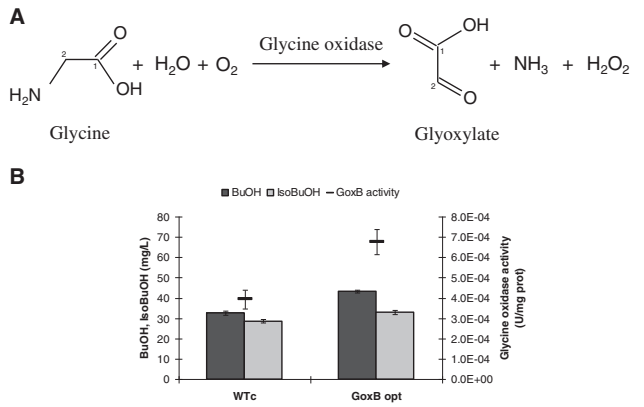

Figure 3 Glycine oxidase: reaction and enzymatic activity assay. (**A**) Reaction catalysed by glycine oxidase. The carbons of the molecules were numbered. (**B**) Glycine oxidase activity (upper bars), butanol (dark gray columns) and isobutanol (pale gray columns) for the wild type and modified yeast strains overexpressing the bacterial *goxB* gene optimized for the yeast codon usage. The data presented here are representative of three independent experiments.

peroxide production. The *B. subtilis* glycine oxidase is a homotetrameric flavoprotein which effectively catalyzes the oxidation of sarcosine (N-methylglycine), N-ethylglycine and glycine. Lower activities using D-alanine, D-valine, and D-proline as substrates were described although no activities were shown on L-amino acids and other D-amino acids [24]. Consequently, the *B. subtilis goxB* gene was synthesized with an optimized codon usage (see Additional file 1) for *S. cerevisiae* (*goxB* opt) and constitutively expressed in yeast. The heterologous enzymatic activity was tested using an *in vitro* assay for glycine oxidase (as described in the Methods section [28]), Figure 3B. As expected, in the control (transformed with the empty vector) as well as in the *goxB* opt overexpressing strains the assay revealed the desired activity, being 1.5 fold higher in the recombinant yeast. It has to be mentioned that overall the measured activities are quite low: however, it might be that the assay needs to be optimized. In fact, the activity measured in total protein extract from *E. coli* BL21 strain overexpressing the *B. subtilis goxB* gene was ~ 4.E-03 U/mg proteins (corresponding to ~ 0.004 U/mL), against 0.4 U/mL reported in literature for the purified enzyme [28].

The effect of glycine oxidase overexpression on butanol and isobutanol accumulation was preliminary tested in the two yeast genetic backgrounds, grown like described for Figure 2. In both cases, in the strains overexpressing the *goxB* opt gene we observed a higher butanol and isobutanol accumulation, being about 30% and 15%, respectively (Figure 3, dark and pale gray columns, respectively). The data prove that an activity responsible for glycine conversion into glyoxylate is the first step leading to butanol accumulation, and we also show a first example of how to improve said activity (Figure 3, upper bars).

The second reaction of the pathway: from glyoxylate to β-ethylmalate

In yeasts, no activity able to catalyze the condensation of glyoxylate with butyryl-CoA to form β-ethylmalate has been described yet. However, the malate synthase enzyme catalyzes a similar reaction: the glyoxylate condensation with acetyl-CoA to form malate [29]. In *S. cerevisiae* two isoforms of malate synthase are described, encoded by *MLS*1 and *DAL*7 genes [29]. *MLS*1 expression is repressed by glucose and induced when cells are growing on non-fermentable carbon sources, such as fatty acid, ethanol or acetate. *DAL*7 encodes for an enzyme recycling the glyoxylate generated during allantoin degradation. Its expression is controlled by the nitrogen source present in the medium, resulting repressed in the presence of rich nitrogen sources, such as asparagine and ammonium, and derepressed in the presence of poor nitrogen sources, such as proline [29]. We hypothesized first and then evaluated if butyryl-CoA could also be a substrate of malate synthase enzyme, considering the structural analogy with acetyl-CoA, Figure 4A.

Yeasts were grown in rich YPD medium and malate synthase activity was detected in the presence of acetyl-CoA or butyryl-CoA as acyl-CoA donors, using a modified TNB-based assay (see Methods) (Figure 4B, left

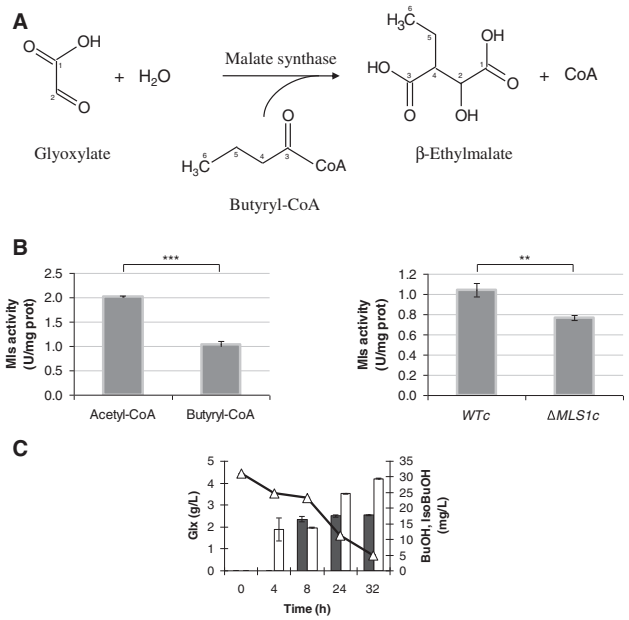

Figure 4 Malate synthase activity and glyoxylate bioconversion into butanol and isobutanol. (**A**) Glyoxylate conversion reaction performed by malate synthase enzyme in the presence of butyryl-CoA. The carbons of the molecules were numbered. (**B**) Malate synthase activity for the glyoxylate conversion into β-ethylmalate. Left panel: malate synthase activity was assayed using acetyl-CoA or butyryl-CoA as donor group. Right panel: effect of *MLS1* deletion on the enzymatic activity. The data presented here are representative of three independent experiments. $p \leq 0{,}05$ = *; $p \leq 0{,}01$ = **; $p \leq 0{,}001$ = ***; $p > 0{,}05$ = n.s. (**C**) Glyoxylate bioconversion. Butanol (full columns) and isobutanol (empty columns) production as well as glyoxylate consumption (triangle) measured at different time point. The data presented here are representative of three independent experiments.

panel). YPD medium was used to have a cultural condition in which both Mls1 and Dal7 were present at similar level, as reported in literature [29]. Remarkably, when butyryl-CoA was added as acyl-CoA donor a malate synthase activity was detected, even if at lower value if compared to the activity measured in the presence of acetyl-CoA (1 U/mg proteins *versus* 2 U/mg proteins, respectively). Based on our information, this is the first experimental evidence that a yeast malate synthase can accept butyryl-CoA as acyl-CoA donor. The *MLS*1 deletion negatively affects the activity (about 25% of reduction, Figure 4B, right panel) and the same impairment is caused by *DAL7* deletion (data not shown), suggesting that the two enzymes might similarly contribute to the reaction of interest.

If our hypothesis is correct, feeding the cells with glyoxylate should result in butanol and isobutanol accumulation. To determine favourable production conditions, yeast cells were grown in minimal medium in the absence or presence of different amount of glyoxylate (0.5, 1, 5 g/L) at different pH (2.5 and 5.5) values. Figure 4C confirms the butanol and isobutanol accumulation, not detectable if glyoxylate is absent (data not shown). In the reported example the production was obtained starting with 5 g/L of glyoxylate at pH 2.5. This pH value has been selected to facilitate the diffusion of undissociated glyoxylic acid inside the cells, since no carrier for this metabolite is reported in literature. In this condition the glyoxylate was almost totally consumed. Cells accumulated during the time about 20 and 30 mg/L of butanol and isobutanol, respectively. This confirms the involvement of glyoxylate as intermediate in the formation of the desired alcohols. At the moment we have no explanation for the higher isobutanol accumulation. One possibility could be that in case of high amount of glyoxylate, Agx1 [30] catalyzes its conversion into glycine, shifting the reaction trough serine formation (see Figure 1).

The third reaction of the pathway: from β-ethylmalate to α-ketovalerate

In *E. coli* the β-isopropylmalate dehydrogenase enzyme, encoded by the *leuB* gene, catalyzes the conversion of β-isopropylmalate into α-ketoisocaproate. Shen and Liao [22] have demonstrated the possibility to use this enzyme to additionally catalyze the conversion of β-ethylmalate into α-ketovalerate in *E. coli* cells (the reaction is depicted in Figure 5A). *LEU*2 is the homologous of *leuB* in *S. cerevisiae* [31]. Therefore, by using the BY4741 strain (deleted in *LEU*2) and the same strain transformed with a *LEU*2 multicopy plasmid, we tested the contribution of the Leu2 activity in the novel pathway. The activity assay was performed using two coupled reactions, since β-ethylmalate is not commercially available. In the first reaction, glyoxylate and butyryl-CoA should be converted into β-ethylmalate by the malate synthase activity, as described in the previous paragraph. The second coupled reaction, catalyzed by the Leu2 activity, utilizes the produced β-ethylmalate to generate α-ketovalerate and releasing NADH as reduced equivalent. Said cofactor can be spectrophotometrically measured to determine the activity. In the *LEU*2 overexpressing strain the activity was about 5 fold higher when compared to the Δ*LEU*2 strain, being 0.1 and 0.02 U/mg proteins, respectively (Figure 5B). When *MLS*1 or *DAL*7 are deleted while Leu2 is present, the dehydrogenase activity significantly decreases, confirming that β-ethylmalate is the substrate of the reaction (Table 1). Table 1 reports all the combinations tested and the registered activities. Interestingly, the residual activity detected whenever *LEU*2 is deleted suggests that other(s) activity(ies) might be responsible for β-ethylmalate conversion.

Concluding, these data indicate that the presence of *LEU*2 coupled with malate synthase activity guarantees the glyoxylate conversion into α-ketovalerate.

The last step: from α-ketoacids to butanol and isobutanol

The last step necessary in the glycine degradation to produce the desired alcohols is the reductive decarboxylation of α-ketovalerate into butanol and of α-isoketovalerate into isobutanol, Figure 6A.

The conversion of α-ketovalerate into α-isoketovalerate was proposed to occur through a dehydratation reaction, catalyzed by dihydroxyacid dehydratase enzyme [21]. However, at the best of our information, no experimental evidences are reported up to now. By looking at the chemical structure of the two ketoacids, this reaction might require an isomerization, like proposed in Figure 1.

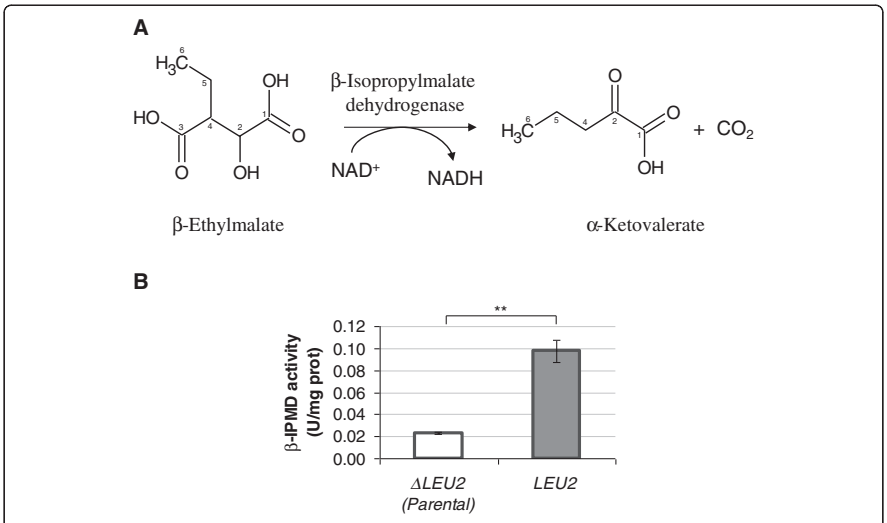

Figure 5 The β-isopropylmalate dehydrogenase involvement in the glycine degradation pathway. The β-isopropylmalate dehydrogenase activity was tested in a coupled reaction using glyoxylate as substrate instead of β-ethylmalate (not commercial available). The carbons of the molecules were numbered. (**A**) Reaction catalysed by the β-isopropylmalate dehydrogenase enzyme. (**B**) Activity of β-isopropylmalate dehydrogenase measured in yeast strain *ΔLEU2* (empty column) and overexpressing *LEU2* gene (grey column). The data presented here are representative of three independent experiments. p ≤ 0,05 = *; p ≤ 0,01 = **; p ≤ 0,001 = ***; p > 0,05 = n.s.

Table 1 β-Isopropylmalate dehydrogenase activity measured with assay coupling the reactions catalyzed by Mls1 and Leu2

Gene			β-IPMD Activity (U/mg prot)
MLS1	*DAL7*	*LEU2*	
+	+	++	0.098 ± 0.010
+	+	-	0.023 ± 0.001
+	-	++	0.019 ± 0.002
+	-	-	0.016 ± 0.002
-	+	++	0.021 ± 0.002
-	+	-	0.018 ± 0.002

The symbols "+" indicate the wild type copy or "++" the overexpression of the corresponding gene in the table. The symbol "-" indicate the deletion of the gene. The data presented here are representative of three independent experiments.

The conversion of α-ketovalerate into butanol requires two reactions: in the first one α-ketovalerate decarboxylation generates the corresponding aldehyde; in the second one the aldehyde is reduced to alcohol, butanol in this case (Figure 6A, upper part). It was reported that in *S. cerevisiae* α-keto-β-methylvalerate, α-ketoisocaproate and α-isoketovalerate [32] can be decarboxylated to the α-ketoacids by pyruvate decarboxylases (Pdc). Going one step forward, Brat *et al.* reported that through the α-isoketovalerate decarboxylation isobutanol can be produced [16], starting from valine as substrate. However, to avoid co-current pyruvate decarboxylation into ethanol, the authors replaced the *PDC* genes with the decarboxylase encoded by *ARO*10 gene, which has no activity on pyruvate [16].

Yeast no data are available about a possible α-ketovalerate decarboxylation in yeast. When pyruvate, α-ketovalerate and α-isoketovalerate were used as substrates, the activities measured using an assay for Pdc activity were 722 ± 2.3, 1.75 ± 0.3 and 0.3 ± 0.05 U/mg proteins, respectively. The involvement of pyruvate decarboxylase in the last reaction was also demonstrated by measuring the butanol and isobutanol production in a *PDC*1, 5, 6 deleted strain. In the presence of α-ketovalerate (1.1612 g/L, 10 mM) as substrate, the deletion of all three isoforms of pyruvate decarboxylase significantly decreases the butanol and isobutanol production, as shown in bioconversion experiment (Figure 6B). In particular, the butanol titer was 5 times lower than in wild type strain, 118 *versus* 583 mg/L respectively. By incubating the triple *PDC* deleted strain with α-isoketovalerate no isobutanol accumulation was observed (data not shown).

It is important to underline that in the presence of α-ketovalerate as substrate both butanol and isobutanol are produced (Figure 6C, left panel) in wild type strain. Considering that more isobutanol is obtained when glycine is added to glucose minimal medium (Figure 2), we could hypothesize that α-isoketovalerate might partially derive from α-ketovalerate and that this reaction is probably irreversible, since in the presence of α-isoketovalerate only isobutanol accumulation was observed (Figure 6C, right panel).

The glyoxylate conversion into butanol and isobutanol requires Mls1, Leu2 and Pdc(s) activities

To further prove the link between glycine and the fusel alcohols we developed an *in vitro* assay in which all reactions of the proposed pathway are coupled. To perform this assay we measured the pyruvate decarboxylase activity using glycine as substrate, monitoring the decrement of OD_{340nm} since NADH is consumed during the last reaction. No data were obtained. We believe that this could be related to (*i*) a lower conversion of glycine to glyoxylate and/or to (*ii*) the very different physiochemical assay conditions required by glycine oxidase (the first enzyme of the pathway) in respect to all the other enzymes. Indeed, a Pdc activity was detected when glyoxylate was used as substrate, confirming the conversion of glyoxylate to the α-ketovalerate.

Figure 7 shows the complete panel of the Pdc activities measured in the different strains. The higher activity was registered in the wild type strain overxpressing the *LEU*2 gene, the minimal (almost undetectable) in the double *MLS*1/*LEU*2 deleted strain and an intermediate situation when only one of the two genes was deleted. To be more precise, the *LEU*2 deletion affects more the activity, very likely because in the case of *MLS*1 deletion, Dal7 is able to replace its function (and vice versa) [29].

Conclusions

This study describes a novel pathway to produce butanol and isobutanol in the yeast *S. cerevisiae* through the glycine degradation pathway.

We characterized the entire pathway identifying for each step at least one enzymatic reaction with at least one relative gene for butanol production. 92 mg/L of butanol were produced starting from glycine as substrate.

It might be speculated that butanol derives from butyryl-CoA and that glycine is solely used to drive the flux. Remarkably, the proposed pathway implies catalytic reactions that justify how glycine is not simply burnt to carbon dioxide, but is an effective co-substrate for the butanol production, as highlighted by the numbered carbons (see Figures 3, 4, 5 and 6, panels A).

Despite the yield on glycine is still quite low, it should be underlined that butanol was obtained through endogenous activities which are in general involved in other reactions and specific for other substrates. Therefore, it can be anticipated that there are many different possibilities for optimizing the pathway, considering every single enzyme involved, the pool of substrates and their compartmentalization.

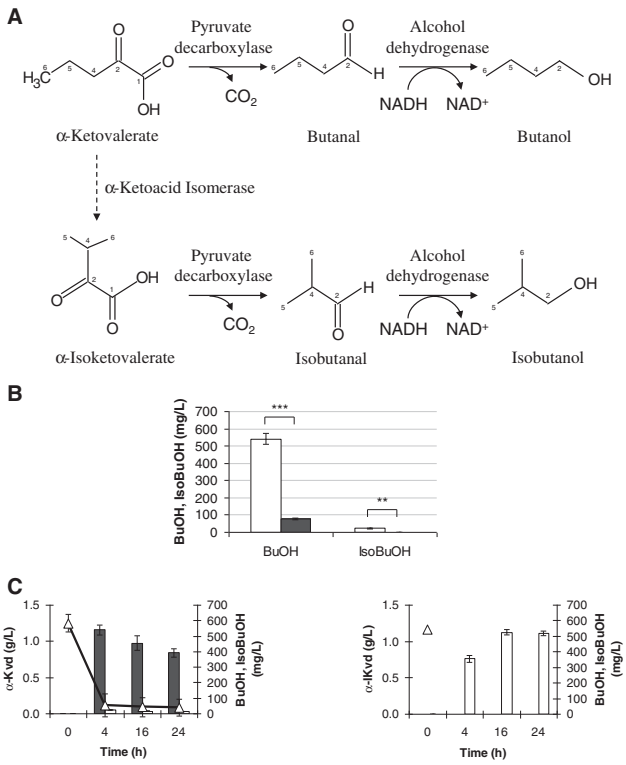

Figure 6 Pyruvate decarboxylase activity and α-ketoacids bioconversion into butanol and isobutanol. (**A**) α-ketovalerate and α-isoketovalerate conversion reaction performed by pyruvate decarboxylase enzyme. The carbons of the molecules were numbered. (**B**) Pyruvate decarboxylase deletion effect on butanol and isobutanol accumulation using α-ketovalerate as substrate. Wild type (empty column) and *PCD*1, 5, 6 deleted strains (full column). The data presented here are representative of three independent experiments. $p \leq 0,05$ = *; $p \leq 0,01$ = **; $p \leq 0,001$ = ***; $p > 0,05$ = n.s. (**C**) α-Ketovalerate (left panel) and α-isoketovalerate (right panel) bioconversion. Butanol (dark grey), isobutanol (white) and α-ketovalerate consumption (triangle) were reported. For α-isoketovalerate (triangle), the sole estimated initial concentration is given. The data presented here are representative of three independent experiments.

From an economical point of view the production of higher alcohols starting from purified glycine cannot be considered as a sustainable process. Metabolic engineering and synthetic biology can then help in the construction of a yeast redirecting sugars to glycine production, and from there to optimize the sole butanol production, but this appears at the moment as a long way to run. However, an alternative seems closer to reality: a considerable fraction of proteins accumulate as waste product deriving from exhausted biomasses of different microbial productions and currently is not fully absorbed by the market [12]. It is then possible to imagine a side-stream process of production which is based on protein hydrolysates; the different aminoacids fed to a yeast strain optimized for desired fusel alcohol production could generate a blend with good properties as biofuel [12], adding value and completing the concept of biorefinery.

Considering the potentiality of *S. cerevisiae* as ethanol producer and considering the potentiality of the aminoacid degradation pathway for fusel alcohol productions [12], it

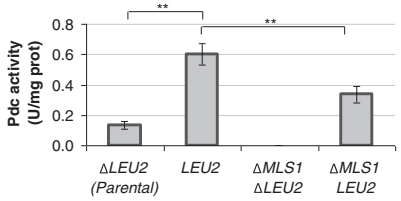

Figure 7 The evidence of glyoxylate degradation through the Mls, β-IPMD and Pdc(s) activities. The *MLS*1 deletion effect was evaluated coupled with the *LEU2* deletion or overexpression (respectively indicated as *ΔMLS1ΔLEU2* and *ΔMLS1 LEU2*). The data presented here are representative of three independent experiments. p ≤ 0,05 = *; p ≤ 0,01 = **; p ≤ 0,001 = ***; p > 0,05 = n.s.

really seems the right moment to intensify the effort in studying and improving yeast tolerance to a mixture of different organic solvents.

Methods

Strains and growth conditions

The *S. cerevisiae* strains used in this study were CEN.PK 102-5B (*MATa,ura3-52, his3-11, leu2-3/112, TRP1, MAL2-8c, SUC2* - Dr. P. Kötter, Institute of Microbiology, Johann Wolfgang Goethe-University, Frankfurt, Germany) [33] and BY4741 (*MATa, ura3Δ0, leu2Δ0, met15Δ0, his 3Δ1*) (EUROSCARF collection, Heidelberg, Germany). The strains BY4741Δ*MLS*1 (*MATa; his3 Δ1; leu2 Δ0; met15 Δ0; ura3 Δ0; YNL117w::kanMX4*) and BY4741Δ*DAL7* (*MATa; his3 Δ1; leu2 Δ0; met15 Δ0; ura3 Δ0; YIR031c::kanMX4*) are provided by EUROSCARF deleted strain collection (EUROSCARF collection, Heidelberg, Germany). The strain deleted in all three isoform of pyruvate decarboxylase (*ΔPDC*1, 5, 6) is CEN.PK RWB837 (*MATa; pdc1::loxP, pdc5::loxP, pdc6::loxP, ura3-52*) [34]. Strains designed with "c" correspond to the respective parental strain transformed with empty plasmid(s) (see below) to render them prototrophic. Strains designed with "*goxB* opt" are the corresponding parental strain transformed with plasmid pYX212 (see below) with the *B. subtilis goxB* coding sequence optimized for the *S. cerevisiae* codon usage. *goxB* opt gene was expressed under the control of the *S. cerevisiae TPI*1 promoter. Yeast transformations were performed according to the LiAc/PEG/ss-DNA protocol [35]. All the parental and transformed strains are reported in the Table 2.

Media composition for cell growth and bioconversion

Independent transformants and the respective control strains (at least three for each transformation) were cultivated in shake flasks with 5/1 ratio of flask volume/medium in minimal synthetic medium with 20 g/L of glucose and supplemented with glycine, glyoxylate, α-ketovalerate or α-isoketovalerate, as specifically indicated in the experiments. YPD and YPGE (for the triple *PDC* deleted strains) media were prepared as follows: yeast extract 1% (w/v), tryptone 2% (w/v) and glucose 2% (w/v) for the YPD. In the YPGE the glucose was replaced with glycerol 1% (v/v) and ethanol 1% (v/v). All strains were grown at 30°C on orbital shaker at 160 rpm for 72 hours.

Table 2 Strains and plasmids used in this work

Parental strain	
Strain	**Genotype**
CEN.PK 102-5B	*MATa, ura3-52, his3-11, leu2-3/112, TRP1, MAL2-8c, SUC2*
CEN.PK RWB837	*MATa, pdc1::loxP, pdc5::loxP, pdc6::loxP, ura3-52*
BY4741	*MATa, ura3Δ0, leu2Δ0, met15Δ0, his 3Δ1*
BY4741Δ*MLS1*	*MATa; his3 Δ1; leu2 Δ0; met15 Δ0; ura3 Δ0; YNL117w::kanMX4*
BY4741Δ*DAL7*	*MATa; his3 Δ1*; leu2 Δ0; met15 Δ0; ura3 Δ0; *YIR031c::kanMX4*

Plasmids		
Expression plasmid	**Segregation**	**Markers, genes**
pYX212	multicopy (2μ derived)	*URA*3
pYX212*goxB* opt	multicopy (2μ derived)	*URA*3, optimised *goxB*
pYX022	integrative	*HIS*3
pYX242	multicopy (2μ derived)	*LEU2*

Transformed strain		
Strain	**Plasmid**	**Obtained strain**
CEN.PK 102-5B	pYX212, pYX022, pYX242	CEN.PKc
BY4741	pYX212, pYX022, pYX242	BY4741c
BY4741	pYX212*goxB* opt, pYX022, pYX242	BY4741c *goxB* opt
BY4741Δ*MLS1*	pYX212, pYX022, pYX242	BY4741ΔMLS1c
BY4741Δ*MLS1*	pYX212*goxB* opt, pYX022, pYX242	BY4741ΔMLS1c *goxB* opt
BY4741Δ*DAL7*	pYX212, pYX022, pYX242	BY4741ΔDAL7c

Kinetic experiment

The butanol and isobutanol production starting from glycine (Figure 2) was performed by growing the cells in Verduyn medium [36] with glucose 20 g/L and glycine 15 g/L as substrates.

Bioconversion experiment

The bioconversion experiments were performed in two phases: 1) cells were grown in YPD or YPGE (for the triple *PDC* deleted strains) medium until the stationary phase; 2) cells were collected by centrifugation (10 min

at 4000 rpm) washed once with water and inoculated in appropriate medium to perform the bioconversion phase. The medium for glyoxylate bioconversion (Figure 4C) was minimal synthetic medium with glucose 20 g/L and glyoxylate 5 g/L at pH 2.5. The medium for α-ketovalerate (or α-isoketovalerate) bioconversion (Figure 6C) was minimal synthetic medium with glucose 20 g/L and α-ketovalerate (or α-isoketovalerate) 1.1612 g/L (corresponding to 10 mM).

Gene amplification and plasmids construction

The *B. subtilis goxB* gene was designed with codon usage adaptation for *S. cerevisiae* by Eurofins MWG Operon. In the Additional file 1 was reported the complete sequence of *goxB* synthesized. *goxB* opt gene was subcloned into the multicopy yeast expression plasmid pYX212 (R&D Systems, Inc., Wiesbaden, D, *URA*3 marker), resulting in the plasmid pYX212*goxB* opt. The heterologous gene is under the control of the *S. cerevisiae TPI*1 promoter. For the construction of the plasmid pYX212*goxB* opt, the recipient vector was *EcoR*I cut, blunted and dephosphorylated, while the insert was *EcoR*I blunt excised from the Eurofins plasmid. DNA manipulation, transformation and cultivation of *E. coli* (Novablue, Novagen) were performed following standard protocols [37]. All the restriction and modification enzymes utilised are from NEB (New England Biolabs, UK) or from Roche Diagnostics.

Cell growth and metabolites determination

The cellular growth was spectrophotometrically monitored at 660nm and was reported as variation of the optical density (OD) as a function of time (h). The amount of extracellular glucose, butanol, isobutanol, glyoxylate and α-ketovalerate were determined by HPLC based method using H_2SO_4 5 mM as mobile phase and Aminex HPX-87P column, 300 × 7.8 mm with a polystyrene divinylbenzene-based matrix (BioRad). The glycine quantification was performed using a previously described assay [38].

Determination of enzymatic activities

Exponentially growing cells were harvested by centrifugation at 4000 rpm for 10 min and washed with cold deionised water. The cell pellet was then re-suspended in 25 mM Tris-HCl pH 8.0 with protease inhibitor cocktail (Roche diagnostics, Cat. No. 04906837001) and 1 mM of phenylmethylsulfonyl fluoride (PMSF) and mechanically disrupted using glass microbeads (600 μm, Sigma-Aldrich). Cells debris was removed by centrifugation at 14000 rpm for 10 min at 4°C and the clarified crude extract was used for enzymatic analysis. The protein concentration in cell-free extracts was estimated according to Bradford [39] using bovine serum albumin as reference.

Enzyme activities were measured on cell-free extracts by spectrophotometric assays. Activities were expressed as U/mg of total proteins.

Glycine oxidase activity

Glycine oxidase activity was assayed spectrophotometrically via determination of H_2O_2 with an enzyme-coupled assay using horseradish peroxidase and *o*-dianisidine, as previously described with some modifications [28]. The assay was performed on a final volume of 1 ml as follows: Tris-HCl 100 mM pH 8, phosphoric acid 10 mM, glycine 50 mM, *o*-dianisidine 1 mM, FAD 0.198 μM, horseradish peroxidase 14.72 U/mL, cell-free protein extract (0.5 mg/mL). The reaction was incubated at 37°C for 90 minutes and yellow colour, developed by o-dianisidine oxidation, was monitored at 530 nm. The glycine oxidase activity was expressed as U/mg of total proteins using the following equation:

$$\text{Activity (U/mg prot tot)} = (((\text{OD 530nm/min})/\varepsilon) \cdot \text{dilution factor})/\text{mg prot tot}$$

Were $\varepsilon = 8.3 \cdot 1/(\text{mM} \cdot \text{cm})$

One glycine oxidase unit is defined as the amount of enzyme that converts 1 mole of substrate (glycine) per minute at 25°C.

Malate synthase activity

The malate synthase activity was performed as described in Sigma-Aldrich protocol [40] using acetyl-CoA (or butyryl-CoA) + glyoxylate. The assay take into consideration that glyoxylate condensation with acetyl-CoA (or butyryl-CoA) produces malate (or β-ethylmalate) and CoA. The free CoA can react with the Ellman reagent DTNB (5,5'-Dithio-bis(2-Nitrobenzoic Acid)) which reacts with free thiol groups, producing CoA-derivative and TNB (5-Thio-2-Nitrobenzoic Acid) [41]. The quantity of TNB produced is in stoichiometric ratio (1:1) with free thiol groups and was monitored spectrophotometrically at 412 nm.

β-isopropylmalate dehydrogenase activity (using glyoxylate and butyryl-CoA as substrates)

The β-isopropylmalate dehydrogenase enzyme catalyzes the NAD-dependent oxidation of the substrate with simultaneously conversion of NAD^+ to NADH. The activity was spectrophotometrically determined at 340 nm. The assay was performed on a final volume of 1 mL in cuvette with imidazole 50 mM pH 8, $MgCl_2$ 10 mM, butyryl-CoA 0.125 mM, glyoxylate 0.5 mM, NAD^+ 1.575 mM. After incubation at 30°C for 10 min cell-free protein extract (0.6 mg/mL) were added and increasing of absorbance at 340 nm was monitored for 10 min.

The β-isopropylmalate dehydrogenase activity was expressed as U/mg total proteins using the following equation:

$$\text{Activity (U/mg prot tot)} = (\text{OD 340nm/min} \cdot \text{dilution factor})/\varepsilon \cdot \text{Ev}$$

Were ε is the millimolar extinction coefficient of NADH at 340 nm ($6.22 \cdot 1/(\text{mM} \cdot \text{cm})$) and Ev is the volume of cell extract used (expressed in millilitres).

Pyruvate decarboxylase activity (using glycine or glyoxylate and butyryl-CoA as substrates)

The pyruvate decarboxylase enzyme catalyzes the decarboxylation of ketoacid to form the derived aldehyde which is reduced by alcohol-dehydrogenase NADH-dependent activity. The conversion of NADH to NAD^+ is spectrophotometrically revealed at 340 nm.

The assay was performed based on pyruvate decarboxylase assay protocol of Sigma-Aldrich [40] with some modifications. When glycine was used as substrate Tris-HCl 100 mM pH 8, phosphoric acid 10 mM, glycine 50 mM, FAD 0.198 μM, $MgCl_2$ 10 mM, butyryl-CoA 0.125 mM and NADH 0.16 mM were added in cuvette in a final volume of 1 mL. After incubation at 37°C for 30 minutes, alcohol dehydrogenase enzymatic solution (200 U/mL) and 0.2 mg/mL of cell-free extract were added. The decrease of absorbance at 340 nm was monitored for 15–30 min.

When glyoxylate and butyryl-CoA were used as substrates imidazole buffer 35 mM, $MgCl_2$ 10 mM, butyryl-CoA 0.125 mM, glyoxylate 0.5 mM and NADH 0.16 mM were added in cuvette in a final volume of 1 mL. After incubation at 30°C for 10 min 20 μL of alcohol dehydrogenase enzyme solution (200 U/mL) and 0.2 mg/mL of cell-free extract were added. The decrease of absorbance at 340 nm was monitored for 15 min.

The activity was expressed as U/mg total proteins using the following equation: Activity (U/mg prot tot) = $(\text{OD 340nm/min} \cdot \text{dilution factor})/\varepsilon \cdot \text{Ev}$.

Were ε is the millimolar extinction coefficient of NADH at 340 nm ($6.22 \cdot 1/(\text{mM} \cdot \text{cm})$) and Ev is the volume of cell extract used (expressed in millilitres).

Additional file

Additional file 1: Sequence of synthesized *goxB* gene with codon usage optimized for *Saccharomyces cerevisiae*.

Abbreviations

GAP1: General Amino acid Permease gene; Shm2: Serine HydroxyMethyltransferase enzyme; GDC: Glycine Decarboxylase (enzymatic) Complex; *goxB*: Glycine OXidase gene, *B. subtilis*; *MLS1*: MaLate Synthase gene; *DAL7*: Malate synthase gene (name description: Degradation of ALlantoin); Agx1: Alanine:Glyoxylate aminotrans(X)ferase enzyme; *leuB*: LEUcine Biosynthesis (β-isopropylmalate dehydrogenase gene), *E. coli*; *LEU2*: LEUcine biosynthesis (β-isopropylmalate dehydrogenase gene); β-IPMD: β-IsopropylMalate Dehydrogenase enzyme; pTPI: Triose-Phosphate Isomerase, promoter; *PDC*: Pyruvate DeCarboxylase gene(s); *ARO10*: AROmatic amino acid requiring gene; $NAD(H)^+$: Nicotinamide Adenine Dinucleotide (oxidized and reduced); $FAD(H_2)$: Flavin Adenine Dinucleotide (oxidized and reduced); -CoA: Coenzyme A; YPD: Yeast extract, Peptone, Dextrose; YPGE: Yeast extract, Peptone, Glycerol, Ethanol; PMSF: PhenylMethaneSulfonyl Fluoride; DTNB/TNB: 5,5'-DiThio-bis(2-Nitrobenzoic Acid)/5-Thio-2-Nitrobenzoic Acid; OD: Optical Density; HPLC: High-Performance Liquid Chromatography; *: if not differently specified, the listed genes and enzymes refer to *S. cerevisiae*.

Competing interests

PB recently applied as inventor of a patent application related to the content of the manuscript. In any way PB, or whatever organization, will gain or lose financially from the publication of this manuscript, either now nor in the future. The other authors declare that they have no competing interests.

Authors' contributions

VL carried out the experiments for butanol and isobutanol production and the enzymatic assays, participated in the evaluation of the data and in compiling the manuscript. NB developed the *goxB* optimized strains and took part in the data analysis. GR carried out the bioconversion experiments on alpha-ketoacids and took part in the data analysis. DP participated in the experimental work design and contributed to the data interpretation. PB conceived the study, participated in its design and compiled the manuscript. All the authors have read and approved the final manuscript.

Acknowledgements

This work was supported by Eni S.p.A. – Corporate. The authors gratefully acknowledge Alessandro Scardua for technical contribution and Francesca De Ferra for fruitful discussions.

Author details

[1]University of Milano Bicocca, Piazza della Scienza 2, 20126, Milano, Italy. [2]Current address: PTA (Schweiz) GmbH, Hohlstrasse 192, CH-8004, Zürich, Switzerland.

Received: 1 February 2013 Accepted: 25 April 2013
Published: 4 May 2013

References

1. Savage N: **Fuel options: The ideal biofuel.** *Nature* 2011, **474:**S9–S11.
2. Dong H, Tao W, Dai Z, Yang L, Gong F, Zhang Y, Li Y: **Biobutanol.** *Adv Biochem Eng Biotechnol* 2012, **128:**85–100.
3. Atsumi S, Cann AF, Connor MR, Shen CR, Smith KM, Brynildsen MP, Chou KJ, Hanai T, Liao JC: **Metabolic engineering of *Escherichia coli* for 1-butanol production.** *Metab Eng* 2008, **10:**305–311.
4. Steen EJ, Chan R, Prasad N, Myers S, Petzold CJ, Redding A, Ouellet M, Keasling JD: **Metabolic engineering of *Saccharomyces cerevisiae* for the production of n-butanol.** *Microb Cell Fact* 2008, **7:**36.
5. Bond-Watts BB, Bellerose RJ, Chang MC: **Enzyme mechanism as a kinetic control element for designing synthetic biofuel pathways.** *Nat Chem Biol* 2011, **7:**222–227.
6. Trinh CT: **Elucidating and reprogramming *Escherichia coli* metabolisms for obligate anaerobic n-butanol and isobutanol production.** *Appl Microbiol Biotechnol* 2012, **95:**1083–1094.
7. McKee AE, Rutherford BJ, Chivian DC, Baidoo EK, Juminaga D, Kuo D, Benke PI, Dietrich JA, Ma SM, Arkin AP, *et al*: **Manipulation of the carbon storage regulator system for metabolite remodeling and biofuel production in *Escherichia coli*.** *Microb Cell Fact* 2012, **11:**79.
8. Ohno S, Furusawa C, Shimizu H: **In silico screening of triple reaction knockout *Escherichia coli* strains for overproduction of useful metabolites.** *J Biosci Bioeng* 2013, **115:**221–228.
9. Shen CR, Lan EI, Dekishima Y, Baez A, Cho KM, Liao JC: **Driving forces enable high-titer anaerobic 1-butanol synthesis in *Escherichia coli*.** *Appl Environ Microbiol* 2011, **77:**2905–2915.
10. Lan EI, Liao JC: **Microbial synthesis of n-butanol, isobutanol, and other higher alcohols from diverse resources.** *Bioresour Technol* 2013, **135:**339–349.
11. Dellomonaco C, Clomburg JM, Miller EN, Gonzalez R: **Engineered reversal of the β-oxidation cycle for the synthesis of fuels and chemicals.** *Nature* 2011, **476:**355–359.

12. Huo YX, Cho KM, Rivera JG, Monte E, Shen CR, Yan Y, Liao JC: **Conversion of proteins into biofuels by engineering nitrogen flux.** *Nat Biotechnol* 2011, **29:**346–351.
13. Chen X, Nielsen KF, Borodina I, Kielland-Brandt MC, Karhumaa K: **Increased isobutanol production in *Saccharomyces cerevisiae* by overexpression of genes in valine metabolism.** *Biotechnol Biofuels* 2011, **4:**21.
14. Kondo T, Tezuka H, Ishii J, Matsuda F, Ogino C, Kondo A: **Genetic engineering to enhance the Ehrlich pathway and alter carbon flux for increased isobutanol production from glucose by *Saccharomyces cerevisiae*.** *J Biotechnol* 2012, **159:**32–37.
15. Lee WH, Seo SO, Bae YH, Nan H, Jin YS, Seo JH: **Isobutanol production in engineered *Saccharomyces cerevisiae* by overexpression of 2-ketoisovalerate decarboxylase and valine biosynthetic enzymes.** *Bioprocess Biosyst Eng* 2012, **35:**1467–1475.
16. Brat D, Weber C, Lorenzen W, Bode HB, Boles E: **Cytosolic re-localization and optimization of valine synthesis and catabolism enables inseased isobutanol production with the yeast *Saccharomyces cerevisiae*.** *Biotechnol Biofuels* 2012, **5:**65.
17. Brat D, Boles E: **Isobutanol production from d-xylose by recombinant *Saccharomyces cerevisiae*.** *FEMS Yeast Res* 2013, **13:**241–244.
18. Hofman-Bang J: **Nitrogen catabolite repression in *Saccharomyces cerevisiae*.** *Mol Biotechnol* 1999, **12:**35–73.
19. McNeil JB, McIntosh EM, Taylor BV, Zhang FR, Tang S, Bognar AL: **Cloning and molecular characterization of three genes, including two genes encoding serine hydroxymethyltransferases, whose inactivation is required to render yeast auxotrophic for glycine.** *J Biol Chem* 1994, **269:**9155–9165.
20. Sinclair DA, Dawes IW: **Genetics of the synthesis of serine from glycine and the utilization of glycine as sole nitrogen source by *Saccharomyces cerevisiae*.** *Genetics* 1995, **140:**1213–1222.
21. Villas-Bôas SG, Kesson M, Nielsen J: **Biosynthesis of glyoxylate from glycine in *Saccharomyces cerevisiae*.** *FEMS Yeast Res* 2005, **5:**703–709.
22. Shen CR, Liao JC: **Metabolic engineering of *Escherichia coli* for 1-butanol and 1-propanol production via the keto-acid pathways.** *Metab Eng* 2008, **10:**312–320.
23. Atsumi S, Hanai T, Liao JC: **Non-fermentative pathways for synthesis of branched-chain higher alcohols as biofuels.** *Nature* 2008, **451:**86–89.
24. Nishiya Y, Imanaka T: **Purification and characterization of a novel glycine oxidase from *Bacillus subtilis*.** *FEBS Lett* 1998, **438:**263–266.
25. Rabin R, Reeves HC, Ajl SJ: **Beta-ethylmalate synthetase.** *J Bacteriol* 1963, **86:**937–944.
26. Hazelwood LA, Daran JM, van Maris AJ, Pronk JT, Dickinson JR: **The Ehrlich pathway for fusel alcohol production: a century of research on *Saccharomyces cerevisiae* metabolism.** *Appl Environ Microbiol* 2008, **74:**2259–2266.
27. Piper MD, Hong SP, Eissing T, Sealey P, Dawes IW: **Regulation of the yeast glycine cleavage genes is responsive to the availability of multiple nutrients.** *FEMS Yeast Res* 2002, **2:**59–71.
28. Job V, Marcone GL, Pilone MS, Pollegioni L: **Glycine oxidase from *Bacillus subtilis*. Characterization of a new flavoprotein.** *J Biol Chem* 2002, **277:**6985–6993.
29. Hartig A, Simon MM, Schuster T, Daugherty JR, Yoo HS, Cooper TG: **Differentially regulated malate synthase genes participate in carbon and nitrogen metabolism of *S. cerevisiae*.** *Nucleic Acids Res* 1992, **20:**5677–5686.
30. Schlösser T, Gätgens C, Weber U, Stahmann KP: **Alanine : glyoxylate aminotransferase of *Saccharomyces cerevisiae*-encoding gene *AGX1* and metabolic significance.** *Yeast* 2004, **21:**63–73.
31. Kohlhaw GB: **Beta-isopropylmalate dehydrogenase from yeast.** *Methods Enzymol* 1988, **166:**429–435.
32. ter Schure EG, Flikweert MT, van Dijken JP, Pronk JT, Verrips CT: **Pyruvate decarboxylase catalyzes decarboxylation of branched-chain 2-oxo acids but is not essential for fusel alcohol production by *Saccharomyces cerevisiae*.** *Appl Environ Microbiol* 1998, **64:**1303–1307.
33. van Dijken JP, Bauer J, Brambilla L, Duboc P, Francois JM, Gancedo C, Giuseppin ML, Heijnen JJ, Hoare M, Lange HC, *et al*: **An interlaboratory comparison of physiological and genetic properties of four *Saccharomyces cerevisiae* strains.** *Enzyme Microb Technol* 2000, **26:**706–714.
34. van Maris AJ, Winkler AA, Porro D, van Dijken JP, Pronk JT: **Homofermentative lactate production cannot sustain anaerobic growth of engineered *Saccharomyces cerevisiae*: possible consequence of energy-dependent lactate export.** *Appl Environ Microbiol* 2004, **70:**2898–2905.
35. Gietz RD, Woods RA: **Transformation of yeast by lithium acetate/single-stranded carrier DNA/polyethylene glycol method.** *Guide to Yeast Genetics and Molecular and Cell Biology, Pt B* 2002, **350:**87–96.
36. Verduyn C, Postma E, Scheffers W, Van Dijken J: **Effect of benzoic acid on metabolic fluxes in yeasts: a continuous-culture study on the regulation of respiration and alcoholic fermentation.** *Yeast* 1992, **8:**501–517.
37. Sambrook J, Maniatis T, Fritsch EF: *Molecular cloning : a laboratory manual.* 2nd edition. Cold Spring Harbor, N.Y.: Cold Spring Harbor Laboratory; 1989.
38. Stella CA, Sáenz DA, Chianelli MS, Kaminszczik S: **A simple protocol to evaluate nitrogen utilisation in *Saccharomyces cerevisiae*.** *Biochem Educ* 2000, **28:**169–170.
39. Bradford MM: **A rapid and sensitive method for the quantitation of microgram quantities of protein utilizing the principle of protein-dye binding.** *Anal Biochem* 1976, **72:**248–254.
40. Sigma L: URL: [http://www.sigmaaldrich.com].
41. Ellman GL: **Tissue sulfhydryl groups.** *Arch Biochem Biophys* 1959, **82:**70–77.

doi:10.1186/1754-6834-6-68
Cite this article as: Branduardi *et al.*: A novel pathway to produce butanol and isobutanol in *Saccharomyces cerevisiae*. *Biotechnology for Biofuels* 2013 **6**:68.

Additional file

Additional file 1 – Sequence of synthesized *goxB* gene with codone usage optimized for *Saccharomyces cerevisiae*

ATGAAGAAACACTACGACACTGCAGTTATAGGTGGAGGGATCATT
GGTTGTGCGATATCGTACGAATTGGCCAAAACTCAACAGAAGGTT
GTCCTGCTAGAAGCTGGAGAAGTAGGTAGAAAGACTACTAGTGCT
GCTGCTGGAATGCTTGGAGCTCATGCCGAATGCGAAAACAGGGAT
GCTTTCTTTGACTTTGCCATGCACTCACAAAGGCTTTATGAACCA
GCAGGGCAAGAATTGGAAGAAGCATGTGGTATTGATATTAGACGT
CATAATGGCGGAATGTTGAAGTTAGCCTATACGGAAGAGGATATT
GCCTGTTTAAGAAAGATGGATGATTTACCTAGCGTTACCTGGTTG
TCTGCTGAAGATGCATTGGAGAAGGAACCTTATGCATCGAAAGAC
ATACTAGGTGCATCCTTTATAAAAGATGATGTGCACGTAGAACCG
TATTATGTCTGCAAAGCCTACGCTAAAGGGGCTAGGAGATATGGT
GCTGACATTTACGAACACACACAAGTCACCTCAGTGAAAAGAATG
AACGGAGAGTATTGCATCACAACATCAGGTGGAGATGTTTATGCC
GACAAGGTTGCAGTTGCTTCTGGTGTATGGTCTGGTCGTTTCTTT
TCCCAGTTAGGTTTAGGTCAACCATTCTTTCCAGTAAAAGGCGAG
TGTTTGAGTGTTTGGAATGACGATACCCCATTAACCAAGACTCTT
TACCATGACCATTGTTACGTGGTTCCAAGAAAGTCCGGCAGATTG
GTCATTGGTGCCACTATGAAACATGGTGATTGGTCTGATACACCT
GACATTGGTGGCATTGAAGCTGTGATTGGTAAGGCGAAAACGATG
CTACCAGCAATTGAGCACATGAAAATCGATAGATTTTGGGCGGGT
TTAAGACCGGGAACAAGAGATGGCAAACCCTTCATTGGGAGACAT
CCCGAAGATAGCGGCATAATCTTTGCAGCCGGTCATTTCAGAAAT
GGCATACTGCTGGCTCCTGCAACAGCTGAAATGGTCAGAGACATG
ATCTTGGAACGTCAGATAAAACAAGAGTGGGAAGAGGCATTTAGG
ATCGATAGAAAAGAGGCGGTTCATATCTAA